Paleobiodiversity and paleoenvironments of the eastern Paratethys Pleistocene lacustrine-palustrine sequence in the Baklan Basin (SW Anatolia, Turkey)

Hülya Alçiçek, Martin Gross, Johannes M. Bouchal, Frank P. Wesselingh, Thomas A. Neubauer, Tom Meijer, Lars W. van den Hoek Ostende, Alexey Tesakov, Alison M. Murray, Serdar Mayda, Mehmet Cihat Alçiçek

DOI:
https://doi.org/10.1016/j.palaeo.2023.111649

Palaeogeography, Palaeoclimatology, Palaeoecology 626 (2023) 111649

Contents lists available at ScienceDirect

Palaeogeography, Palaeoclimatology, Palaeoecology

journal homepage: www.elsevier.com/locate/palaeo

Paleobiodiversity and paleoenvironments of the eastern Paratethys Pleistocene lacustrine-palustrine sequence in the Baklan Basin (SW Anatolia, Turkey)

Hülya Alçiçek [a,*], Martin Gross [b], Johannes M. Bouchal [c], Frank P. Wesselingh [d,e], Thomas A. Neubauer [f,g], Tom Meijer [d], Lars W. van den Hoek Ostende [d], Alexey Tesakov [h], Alison M. Murray [i], Serdar Mayda [j], Mehmet Cihat Alçiçek [a]

[a] Pamukkale University, Department of Geology, 20160 Denizli, Türkiye
[b] Universalmuseum Joanneum, Geology and Palaeontology, Weinzöttlstrasse 16, 8045 Graz, Austria
[c] University of Vienna, Department of Botany and Biodiversity Research, Division of Structural and Functional Botany, Rennweg 14, 1030 Vienna, Austria
[d] Naturalis Biodiversity Center, P.O. Box 9517, 2300 RA Leiden, the Netherlands
[e] Department of Earth Sciences, Utrecht University, Princetonlaan 8a, 3584 CB Utrecht, the Netherlands
[f] Department of Animal Ecology and Systematics, Justus Liebig University, Heinrich-Buff-Ring 26-32 IFZ, Giessen 35392, Germany
[g] SNSB - Bavarian State Collection for Paleontology and Geology, Richard-Wagner-Straße 10, 80333 Munich, Germany
[h] Russian Academy of Sciences, Geological Institute, Pyzhevsky Lane, 7, Moscow, 119017 Moscow, Russia
[i] Department of Biological Sciences, University of Alberta, Edmonton, AB T6G2E9, Canada
[j] Natural History Museum, Ege University, 35100 Izmir, Türkiye

ARTICLE INFO

Editor: L Angiolini

Keywords:
SW Anatolia
Pontocaspian fauna
Biodiversity
Paleoenvironments
Paleoclimate
Paleobiogeography

ABSTRACT

The Lower-Upper Pleistocene sedimentary record of the Baklan Basin, a long-lived continental half-graben basin in SW Turkey, is characterized by shallow lacustrine and palustrine deposits. The paleoenvironmental changes recorded in the basin succession allow for a multiproxy approach in reconstructing the paleoclimatic, paleoecological, and paleobiogeographical evolution of southwestern Anatolia during the Early-Late Pleistocene. Based on sedimentological, paleontological, and geochemical data, three main types of depositional intervals have been identified, corresponding to different phases of a lake expansion cycle: The first interval is characterized by the perennial shallow lake environment (PSL deposits), which represents the very early stage of the Early Expansion System Tract (VEEST). This suggests a very early stage of lake transgression in arid climate conditions. The second interval is represented by the palustrine carbonate lake center environment (PLC deposits), which corresponds to the late stage of the Early Expansion System Tract (LEEST). This indicates a late early stage of lake transgression in semiarid to subhumid climates. The third interval is marked by the palustrine lake margin environment (PLM deposits), which represents the Late Expansion System Tract (LEST) under humid conditions.

The Lower-Upper Pleistocene successions of the Baklan Basin provide an excellent example of lacustrine and palustrine deposition in a laterally extensive, low-gradient, shallow lake system in the semi-isolated Pontocaspian freshwater to slightly brackish water (oligohaline-low mesohaline) long-lived lake. The presence of Pontocaspian ostracod and mollusc faunas in the studied successions indicates that the largest major Caspian transgression around 2.6 millon years ago extended to SW Anatolia. The studied successions represent a rich archive of landscape, climate, and biotic development in the eastern Paratethys region during the Early-Late Pleistocene. The biogeographic signature of fossil faunas (mammals, ostracods, molluscs, and fishes) and floras (Characeae) is predominantly modern Palearctic and Holarctic, with a minor amount of endemic Pontocaspian elements. This study presents the Pleistocene Pontocaspian species of the Anatolian lakes that may have served as refugia for the Palearctic taxa during adverse time intervals. Consequently, this study shows that Lower-Upper Pleistocene lacustrine to palustrine sedimentation in the Baklan Basin has been controlled by the combination of tectonics, climate changes, and the largest major Caspian Sea transgression. The findings of this study could be used to evaluate the impact of similar allocyclic factors on the sedimentological, hydrological, and geochemical development of other intermontane lake basins.

* Corresponding author.
E-mail address: halcicek@pau.edu.tr (H. Alçiçek).

https://doi.org/10.1016/j.palaeo.2023.111649
Received 17 September 2021; Received in revised form 15 May 2023; Accepted 16 May 2023
Available online 18 May 2023

1. Introduction

During the Neogene-Quaternary, the Paratethys region, which includes the Black Sea, Azov Sea, Caspian Sea, and Lake Aral, experienced significant changes in their paleogeography and paleoclimate (e.g., Krijgsman et al., 2019). The Caspian Sea and Black Sea underwent major fluctuations in their sea/lake levels since the Pliocene, potentially influenced by tectonics and glacio-eustatic sea level changes, and hydrological and climatic changes triggered by glacial-interglacial cycles. These changes may have led to intermittent periods of connectivity between the Caspian Sea, Black Sea, and Aegean Sea basins (e.g., Badertscher et al., 2011; Yanina, 2014; Krijgsman et al., 2019).

During the latest Pliocene-earliest Pleistocene, a major transgression occurred in the Caspian Sea region, resulting in the establishment of connectivity between the Caspian Sea, Black Sea, and Aegean Sea (Krijgsman et al., 2019). This facilitated the migration of various fauna, such as fishes, molluscs, and ostracods, from the Caspian Sea to the Black Sea and eventually to the Aegean Sea. As a result, the Black Sea, Caspian Sea, and Lake Aral had high biodiversity of Pontocaspian fauna. The Pontocaspian fauna evolved in the past two million years and adapted to the unusual salinity regimes in these lakes and seas (Nevesskaya et al., 2005). Although the Pontocaspian biota developed around the Caspian Sea, the Black Sea, and the Marmara Sea basins (e.g., Nevesskaja et al., 2001; Yanina, 2014), satellite areas such as the Balkans and Anatolia may have played a role in their evolution as well (Büyükmeriç and Wesselingh, 2018). Some fossil and modern Pontocaspian taxa have been recorded in southwestern Anatolian lake systems (Alçiçek et al., 2007, 2015; Wesselingh et al., 2008; Wesselingh and Alçiçek, 2010; Rausch et al., 2019, 2020; Lazarev, 2020a, 2020b; Wilke et al., 2007; Glöer and Girod, 2013). The Pontocaspian ostracod and mollusc fauna have been documented in the Pliocene-Pleistocene Lake Denizli (Taner, 1974a, 1974b, 1975; Alçiçek et al., 2007, 2015; Wesselingh et al., 2008) in southwestern Anatolia, Late Pleistocene Lake Karapınar (Büyükmeriç and Wesselingh, 2018) in central Anatolia, and Late Pleistocene Lake İznik (İslamoğlu, 2009) and Lake İzmit (Büyükmeriç et al., 2016) in northwestern Anatolia.

Extensive literature has been devoted to the Miocene to Pleistocene paleogeographic development of the Western Paratethys (Alpine), the Central Paratethys (Carpathian, Balkan), and the northern parts of the Eastern Paratethys (Crimean-Caucasian). However, studies regarding paleogeographical reconstructions of the southern part of the Eastern Paratethyan lakes, including Anatolia, are still very scarce (Alçiçek et al., 2007, 2015; Wesselingh et al., 2008; Wesselingh and Alçiçek, 2010; Rausch et al., 2019, 2020; Lazarev, 2020a, 2020b). The spatial and temporal evolution of the Paratethys region during the Neogene-Quaternary is still poorly constrained in Anatolia.

In this study, we report Pontocaspian ostracod and mollusc fauna in the Baklan Basin in southwestern Anatolia. This new record has the potential to help us understand the role of satellite regions in the evolution of Pontocaspian biota. The lacustrine-palustrine deposits containing endemic Pontocaspian biota of the Baklan Basin provide notable continental records of paleoclimatic, paleobiogeographical and paleoecological conditions for this period in the Eastern Paratethys region. This succession allows us to understand the southern boundary of the Paratethys, the location of the gateways, and the time when the region served as a refugium for the Pontocaspian fauna during the Early-Late Pleistocene. Therefore, this study aims to (i) reconstruct the paleoenvironmental, paleohydrological, and paleoclimatic evolution of the Lower-Upper Pleistocene succession by using mineralogical, sedimentological, geochemical, and paleontological data, (ii) describe the drivers of faunal evolution, and (iii) synthesize regional conclusions about paleogeographical, paleoclimatic, paleoecological, paleobiogeographical, and tectonic events. This study as a whole contributes to a better understanding of the Early-Late Pleistocene paleogeographic history of the eastern Paratethys region.

2. Geological setting and basin stratigraphy

The Western Anatolian domain is characterized by intra-continental extensional tectonics (Ten Veen et al., 2009). Its southern part is distinguished by the Western Taurides which constitutes the eastern extension of the Alpine orogeny and are subdivided into thre structural units of Beydağları autochthon, Lycian and Antalya nappes, and were attributed to diverse orogenic stages on a regional scale and represent the closure of the Neotethyan oceanic domains during the Mesozoic-early Cenozoic (Fig. 1B; Özgül and Arpat, 1973; Bernoulli et al., 1974; Collins and Robertson, 1998; Nemec et al., 2018). The late Cenozoic Neotectonic deformation in SW Anatolia (Fig. 1B) caused the formation of an array of NE-trending extensional grabens hosted by the Paleozoic–Mesozoic metamorphic bedrock of the Menderes Massif and the Mesozoic Lycian allochthonous units (Ten Veen et al., 2009; Alçiçek and Ten Veen, 2008). These grabens were filled by Neogene to Quaternary alluvial fan, fluvial, lacustrine, and fluvio–lacustrine deposits (Alçiçek et al., 2019). The Baklan Basin is an arcuate graben (Fig. 2) with a Neogene–Quaternary basin-fill that is the subject of this study. The regional geological maps, including the Baklan Basin, were first charted by Konak et al. (1986) at a scale of 1:25000 scale, and its rock units were described in a lithostratigraphic context. Sun (1990) compiled the regional geological map at a scale of 1:100000 scale and described the basin-fill units as the Denizli Group. Sözbilir (1997) followed a similar nomenclature and locally subdivided the units into the Belevi Group consisting of terrestrial deposits that unconformably overlie marine Oligocene deposits. Later, Konak and Şenel (2002) and Konak (2002) compiled the regional geological map at a scale of 1:500000 scale. The fossil materials from the lower basin-fill succession (Mahmutgazi locality, mammal unit MN11-12, Fig. 3) have been studied by Sickenberg and Tobien (1971), Luttig and Steffens (1976), and Rutte and Becker-Platen (1980), with recent paleontological work done by Pickford (2016) and Geraards (2017). The mollusc assemblages from the upper part the succession was presented by Wesselingh and Alçiçek (2010).

Alçiçek et al. (2013) conducted the first attempt to explain the tectonic development of the Baklan Basin in its regional geodynamic context. The detailed kinematic documentation revealed that basin subsidence was initiated by the initial transfer motion of the Dinar Fault Zone, which orthogonally bounds the basin to the northeast. The SW-NE–trending Baklan Basin, approximately 60 km long and 20 km wide, rests on the Paleozoic metamorphic rocks of the Menderes Massif, the Mesozoic carbonates and ophiolites of the Lycian Nappes, and the Eocene-Oligocene siliciclastic rocks (Fig. 3). The basin is bordered by the Çivril Fault to the northwest and the Baklan Fault to the southeast (Fig. 2). The basin's sedimentary fill reaches a thickness of up to 350 m and consists of alluvial fan to fluvial deposits (Upper Miocene) and lacustrine deposits (Upper Miocene–Upper Pleistocene). The lacustrine deposits are subdivided into two stages: the first lacustrine stage (Lower-Upper Pliocene) and the second lacustrine stage (Lower-Upper Pleistocene) (Fig. 3). This study is focused on the second lacustrine stage, which includes the lacustrine-palustrine successions (Fig. 3). The age of studied succession has been determined based on the presence of MNQ1-Q2 micromammal fauna (the gerbiline *Meriones* sp. and the arvicoline *Microtus* sp., Biharian-Toringian).

3. Material and methods

The studied Lower-Upper Pleistocene outcrops are located between Aşağıseyit and Gelinören villages in the northern part of the Baklan Basin (Fig. 2). Three sections in the study area were logged and compiled in Fig. 4. Analytical methods are presented below.

The macroscopic facies analysis was supplemented by the observation of 30 thin sections of collected samples. The studied deposits were divided into fourteen sedimentary facies, which have been further grouped into three facies associations. The Dunham classification system

(Dunham, 1962) was used for descriptive carbonate terminologies.

The mineral composition of 65 powdered samples was determined by X-ray diffraction (XRD) at a laboratory of Hacettepe University (Turkey). The powder X-ray diffraction patterns of the samples were recorded on a Rigaku D/Max 2200 PC diffractometer using CuKa radiation ($k = 1.542A°$). The semi-quantitative ratios were determined from the powder diffractogram using an external standard method developed by Gündoğdu (1982) and Temel and Gündoğdu (1996). Clay-fraction analysis was performed on 12 powdered dolomitic limestone, mudstone and marlstone samples. Clay mineralogy of the <2 μm grain-size fraction was also determined by X-ray diffraction. Samples were pre-treated with 0.2 N HCl to remove carbonates. After centrifuging and microhomogenisation, the <2 μm fraction was separated by gravity settling on glass slides. Selected samples were examined in three forms:

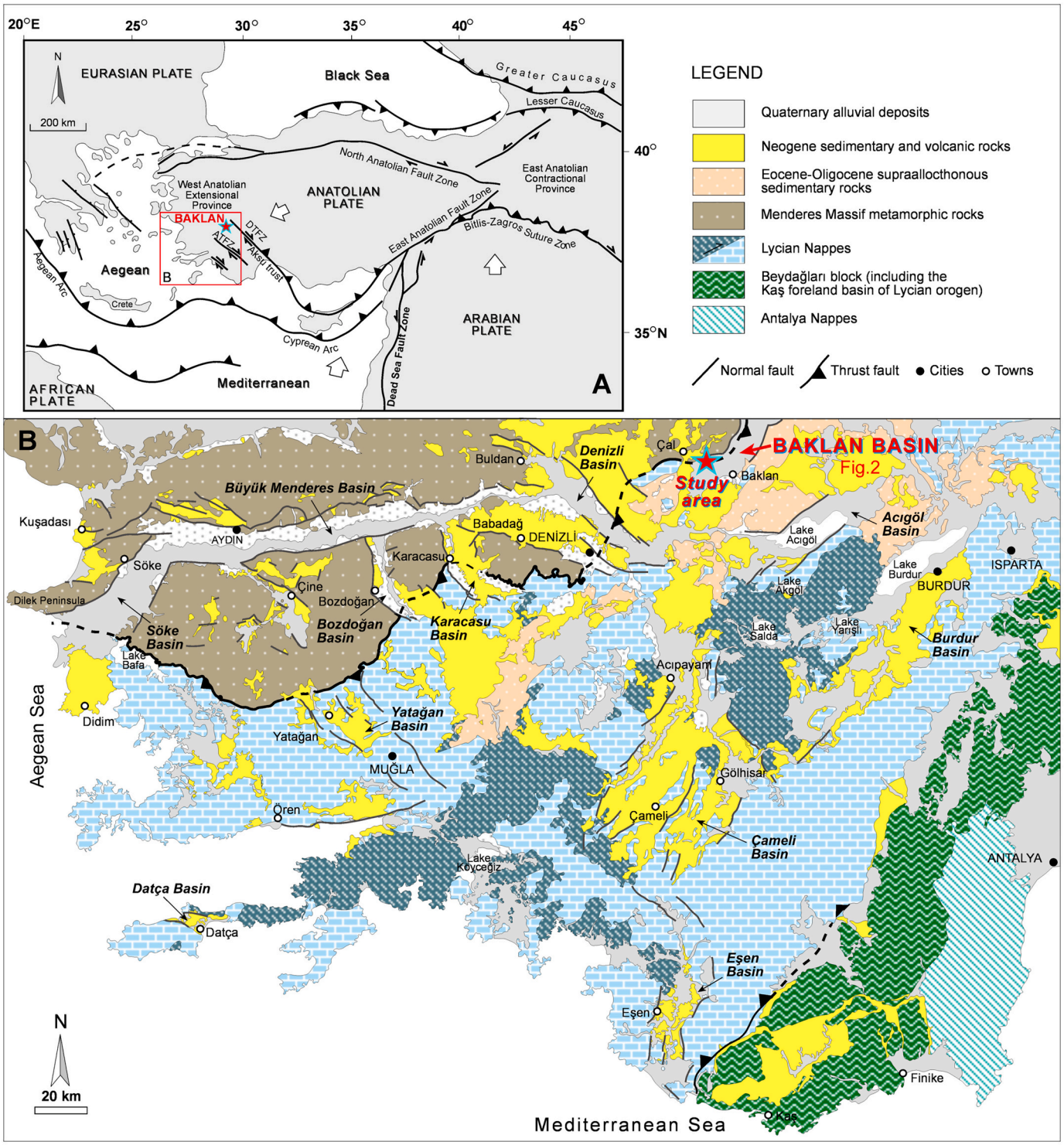

Fig. 1. (A) Tectonic map of the eastern Mediterranean showing major tectonic structures (after Bozkurt, 2003; Alçiçek et al., 2013; Kaymakçı et al., 2018; Nissen et al., 2022), DTFZ: Dinar Transfer Fault Zone, ATFZ: Acıpayam Transfer Fault Zone; (B) Geological map of SW Anatolia showing the main tectonic and sedimentary units (based on Şenel, 1997).

as an oriented clay sample (untreated), as an ethyleneglycol-treated clay sample, and as an oriented clay sample heated to 500 °C for 2 h (oven-dried). The external standard method of Gündoğdu (1982) was used as a guide for quantitative estimates of the mineral composition. The percentage evaluations were based on peak heights, corrected for mineral crystallinity.

Samples for stable isotope analyses were collected by drilling micritic carbonate textures and obtaining approximately 3 mg of powdered sediment. Samples with diagenetic alteration were discarded, and only dense micritic areas were drilled for $\delta^{18}O$ and $\delta^{13}C$ isotope analysis. For mixed carbonate samples, both calcite and dolomite were analyzed if the lesser mineral constituted at least 10% of the total carbonate. Otherwise, only the dominant mineral (calcite or dolomite) was analyzed. For $\delta^{18}O$ and $\delta^{13}C$ analysis, approximately 3 mg of powder of the carbonate samples (dolomitic limestones and dolostones) were extracted from polished slabs of samples under a stereomicroscope (Leica S8APO) with a micro-drill. Additionally, approximately 3 mg of powder of marlstone and mudstone samples was also drilled from the fresh surface using a microdrill under the stereomicroscope. These samples were analyzed at the Stable Isotope Ratio Facility for Environmental Research (SIRFER), University of Utah (USA), using a Thermo Fisher Scientific GasBench II with a PAL autosampler, coupled to a ConFlow IV interface and a MAT 253 mass spectrometer (Thermo Fisher Scientific) to obtain their $\delta^{18}O$ and $\delta^{13}C$ isotopic compositions. The samples were reacted with 10 droplets of phosphoric acid (H_3PO_4) (kept at 50 °C) to produce CO_2 gas. The results are reported using standard delta notation ($\delta^{18}O$ and $\delta^{13}C$) with respect to Vienna Pee Dee Belemnite (VPDB). Carrara marble and LSVEC were used as primary reference materials, and Marble-Std was used as secondary reference material to cross-check the final values. Internal reference materials were calibrated against international standards NBS-18 and NBS-19. The oxygen fractionation factor was calculated using the alpha value proposed by Swart et al. (1991). Analytical errors for $\delta^{18}O$ and $\delta^{13}C$ are smaller than ±0.05‰ and ± 0.02‰, respectively. The $\delta^{18}O$ and $\delta^{13}C$ values of 72 mollusc specimens were analyzed at Vrije Universiteit (The Netherlands), following procedures outlined in Vonhof et al. (1998). About 0.5 mg of the powdered shell was dissolved in orthophosphoric acid at 50 °C. The evolved CO_2 was purified and run off-line on a Finnigan Mat 251 mass spectrometer. The $\delta^{18}O$ and $\delta^{13}C$ compositions are reported in ‰ notation with respect to the V-PDB standard, using NBS-19 as a primary reference. Analytical precision of an internal standard was ±0.10 and ± 0.06‰ (1σ) for $\delta^{18}O$ and $\delta^{13}C$, respectively, for the measuring period.

Micromammals were collected from ten levels through wet-screening (mesh 0.7 mm) of approximately 10 kg of fossiliferous sediments. All molars were picked out and photographed using a Leica S8APO measuring microscope with associated software. About 2 kg of sediments from each level were washed through sieves using diluted hydrogen peroxide for disintegration, to determine mollusc, ostracod, fish and chara fossils. Ostracod specimens were collected from twenty

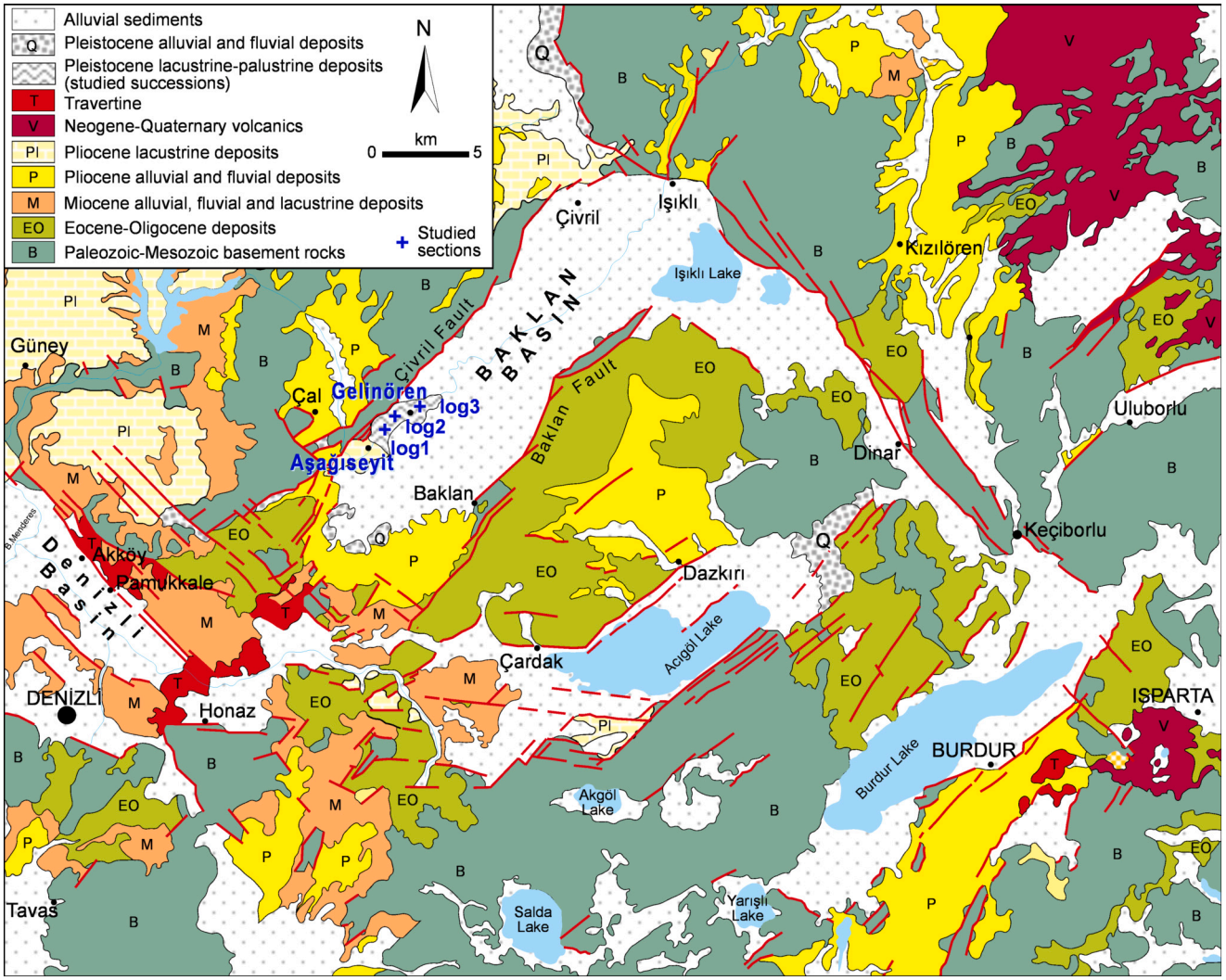

Fig. 2. Geological map of the Baklan Basin (revised and complied after Konak, 2002; Konak and Şenel, 2002; Şenel, 2002; Turan, 2002; Alçiçek et al., 2013).

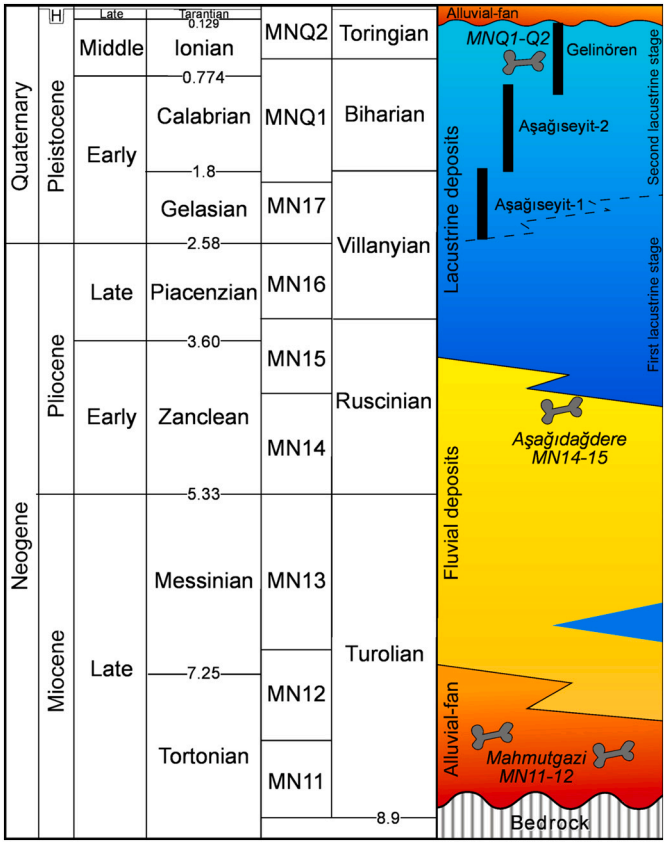

Fig. 3. Stratigraphy of the Late Miocene-Pleistocene succession in the Baklan Basin (Studied logs are shown in solid lines) (based on Göktaş et al., 1989; Şenel, 1997; Alçiçek et al., 2013; Alçiçek et al., 2019).

levels and picked out of the residuals under a stereozoom microscope (Leica S8APO) for SEM (JEOL, JSM-6610LV) studies. Molluscs were collected from eighteen levels and sieved from sediment samples (mesh 1 mm). Mollusc shells were identified to the lowest possible taxon and counted following the methods outlined in van de Velde et al. (2019). Ecological information on the living counterparts of the encountered mollusc species was obtained from Gittenberger et al. (1998), Glöer (2002), and Welter-Schultes (2012). Data on Pontocaspian taxa are retrieved from Wesselingh et al. (2019) and Gogaladze et al. (2021). Fish fossils were collected from thirteen levels and photographed using a Nikon 1200C digital camera mounted on a Zeiss Discovery V8 stereomicroscope. Between five and nine photographs with varying focal points were taken of each view, and the focus was stacked into a single image using Adobe Photoshop imaging software. Chara samples were collected from nine levels and photographed using an Olympus BX51 microscope equipped with an Olympus DP71 camera.

4. Results

4.1. Studied sections

To better define the stratigraphy of the Lower-Upper Pleistocene deposits on the northern margin of the Baklan Basin, three significant locations have been selected (Figs. 2 and 4A-C). The studied succession is divided into three sections:

The Aşağıseyit-1 section is the lower part of the succession and is located 1.5 km northeast of Aşağıseyit village (38°03′56″N, 29°29′07″E) (Figs. 2 and 3). This section is up to 20 m thick and extends laterally over tens of meters. These deposits, which are found at +808 m a.s.l., mainly consist of dolomitic limestone, dolostone, mudstone, and marlstone alternations (Figs. 4A and 5A).

The Aşağıseyit−2 section is the middle part of the succession and conformably overlies the Aşağıseyit-1 section (Figs. 3 and 5A). It is also located in the approximately 200 m northeast of Aşağıseyit-1 section and 1.7 km northeast of Aşağıseyit village (38°03′57″N, 29°29′16″E) (Fig. 2). This section is up to 14 m thick and extends laterally over tens of meters (Fig. 5A). The section is located at a higher altitude of +821 m a.s.l. and is mainly composed of dolomitic limestone, dolostone, siltstone, and mudstone alternations (Fig. 4B).

The Gelinören section is the upper part of the succession and located 250 m north of Gelinören village (38°05′41″N, 29°31′40″E) (Figs. 2 and 3). It is up to 25 m thick (Fig. 4C) and extends laterally over tens of meters (Fig. 5B). This section is located at the same altitude (+817 m a.s.l.) as the Aşağıseyit sections. It is composed of dolomitic limestone, limestone, siltstone-sandstone, mudstone, and marlstone alternations.

4.2. Facies associations and depositional environments

Three facies associations are recognized in the studied succession and are subdivided based on systematic differences in lithology, texture, sediment constituents, sedimentary structures, characteristic styles of stratification, and fossils. The main sedimentological features and associated biota of the fourteen depositional facies identified in the study area are summarized in Table 1.

4.2.1. Perennial shallow lake facies association (PSL)

This association constitutes the lower part of the studied succession (Fig. 3) and is particularly well developed in the basin`s northern part (Fig. 2). It comprises six facies: ostracodal packstone (facies PSL1), mudstone (facies PSL2), peloidal-brecciated-nodular wackestone (facies PSL3), ostracodal-molluscan wackestone (facies PSL4), organic-rich mudstone (facies PSL5), and laminated marlstone (facies PSL6) (Table 1). These deposits can reach a thickness of up to 20 m (Aşağıseyit-1 section, Fig. 4A) and extend laterally for tens of meters (Fig. 5A).

Facies PSL1: Ostracodal packstone is present in the lower and middle parts of the Aşağıseyit-1 section (Fig. 4A). It is beige to yellow, porous, and well-cemented (Fig. 5C). The facies consists of massive (non-laminated) tabular beds that are approximately 20–100 cm thick and alternate with laminated marlstone (facies PSL6). The textural characteristics of this facies are packstones with a homogeneous micritic matrix, diffuse ostracods, siliciclastic grains, iron-oxide stained voids, and circumgranular cracks (cc) (Fig. 6A-6B). The ostracod shell cavities may be open or filled with microsparite, while circumgranular cracks and voids are typically filled with sparite.

Facies PSL2: Mudstone occurs in the middle part of the Aşağıseyit-1 section (Fig. 4A). This facies is beige to yellow, porous, and well-cemented. It contains planar cracks and voids filled with microsparite. The facies consists of massive (non-laminated) tabular beds that are approximately 10–30 cm thick and alternate with laminated marlstone (facies PSL6). The facies is primarily composed of structureless layers (Fig. 5C) of homogeneous, micritic limestones that lack any fossils or intraclasts (Fig. 6C-6D).

Facies PSL3: Peloidal-brecciated-nodular wackestone is located in the upper part of the Aşağıseyit-1 section (Fig. 4A). It is beige to light yellow color, porous, and well-cemented (Fig. 5E). This facies is a texturally wackestone, with a homogeneous micritic matrix, circumgranular cracks, and micritic nodules, iron-oxide stained voids. It is heavily cracked and partly or completely filled with microsparite or sparite cement (Fig. 6F). Circumgranular cracks are common and filled with microsparite and micritic fragments (Fig. 6E) or locally stained by iron oxide (Fig. 6F). This facies is 20–40 cm thick and alternates with laminated marlstone (facies PSL6).

Facies PSL4: Ostracodal-molluscan wackestone occurs in the uppermost part of the Aşağıseyit-1 section (Fig. 4A). It is beige to yellow, porous, and well-cemented (Fig. 5D). It forms tabular beds up to 50 m thick and

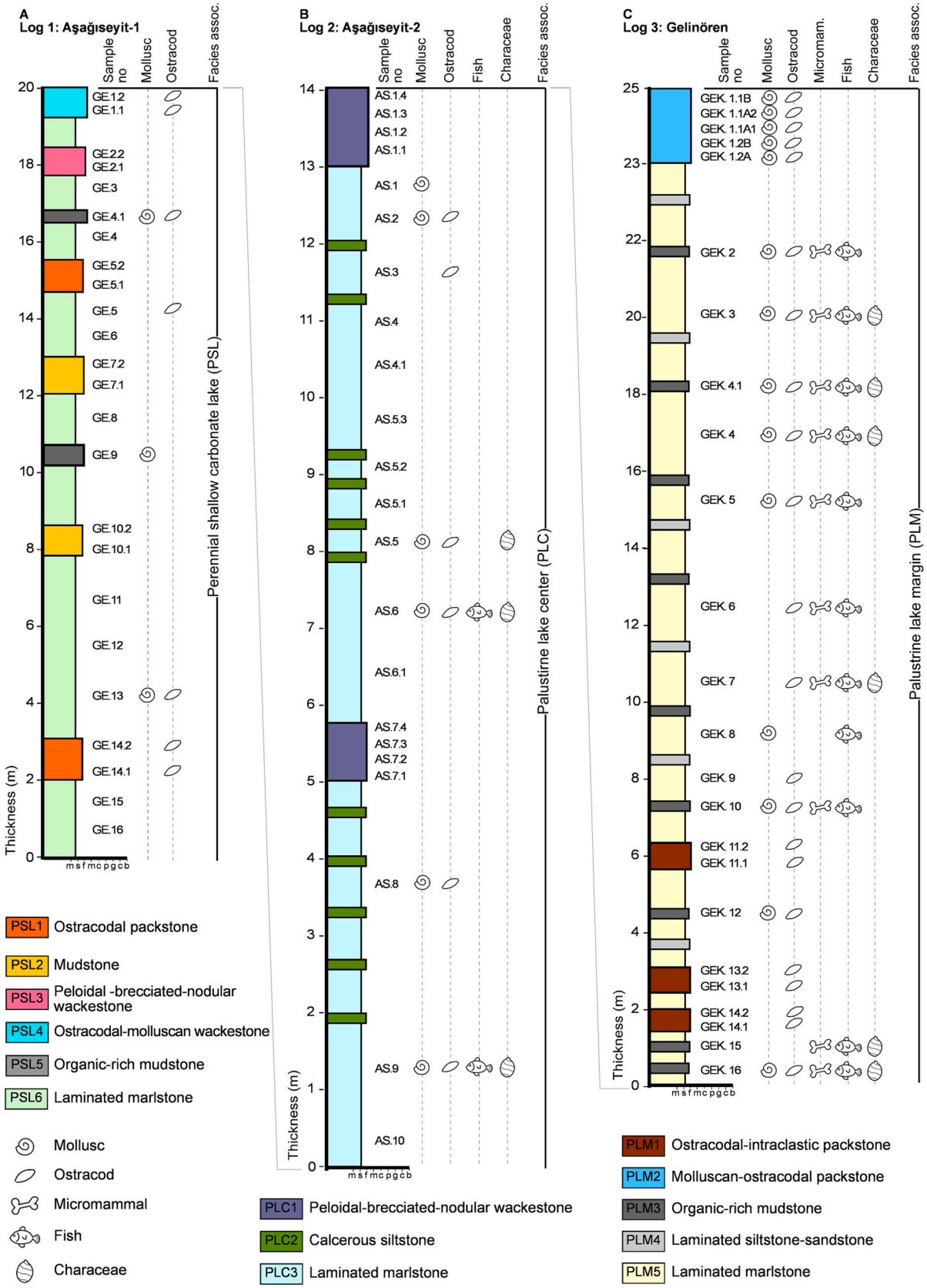

Fig. 4. Measured sedimentological sections of the studied succession: (A) Aşağıseyit-1, (B) Aşağıseyit-2, (C) Gelinören.

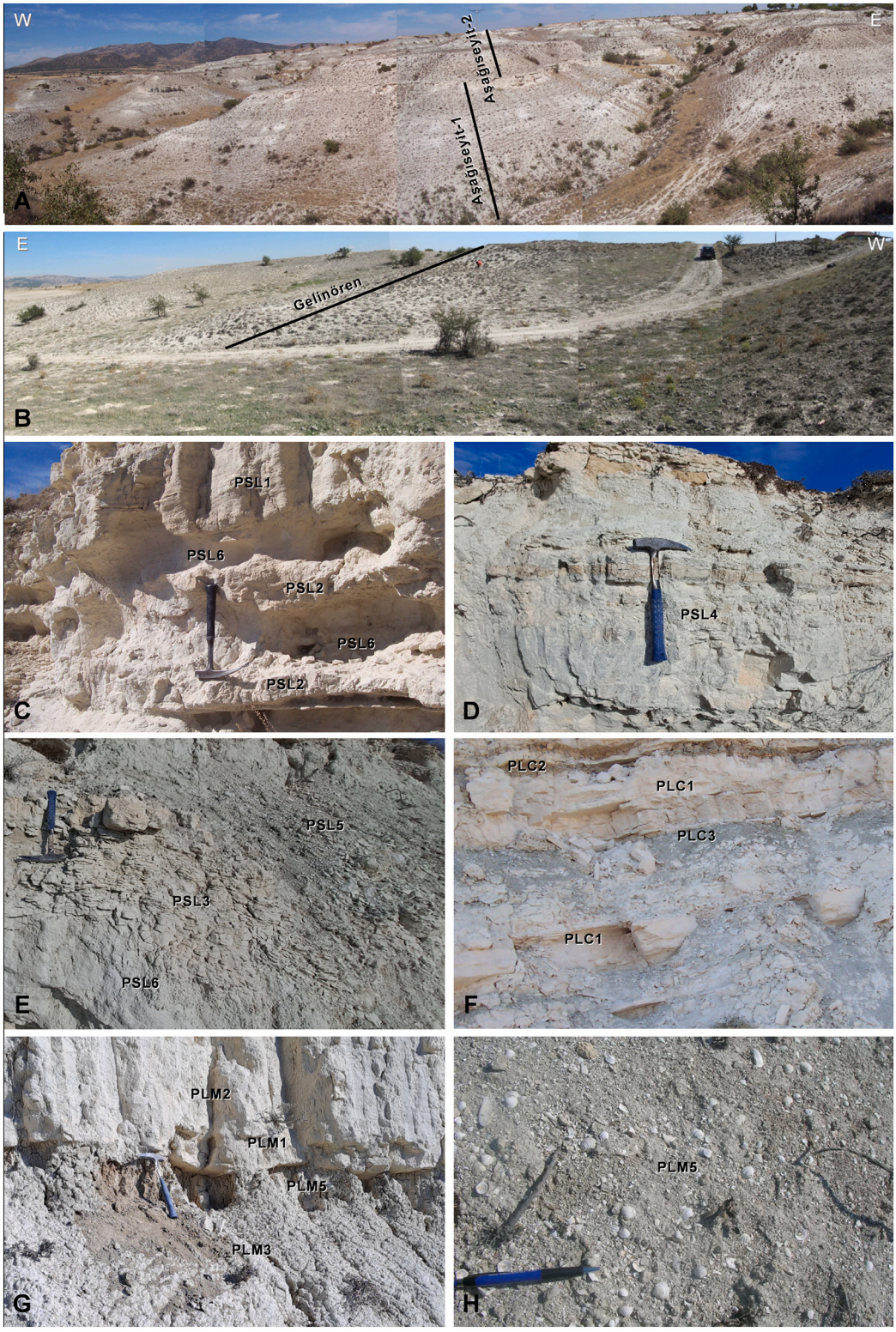

Fig. 5. (A) Outcrop photographs of Aşağıseyit-1 and -2 sections (perennial shallow lake, PSL and palustrine lake centre, PLC facies associations, respectively); (B) Outcrop photograph of Gelinören section (palustrine lake margin facies association, PLM); (C) Alternations of ostracodal packstone (PSL1), mudstone (PSL2) and laminated mudstone (PSL6) of the PSL deposits; (D) Ostracodal-molluscan wackestone (PSL4) beds of the PSL deposits; (E) Alternations of peloidal-brecciated-nodular wackestone (PSL3), organic-rich mudstone (PSL5) and laminated marlstone (PSL6) of the PSL deposits; (F) Alternations of peloidal-brecciated-nodular wackestone (PLC1), calcareous siltstone (PLC2) and laminated marlstone (PLC3) of the PLC facies association; (G) Alternations of ostracodal-intraclastic packstone (PLM1), molluscan-ostracodal packstone (PLM2), organic-rich mudstone (PLM3) and laminated marlstone (PLM5) of the PLM deposits.

alternates with laminated marlstone (facies PSL6). This facies is a texturally wackestone, composed of a micritic texture containing abundant ostracods with a minor amount of molluscs and microsparite-filled voids (Fig. 6E-6F).

Facies PSL5: Organic-rich mudstone is present in the middle and upper parts of the Aşağıseyit-1 section (Fig. 4A). It is dark brown to gray and forms tabular to slightly lenticular beds that are 10–30 cm thick (Fig. 5E). It is parallel–laminated and rarely massive. This facies alternates with laminated marlstone (PSL6). It contains ostracods [Fig. 7 (9–10), (17–20)] and molluscs (Table 1).

Facies PSL6: Laminated marlstone is found in all parts of the Aşağıseyit-1 section (Fig. 4A). This is a light-green to gray in color and forms tabular to slightly lenticular beds that are 20–40 m thick (Fig. 5E). It is parallel-laminated, rarely massive, and is intercalated with facies PSL1, PSL2, PSL3, PSL4 and, PSL5. This facies includes ostracods [Fig. 7 (9–10), (17–20);] and molluscs (Table 1).

Table 1
Summary of the facies, facies associations, and fossil contents in the studied successions of the Baklan Basin.

Facies association	Facies	Fossil content	
Palustrine lake margin (PLM) (Gelinören section)	**Facies PLM1:** Ostracodal-intraclastic packstone **Facies PLM2:** Molluscan-ostracodal packstone-grainstone **Facies PLM3:** Organic-rich mudstone **Facies PLM4:** Laminated siltstone-sandstone **Facies PLM5:** Laminated marlstone	**Ostracods** *Candona* (*Caspiolla*) *fastigata* *Ilyocypris* sp. 1 *Ilyocypris* sp. 3 *Ilyocypris* cf. *monstrifica* *Cyprideis* cf. *pontica* *Amnicythere* cf. *olivia* *Candona* ex. gr. *neglecta* **Fishes** Teleostei Cyprinoidei **Characeae** *Chara* cf. *hispida* *Chara* sp. 1 *Chara* sp. 2 *Chara* sp. 3 *Nitellopsis* (*Tectochara*) *meriani* **Micromammals** *Microtus* sp. *Meriones* sp. Murinae indet.	**Molluscs** *Laevicaspia* ?*lincta* *Monodacna imrei* *Kirelia carinata* ?*Bythinella* sp. *Bithynia pseudemmericia* *Bithynia* sp. (opercula) *Valvata cristata* *Valvata piscinalis* *Lymnaea* cf. *stagnalis* *Stagnicola palustris* *Radix* sp. *Planorbarius corneus* *Planorbis* ?*carinatus* *Gyraulus* cf. *acronicus* *Armiger crista* *Corbicula* aff. *fluminalis* *Corbicula* aff. *fluminea* *Sphaerium rivicola* *Sphaerium corneum* s.l. *Sphaerium* sp. *Pisidium amnicum* *Pisidium clessini* *Pisidium* s.l. sp. *Euglesa nitida* *Euglesa subtruncata* *Euglesa henslowana* *Euglesa ponderosa* *Odhneripisidium tenuilineatum* *Odhneripisidium moitessierianum* Unionoidea sp. indet. *Dreissena polymorpha* s.l.
Palustrine lake center (PLC) (Aşağıseyit-2 section)	**Facies PLC1:** Peloidal-brecciated-nodular wackestone **Facies PLC2:** Calcareous siltstone **Facies PLC3:** Laminated marlstone	**Ostracods** *Candona weltneri* *Heterocypris salina* *Ilyocypris* sp. 2 *Cyprideis* cf. *mehesi* *Tyrrhenocythere* sp. *Limnocythere* aff. *inopinata* *Candona decimai* *Candona* ex. gr. *neglecta* **Characeae** *Chara* cf. *hispida* *Chara* cf. *vulgaris* **Molluscs** *Laevicaspia* ?*lincta* *Bithynia pseudemmericia* *Bithynia* sp. (opercula) *Valvata cristata*	**Molluscs** *Theodoxus bukowskii* *Monodacna imrei* *Valvata piscinalis* *Lymnaea* cf. *stagnalis* *Radix* sp. *Planorbarius corneus* *Planorbis* ?*carinatus* *Gyraulus* cf. *acronicus* *Armiger crista* *Segmentina* aff. *nitida* *Corbicula* aff. *fluminea* *Pisidium amnicum* *Pisidium clessini* *Pisidium* s.l. sp. *Euglesa nitida* *Euglesa subtruncata* *Euglesa henslowana* *Odhneripisidium tenuilineatum* Unionoidea sp. indet. *Dreissena polymorpha* s.l.
Perennial shallow lake (PSL) (Aşağıseyit-1 section)	**Facies PSL1:** Ostracodal packstone **Facies PSL2:** Mudstone **Facies PSL3:** Peloidal-brecciated-nodular wackestone **Facies PSL4:** Ostracodal-molluscan wackestone **Facies PSL5:** Organic-rich mudstone **Facies PSL6:** Laminated marlstone	**Ostracods** *Cypris* cf. *pubera* *Prionocypris zenkeri*	**Molluscs** *Bithynia pseudemmericia* *Valvata cristata* *Planorbarius corneus* *Planorbis* cf. *carinatus* *Gyraulus* ?*acronicus*

Interpretation – Dolomitic limestone-dolostone–marlstone–mudstone alternations of the PSL association are thought to be the deposits of low-gradient, shallow lacustrine setting. The prevalence of carbonates (facies PSL1 to PSL4) with mudstone-wackestone-packestone textures suggests sedimentation in shallow lakes with fluctuating water level (Alonso-Zarza and Wright, 2010). The lack of subaerial exposure features indicates that facies PSL1, PSL2, and PSL4 are fully subaqueous lacustrine in origin. However, pedogenic features such as brecciation, nodularization, cracking of the facies PSL3 imply that marginal lake areas were frequently subaerially exposed (Freytet and Plaziat, 1982). Brecciated carbonate facies (PSL3) indicate short-term subaerial exposure, and thus, they developed by weak pedogenic processes (Alonso-Zarza and Wright, 2010). Such carbonates are thought to result from desiccation-related processes of original lacustrine wackestone. Facies

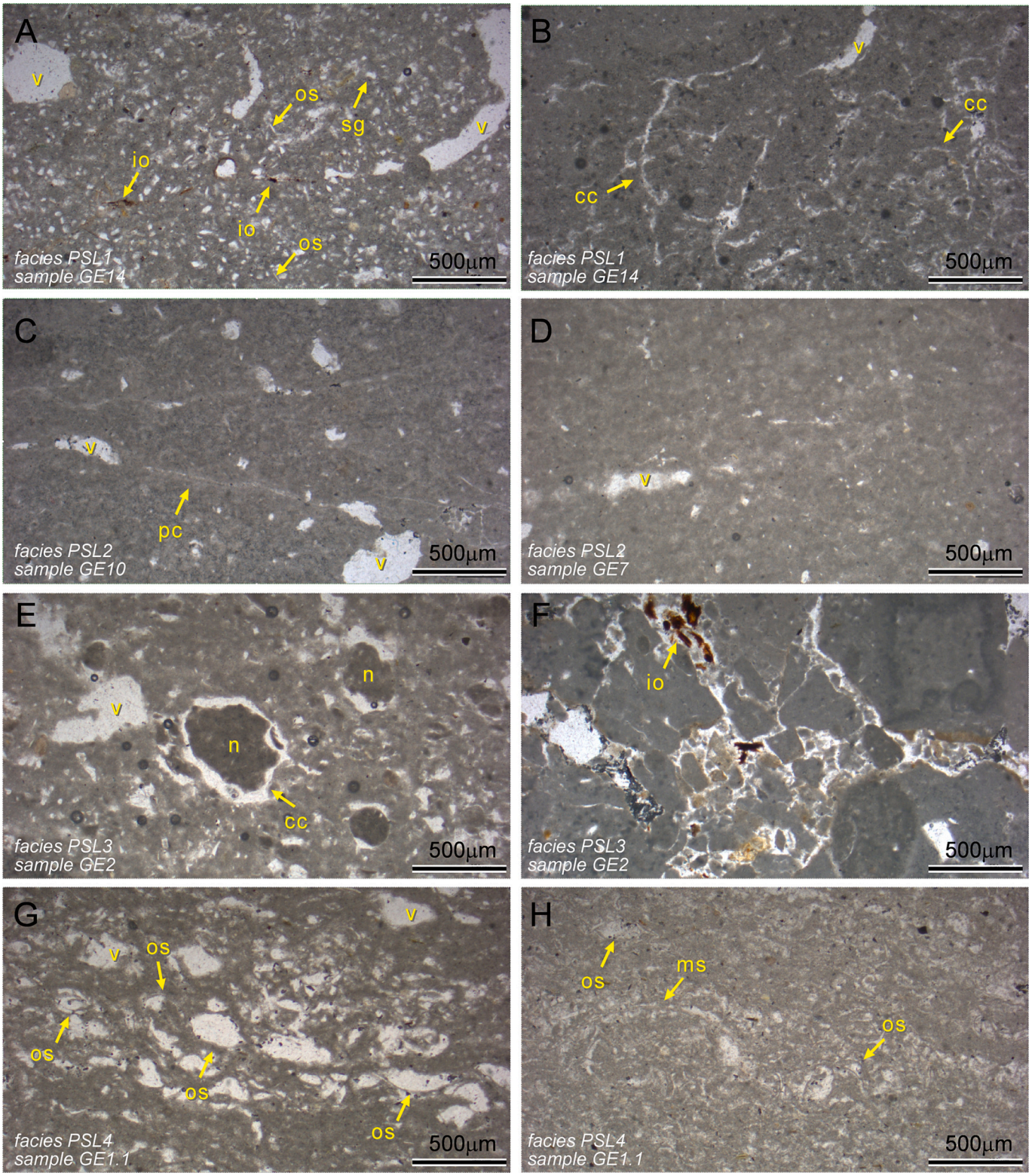

Fig. 6. Microphotographs of shallow lake facies association (PSL): (A-B) ostracodal packstone (PSL1) including ostracods (os), siliciclastic grains (sg), iron-oxide stained (io) voids (v), and circumgranular cracks (cc); (C-D) mudstone (PSL2) containing planar cracks (cc) and voids (v); (E-F) peloidal-brecciated-nodular wackestone (PSL3) including circumgranular cracks (cc), nodules (n), and iron-oxide (io) stained voids (v); (G-H) ostracodal-molluscan wackestone (PSL4) containing ostracods (os), molluscs (ms), and voids (v).

PSL5 represents muddy suspension fallout deposition in the low-energy proximal lacustrine settings, while facies PSL6 reflects mixed terrigenous and carbonate sedimentation in the deeper lacustrine zones.

4.2.2. Palustrine lake center facies association (PLC)

The PLC facies association occurs in the middle part of the studied succession (Fig. 3) (Aşağıseyit-2 section, Fig. 4B). These deposits are particularly well exposed in the northern part of the basin (Fig. 2). It is

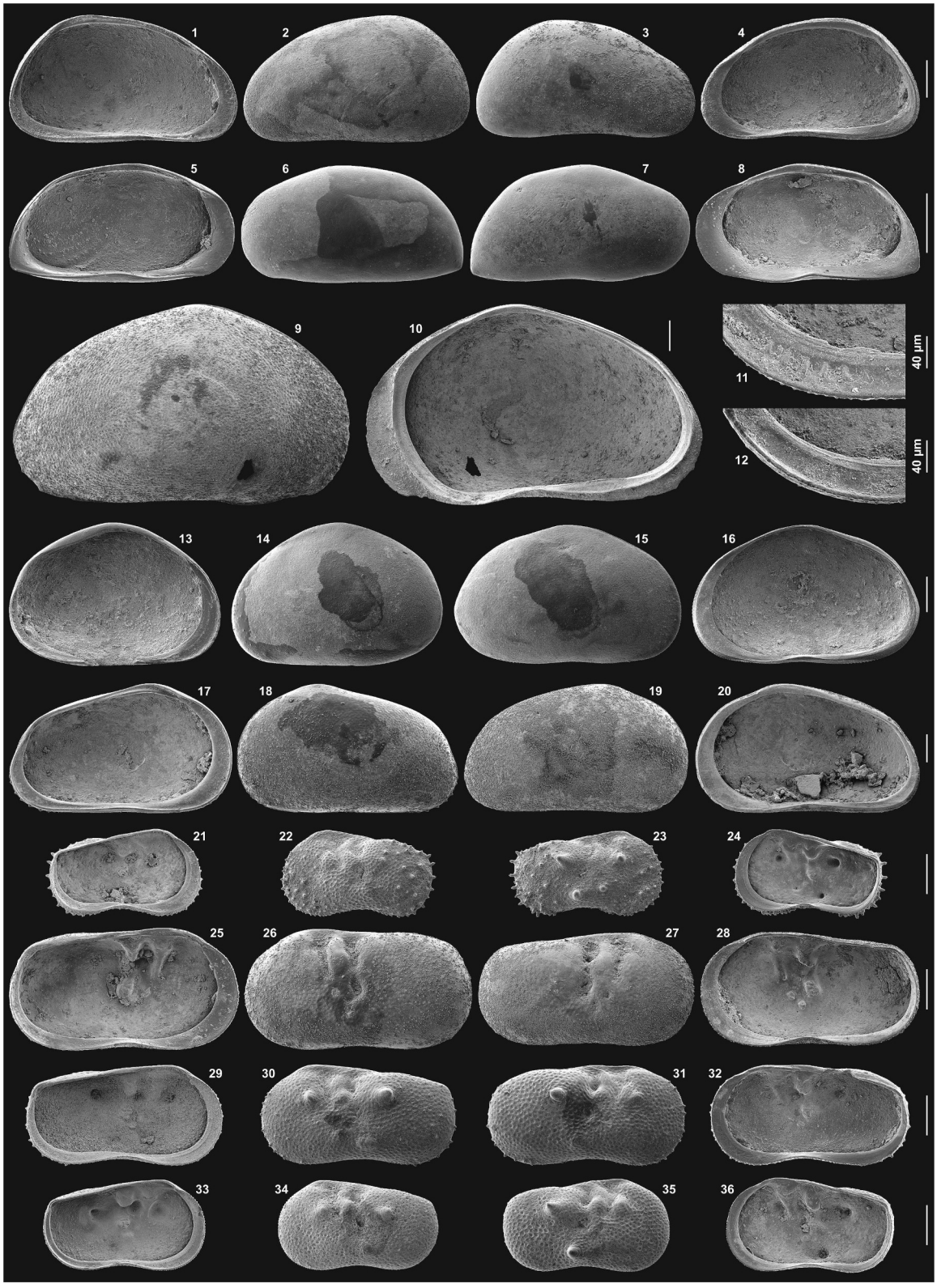

Fig. 7. Ostracods of the perennial shallow lake (PSL, GE samples), palustrine lake center (PLC, AS samples) and palustrine lake margin (PLM, GEK samples) deposits: (1–4) *Candona weltneri*; 1 = Lf, i, 1.22/0.69, AS.9; 2 = 1, e; 3 = Rf, e, 1.13/0.61, AS.9; 4 = Rf, i, 1.25/0.70, AS.9; (5–8) *Candona* (*Caspiolla*) *fastigata*; 5 = Lm, i, 0.75/0.40, GEK.5; 6 = 5, e; 7 = R, e, 0.74/0.40, GEK.5; 8 = 7, e; (9–10) *Cypris* cf. *pubera*; 9 = R, e, 2.21/1.33, GE.5; 10 = 9, i; (11) *Ilyocypris* sp. 1; 11 = L, i, GEK.3, detail of posteroventral margin; (12) *Ilyocypris* sp. 3; 12 = L, i, GEK.9, detail of posteroventral margin; (13–16) *Heterocypris salina*; 13 = L, i, 1.20/0.81, AS.5; 14 = 13, e; 15 = R, e, 1.29/0.79, AS.5; 16 = 15, i; (17–20) *Prionocypris zenkeri*; 17 = L, i, 1.58/0.92, GE.5; 18 = 17, e; 19 = R, e, 1.60/0.92, GE.5; 20 = 19, i; (21–24) *Ilyocypris* cf. *monstrifica*; 21 = L, i, 0.75/0.44, GEK.3; 22 = 21, e; 23 = R, e, 0.74/0.42, GEK.3; 24 = 23, i; (25–28) *Ilyocypris* sp. 1; 25 = L, i, 1.14/0.61, GEK.3; 26 = 25, e; 27 = R, e, 1.08/0.57, GEK.3; 28 = 27, i; (29–32) *Ilyocypris* sp. 2; 29 = L, i, 0.97/0.58, AS.5; 30 = 29, e; 31 = R, e, 0.99/0.51, AS.5; 32 = 31, i; (33–36) *Ilyocypris* sp. 3; 33 = L, i, 0.81/0.45, GEK.3; 34 = 33, e; 35 = R, e, 0.84/0.47, GEK.9; 36 = 35, i. (abbreviations: L = left valve, R = right valve; f = female, m = male; e = lateral view extern, i = lateral view intern; measurements in mm (e.g., 0.89/0.49 = 0.89 mm length, 0.49 mm height); scale bar for each row = 0.2 mm).

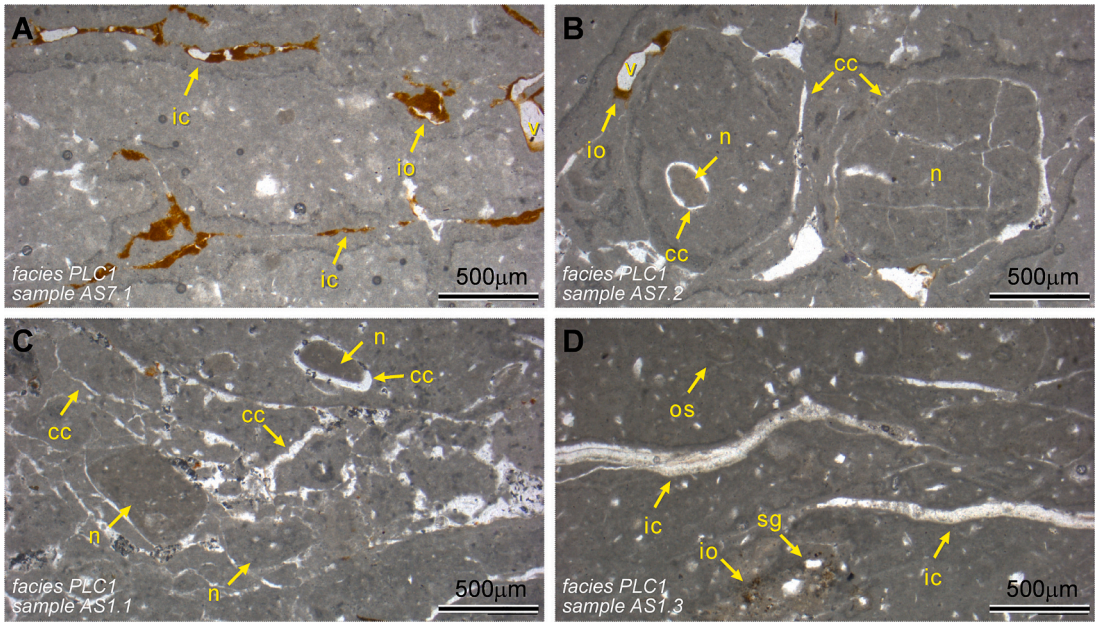

Fig. 8. Microphotographs of palustrine lake centre facies association (PLC): (A-D) Peloidal-brecciated-nodular wackestone (PLC1) including iron-oxide (io) stained irregular cracks (ic) and voids (v), micritic nodules (n), circumgranular cracks (cc), ostracods (os), and siliciclastic grains (sg).

predominantly composed of peloidal-brecciated-nodular wackestone (facies PLC1), calcareous siltstone (facies PLC2), and laminated marlstone (facies PLC3) alternations (Table 1). This association is up to 14 m thick and extends laterally for tens of meters (Fig. 5A). The association passes upward into the palustrine lake margin facies association (PLM).

Facies PLC1: Peloidal-brecciated-nodular wackestone is found in the upper part of the Aşağıseyit-2 section (Fig. 4B). This facies is beige to yellow in color and forms compact, tabular beds up to 100 cm thick (Fig. 5F). It consists of wackestones with rounded micritic nodules (0.2–0.5 mm in diameter), ostracods, siliciclastic grains, iron-oxide stained irregular cracks and voids, and circumgranular cracks (Fig. 8A-8D). Irregular and circumgranular cracks and voids are common in open or partially filled areas with microsparite/sparite cement or iron oxide (Fig. 8A-8D). This facies is intercalated with facies PLC2 and PLC3.

Facies PLC2: Calcareous siltstone is present in all levels of the Aşağıseyit-2 section (Fig. 4B). It is beige to yellow in color (Fig. 5F) and composed of quartz grains with a minor amount of feldspar. It displays planar parallel lamination and the beds are up to 5 cm thick, alternating with facies PLC1 and PLC3.

Facies PLC3: Laminated marlstone occurs in all parts of the Aşağıseyit-2 section (Fig. 4B). It is beige to light-gray in color and forms in tabular to slightly lenticular beds 50–200 cm thick (Fig. 5F). This facies is parallel-laminated, occasionally massive, and includes circumgranular cracks, plant detritus, and root casts (0.5–2.0 cm in length). These deposits are rich in ostracods [Fig. 7 (1–4, 13–16, 29–32) and Fig. 9 (1–4, 9–12, 17–40)], molluscs [Fig. 10 (a, c, j, l-n)], and Characeae [Fig. 11 (a-c)] (Table 1). The facies is intercalated with facies PLC1 and PLC2.

Interpretation – Dolomitic limestone-dolostone-marlstone-siltstone alternations of the PLC association are interpreted as palustrine deposits. The predominance of PLC1 carbonates with wackestone textures indicates palustrine sedimentation in shallow lakes with fluctuating water levels (Alonso-Zarza, 2003; Alonso-Zarza and Wright, 2010). Pedogenic features of the facies PLC1 and PLC3 (i.e., brecciation, nodularization, and cracking) reflect that the lake areas were often subaerially exposed, favoring palustrine deposits (Freytet and Plaziat, 1982). The presence of well preserved Characeae gyrogonites in the PLC3 deposits also supports a deposition formed under low-energy conditions at the margin of a shallow lake (usually depths of less than 10 m) (Anadón et al., 2000; Lettéron et al., 2018). Facies PLC2 indicate the contribution of terrigenous fine-grained deposits by sheetfloods in the marginal lake areas, whereas facies PLC3 is interpreted as settling out of carbonate and fine-grained terrigenous deposits during the relatively high lake level intervals.

4.2.3. *Palustrine lake margin facies association (PLM)*

These deposits form the upper part of the studied succession (Gelinören section, Fig. 4C) and are well exposed in the basin's northern part (Fig. 2). This assemblage conformably overlies the PLC facies association and consists of alternating ostracodal-intraclastic packstone (facies PLM1), molluscan-ostracodal packstone-grainstone (facies PLM2), organic-rich mudstone (facies PLM3), laminated siltstone-sandstone (facies PLM4), and laminated marlstone (facies PLM5) (Table 1). These deposits are up to 25 m thick and extend laterally over tens of meters (Fig. 5B).

Facies PLM1: Ostracodal-intraclastic packstone occurs in the lower part of the Gelinören section (Fig. 4C). This facies is beige to yellow in color and forms compact, tabular beds up to 50 cm thick (Fig. 5F). This facies is a texturally packestone, with a homogeneous micritic matrix, containing ostracods, siliciclastic grains, irregular and circumgranular cracks, and iron-oxide stained voids (Fig. 12A-C). The planar and circumgranular cracks are locally filled with microsparite and iron-oxide. This facies is up to 50 cm thick and alternated with facies PLM3, PLM4, and PLM5.

Facies PLM2: Molluscan-ostracodal packstone-grainstone is found in the uppermost part of the Gelinören section (Fig. 4C). It is texturally packestone-grainstone, with a homogeneous micritic-microsparitic matrix, charophyte stems, molluscs, ostracods, pellets, oncoids, voids, siliciclastic grains, intraclast fragments, and iron-oxide stained voids (Fig. 12D-F). This facies is up to 100 cm thick and alternated with facies PLM5.

Facies PLM3: Organic-rich mudstone occurs in all parts of the Gelinören section (Fig. 4C). This facies is dark brown to gray and forms tabular to slightly lenticular beds that are 15–30 cm thick (Fig. 5G). It is parallel–laminated and rarely massive. This facies includes decimeter- to centimeter-scale mudcracks, macrophytic detritus, and elongated micrite casts (1–5 cm in length). The mollusc-bearing layers contain three micromammals (*Meriones* sp., Murinae indet., and the arvicoline

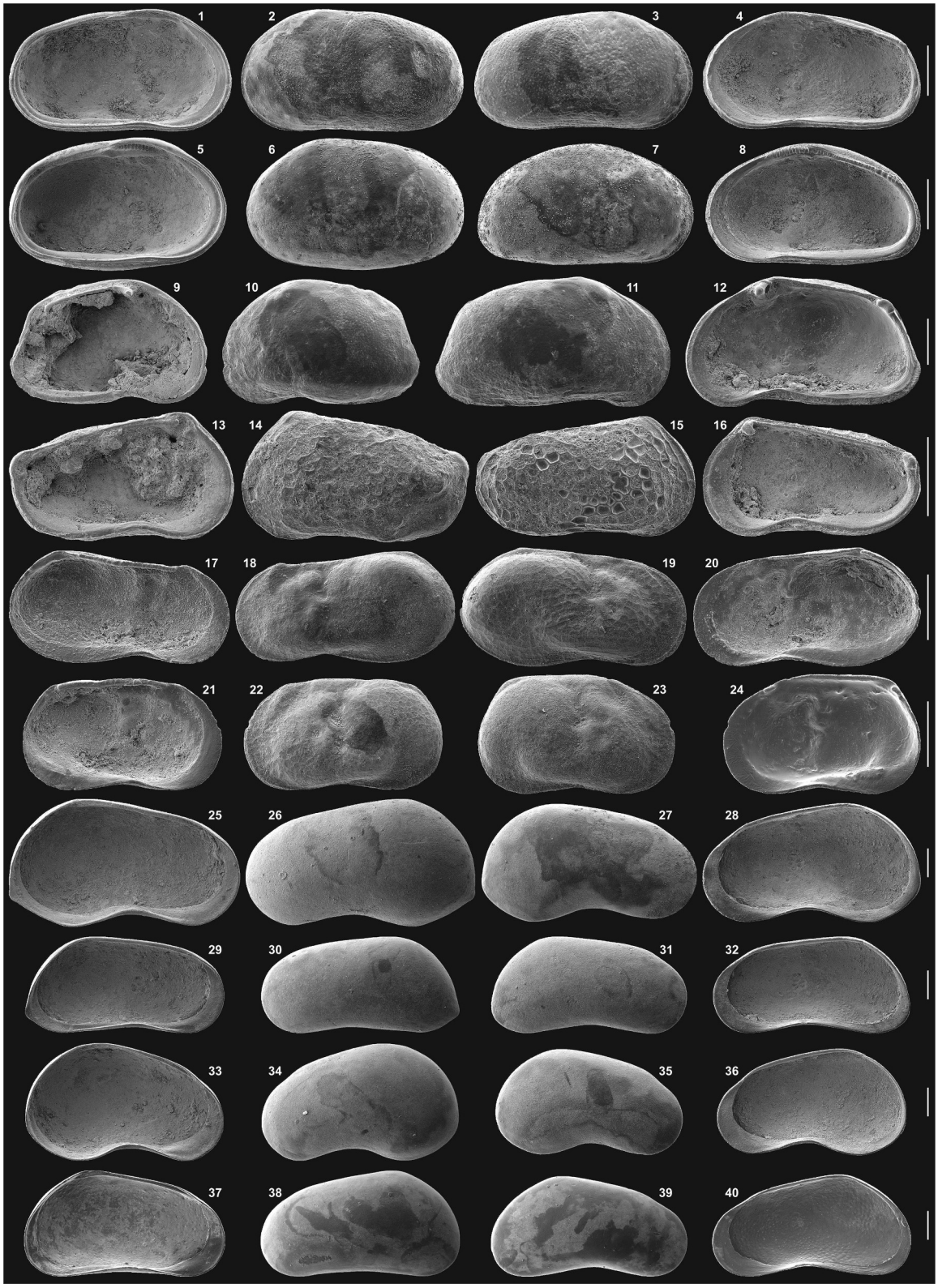

Fig. 9. Ostracods of the palustrine lake center (PLC, AS samples) and palustrine lake margin (PLM, GEK samples) deposits: (1–4) *Cyprideis* cf. *mehesi*; 1 = Lf, i, 0.89/0.49, AS.3; 2 = 1, e; 3 = Rf, e, 0.87/0.47, AS.3; 4 = 3, i; (5–8) *Cyprideis* cf. *pontica*; 5 = Lf, i, 0.87/0.53, GEK.7; 6 = 5, e; 7 = Rf, e, 0.86/0.49, GEK.7; 8 = 7, i; (9–12) *Tyrrhenocythere* sp.; 9 = Lf, i, 0.86/0.54, AS.2; 10 = 9, e; 11 = Rm, e, 1.02/0.57, AS.2; 12 = 11, i; (13–16) *Amnicythere* cf. *olivia*; 13 = L, i, 0.58/0.33, GEK.9; 14 = 13, e; 15 = R, e, 0.56/0.31, GEK.9; 16 = 15, i; (17–24) *Limnocythere* aff. *inopinata*; 17 = Lm, i, 0.67/0.34, AS.5; 18 = 17, e; 19 = Rm, e, 0.69/0.36, AS.5; 20 = 19, i; 21 = Lf, i, 0.61/0.34, AS.5; 22 = 21, e; 23 = Rf, e, 0.64/0.39, AS.5; 24 = 23, i; (25–32) *Candona decimai*; 25 = Lm, i, 1.60/0.89, AS.5; 26 = 25, e; 27 = Rm, e, 1.50/0.83, AS.5; 28 = 27, i; 29 = Lf, i, 1.38/0.67, AS.5; 30 = 29, e; 31 = Rf, e, 1.37/0.67, AS.5; 32 = 31, i; (33–40) *Candona* ex. gr. *neglecta*; 33 = Lm, i, 1.38/0.82, AS.5; 34 = 33, e; 35 = Rm, e, 1.31/0.74, AS.5; 36 = 35, i; 37 = Lf, i, 1.39/0.74, GEK.4.1; 38 = 37, e; 39 = Rf, e, 1.37/0.70, GEK.4.1; 40 = 39, i Abbrev: see Fig. 7.

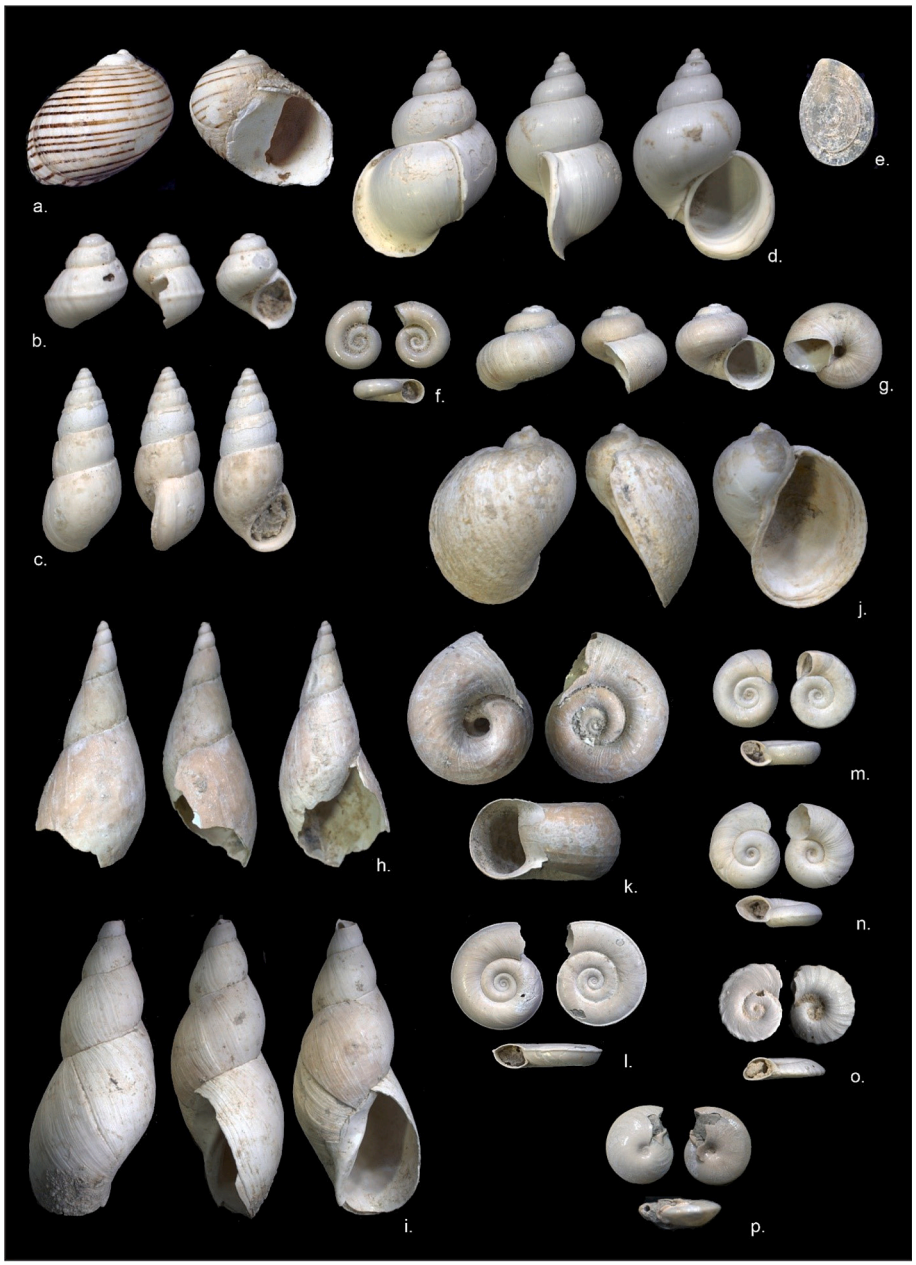

Fig. 10. Molluscs of the palustrine lake center (PLC, AS samples) and palustrine lake margin (PLM, GEK samples) deposits: (a) RGM.1310373. *Theodoxus bukowskii*. Collected from surface of badland, 550 m N of Aşağıseyit village, 38°03′56″N, 29°28′51″E. W 6.8 mm. (b) RGM.1310363. *Kirelia carinata*. GEK5. H 1.3 mm. (c) RGM.1310366. *Laevicaspia* ?*lincta*. AS2. H5.8 mm. (d) RGM. 1310357. *Bithynia pseudemmericia*. GE4.1, GEK6. H 13 mm. (e) RGM.1310358. *Bithynia* sp. operculum. GEK6. L 4.2 mm. (f) RGM.1310372. *Valvata cristata*. GEK6. W 2.4 mm. (g) RGM.1310364. *Valvata piscinalis*. GEK5. W 5.8 mm. (h) RGM.1310362. *Lymnaea* cf. *stagnalis*. GEK5. H 14 mm. (i) RGM.1310355. *Stagnicola palustris*. GEK5. H 33 mm. (j) RGM.1310369. *Radix* sp. AS2. H 10.5 mm. (k) RGM.1310361. *Planorbarius corneus*. GEK5. W 12.5 mm. (l) RGM.1310365. *Planorbis* cf. *carinatus*. AS2. W 9 mm. (m) RGM.1310368. *Gyraulus* cf. *acronicus*. AS2. W 5.7 mm. (n) RGM.1310367. *Gyraulus* ?*acronicus*. AS2. W 4.7 mm. (o) RGM.1310371. *Armiger crista*. GEK1. W 1.8 mm. (p) RGM.1310370. *Segmentina* aff. *nitida*. GEK6. W 1.7 mm.

Microtus sp.; Table 1).

Facies PLM4: Laminated siltstone-sandstone is also found in all parts of the Gelinören section (Fig. 4C). It is beige to yellow, fine- to medium-grained, and well-sorted, forming beds that are 15–25 cm thick. The beds are composed of siliciclastic grains and exhibit planar parallel lamination that is locally disrupted by vertical and horizontal tubes about 2 mm wide and 3 cm long. The tubes are generally filled with micrite or microspar. This facies alternates with facies PLM1, PLM2, and PLM5.

Facies PLM5: Laminated marlstone occurs in all parts of the Gelinören section (Fig. 4C). This facies is light to dark greenish-gray in color and constitute in tabular or lenticular beds that are 10–50 cm thick. This facies is parallel-laminated and only locally massive. It contains mud-cracks, plant detritus, and root casts (0.5–2.0 cm long). These deposits are very rich in ostracods [Fig. 7 (5–8, 11–12, 21–28, 33–36) and Fig. 9 (5–8, 13–16)], molluscs [Fig. 10 (b, d-i, k, o-p) and Fig. 13 (a-r)], Characeae [Fig. 11 (b, d-g)], and fishes [Fig. 14 (a-k)] (Table 1). This facies is intercalated with facies PLM1, PLM2, and PLM4.

Interpretation – Dolomitic limestone-dolostone–marlstone–siltstone-sandstone-mudstone alternations of the PLM association are thought to be the deposits of marginal areas of palustrine setting. The predominance of packstone textures PLM1 and PLM2 carbonates is typically characteristic of low-energy, palustrine lake conditions (Alonso-Zarza et al., 2011). Pedogenic features, such as brecciation and cracking, suggest periodic episodes of subaerial exposure in the palustrine settings (Alonso-Zarza, 2003). Facies PLM3 reflects a low-energy environment dominated by muddy suspension fallout, whereas facies PLM4 is interpreted as the supply of terrigenous fine-grained deposits by sheetfloods or very gently incised channels in terminal zones in the marginal lake zones. Facies PLM5 reflects the deposition of transitional siliciclastic/carbonate mudflats in the marginal areas. The presence of well preserved Characeae gyrogonites in the PLM2 and PLM5 facies indicates shallow water depths (< 10 m) with low-energy conditions, favoring the growth of the green algae (Anadón et al., 2000; Lettéron et al., 2017).

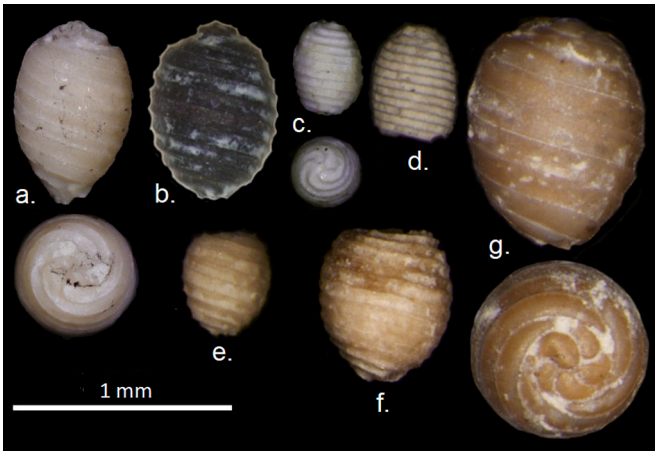

Fig. 11. *Characeae* of the palustrine lake center (PLC, AS samples) and palustrine lake margin (PLM, GEK samples) deposits. (a–b) *Chara* cf. *hispida*, (a) G (AS.9), above LV, below AV, (b) O (GEK.7), LV. (c) *Chara* cf. *vulgaris*, G (AS.9), above LV, below AV. (d) *Chara* sp. 1, G (GEK.4), LV. (e) *Chara* sp. 2., G (GEK.4), LV. (f) *Chara* sp. 3, (GEK.3) G, LV. (g) *Nitellopsis* (*Tectochara*) *meriani*, (GEK.3) G, above LV, below AV. Abbrev.: Gyrogonite (G), oospore (O), lateral view (LV), apical view (AV).

4.3. Mineralogy and stable isotope geochemistry

The mineralogy and stable isotopic composition of lacustrine carbonates and fossil molluscs have been widely used to reconstruct paleosalinity and paleotemperature of lake waters, making them a powerful tool for paleolimnological studies (e.g., Leng and Marshall, 2004). The mineralogical and $\delta^{18}O$ and $\delta^{13}C$ isotope compositions of carbonate samples from three stratigraphic associations in the studied successions are listed in Table 2 and shown in Fig. 15A-15B.

XRD analyses indicate that the lower PSL deposits consist of 23% dolomite and 8% calcite with a rich admixture of siliciclastic minerals (42% clay minerals, 12% mica, 9% aragonite, 3% quartz, 3% feldspar). Carbonate samples of these deposits show mostly positive $\delta^{18}O$ values (+0.28 to +4.08‰, mean = +2.76‰ for calcite and +1.70 to +4.09‰, mean = +2.89‰ for dolomite). The $\delta^{13}C$ values are negative and slightly variable (−4.60 to −1.67‰, mean = −3.19‰ for calcite and −3.10 to −1.03‰, mean = −2.35‰ for dolomite) (Table 2; Fig. 15A). The stable isotope values of molluscs of the PSL deposits exhibit similar $\delta^{18}O$ values (+0.88 to +4.10‰, mean = +2.70‰) and $\delta^{13}C$ values (−3.37 to +0.94‰, mean = −1.70‰) (Table 3; Fig. 15B).

The middle PLM deposits include 19% dolomite and 13% calcite and siliciclastic minerals (40% clay minerals, 13% mica, 6% aragonite, 5% feldspar, 4% quartz). Carbonate deposits of these deposits exhibit positive to slightly negative $\delta^{18}O$ values (−2.03 to +3.87‰, mean = +1.22‰ for calcite and −1.35 to +3.92‰, mean = +1.37‰ for

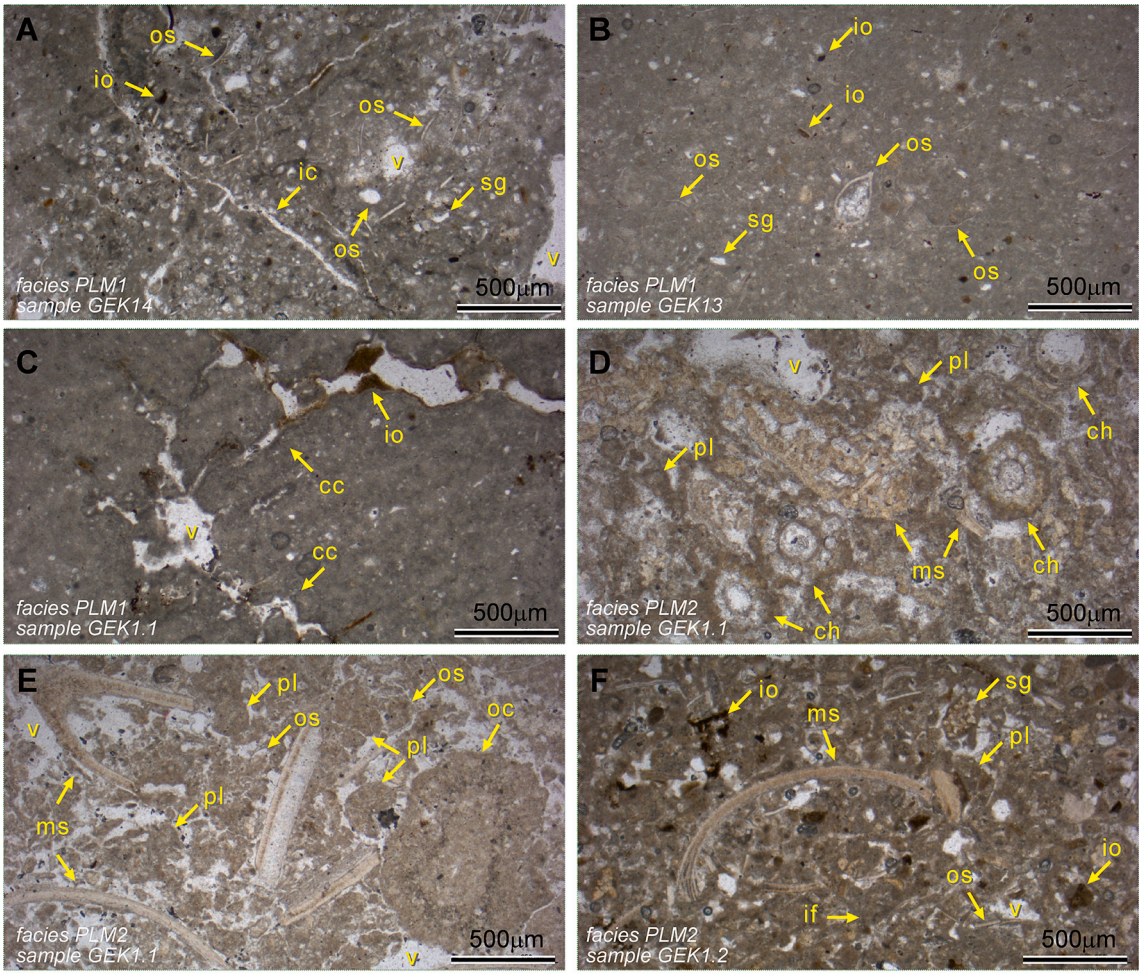

Fig. 12. Microphotographs of palustrine lake margin facies association (PLM) (A-C) Ostracodal-intraclastic packstone (PLM1) contaning ostracods (os), siliciclastic grains (sg), irregular (ic) and circumgranular cracks (cc), and iron-oxide (io) stained voids (v); (D-F) Molluscan-ostracodal packstone-grainstone (PLM2) including charophytes (ch), molluscs (ms), ostracods (os), pellets (pl), oncoids (oc), voids (v), siliciclastic grains (sg), intraclast fragments (if), and iron-oxide (io) stained voids (v).

Fig. 13. Molluscs of the palustrine lake margin deposits (PLM, GEK samples): (a) PAUT.GEK2 *Monodacna imrei* (paratype). GEK2. W 22 mm. (b) RGM. 1310356. *Dreissena polymorpha* s.l. GEK5. L 33 mm. (c) RGM.1310360. *Corbicula* aff. *fluminalis*. GEK1. W 16.5 mm. (d) RGM.1310359. *Corbicula* aff. *fluminea*. GEK5. W 20.5 mm. (e) RGM.1310341. *Sphaerium rivicolum*. GEK5. W 17 mm. (f) RGM.1310342. *Sphaerium corneum*. GEK5. W 7.3 mm. (g) RGM.131043. *Pisidium amnicum*. GEK5. W. 7.5 mm. (h) RGM.131044. *Pisidium amnicum*. GEK5. W. 7.5 mm. (i) RGM.1310353. *Pisidium* cf. *clessini*. GEK13. W 6.2 mm. (j) RGM.1310354. *Pisidium* cf. *clessini*. GEK13. W. 5.3 mm. (k) RGM.1310347. *Euglesa nitida*. GEK5. W 2.4 mm. (l) RGM.1310348. *Euglesa nitida*. GEK5. W 2.4 mm. (m) RGM.1310345. *Euglesa subtruncata*. GEK5. W 3.2 mm. (n) RGM.1310346. *Euglesa henslowana*. GEK5. W 3.3. mm. (o) RGM.1310352. *Euglesa henslowana*. GEK13. W 6.2 mm. (p) RGM.1310351. *Euglesa ponderosa*. GEK4.2. W. 3.3 mm. (q) RGM. 1310350. *Odhneripisidium tenuilineatum*. GEK5. W 1.4 mm. (r) RGM.1310349. *Odhneripisidium moitessierianum*. GEK4.1. W 1.8 mm.

dolomite). The $\delta^{13}C$ values are negative and slightly variable (−5.31 to −0.81‰, mean = −3.74‰ for calcite and −5.71 to −3.84‰, mean = −4.74‰ for dolomite) (Table 2; Fig. 15A). The stable isotope values of molluscs of the PLC deposits show similar $\delta^{18}O$ values (−1.20 to +4.37‰, mean = −1.82‰) and $\delta^{13}C$ values (−8.19 to +0.92‰, mean = −4.53‰) (Table 3; Fig. 15B).

The upper PLM deposits are composed of 24% calcite and 9% dolomite with a significant amount of siliciclastic minerals (43% clay minerals, 10% mica, 6% aragonite, 5% quartz, 3% feldspar). Carbonate samples of these deposits have negative $\delta^{18}O$ values (−6.20 to −0.67‰, mean = −3.03‰ for calcite and −5.55 to −0.20‰, mean = −2.78‰ for dolomite) and negative $\delta^{13}C$ values (−8.45 to −0.75‰, mean = −3.97‰ and −6.44 to −0.87‰, mean = −3.11‰ for dolomite) (Table 2; Fig. 15A). The stable isotope values of molluscs of the PLM deposits also show broad variations ($\delta^{18}O$ values from −6.31 to +5.49‰, mean = −0.27‰ and $\delta^{13}C$ values from −9.13 to +2.80‰, mean = −4.83‰; Table 3; Fig. 15B).

Interpretation – The high $\delta^{18}O$ values of the PSL and PLC carbonates indicate evaporative enrichment of $\delta^{18}O$ in the lake water, while the low $\delta^{18}O$ values in the lower part of the PLM deposits suggest a flux of isotopically light, ^{18}O-depleted meteoric water (Leng and Marshall, 2004). The negative $\delta^{13}C$ values in all deposits imply the input of isotopically light CO_2 resulting from biological processes related to the pond vegetation or organic matter decay (Talbot and Kelts, 1990; Leng and Marshall, 2004).

5. Discussion

5.1. Paleoecology and paleobiogeography

5.1.1. Micromammals

The palustrine marginal lake deposits (PLM) of the Gelinören section (Fig. 4C) contain the micromammal fauna *Microtus* sp., *Meriones* sp., and Murinae indet. (Table 1). This fauna comprises open-steppe genera,

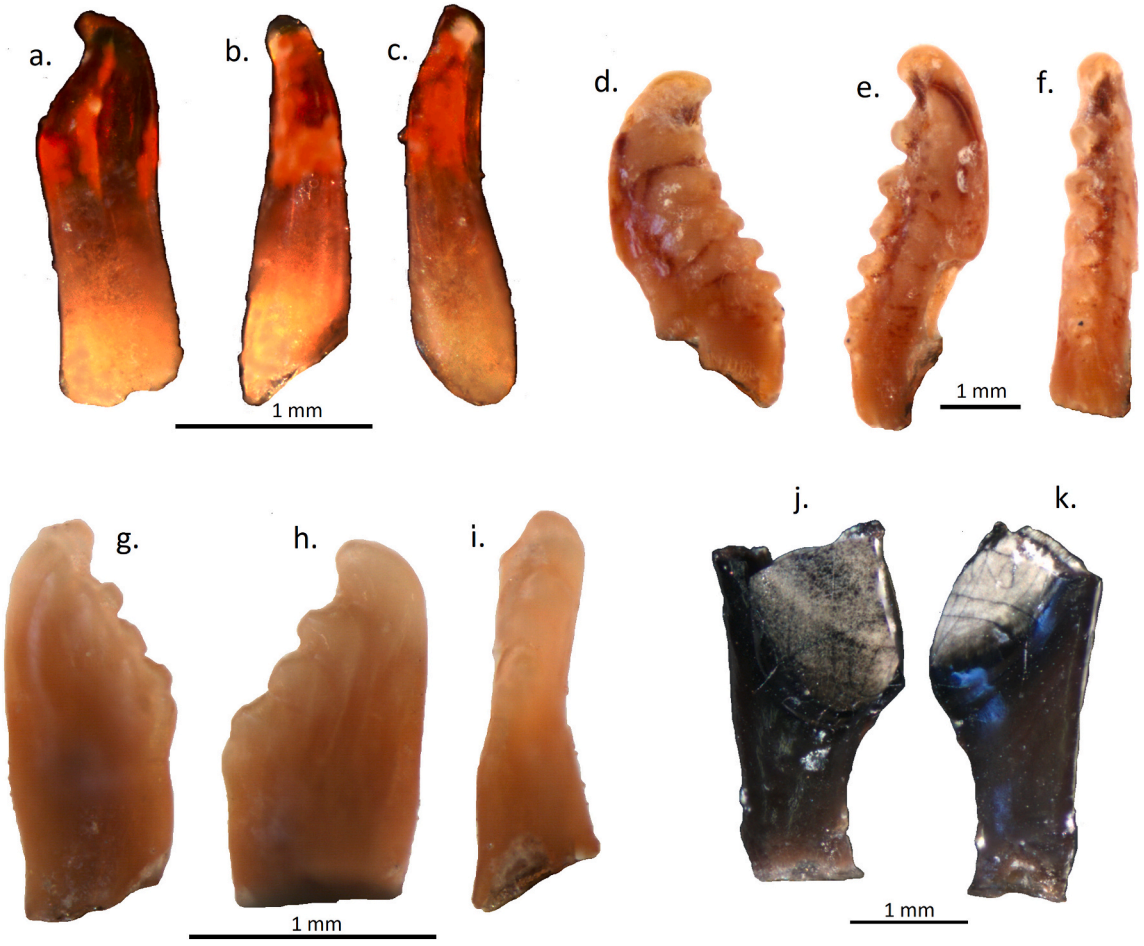

Fig. 14. Fish teeth from the palustrine lake margin (PLM, GEK samples) deposits. (a–c) Morphotype A, from locality GEK 7, Teleostei indeterminate in a, lateral, b, posterior and c, anterior views. (d–f) Morphotype B, from locality GEK 2, Cyprinoidei, in d, posterolateral, e. lateral, and f. posterior views. (g–i) Morphotype B, from locality GEK 7, Cyprinoidei, in g, h, right and left lateral views, and i, posterior view. (j–k) Morphotype C, from locality GEK 5, Cyprinoidei, in two views.

including extant Palearctic forms (Table 4). Wesselingh and Alçiçek (2010) previously reported the presence of *Pseudomeriones tchaltaensis* in the Gelinören section. However, re-examination of the specimen identified as *Pseudomeriones tchaltaensis* revealed that it was actually a very hypsodont M2 of a gerbil that cannot be attributed to *Pseudomeriones*. Therefore, *Pseudomeriones tchaltaensis* is now reclassified as *Meriones* sp. The genera *Microtus* and *Meriones* are both extant in Anatolia and have been found together in the Pleistocene localities in Greece (Kuss and Storch, 1978) and western Turkey (Storch, 1988). The presence of *Microtus* suggests that the Gelinören section is much younger than previously assumed by Wesselingh and Alçiçek (2010) and is therefore of Middle-Late Pleistocene age (Biharian-Toringian, MNQ1-Q2; Fig. 3).

5.1.2. Ostracods

Three samples from the perennial shallow lake deposits (PSL association, Aşağıseyit-1 section, Fig. 4A), six samples from the palustrine lake center deposits (PLC association, Aşağıseyit-2 section, Fig. 4B), and twelve samples from the palustrine lake margin deposits (PLM association, Gelinören section, Fig. 4C) were investigated for their ostracod content and yielded a total of 16 species (Figs. 7 and 9; Table 1) Most ostracod valves are well preserved, and species are usually represented by both adult and juvenile stages.

The three samples from the perennial shallow lake deposits (Table 1) yielded a poor ostracod fauna (3 taxa, 31 valves) indicative of a shallow freshwater environment, such as a lake or slow-flowing stream. Among the recovered ostracod species of the palustrine lake center and palustrine lake margin deposits (Table 1), *Cyprideis* spp., *Tyrrhenocythere* sp., *Amnicythere* cf. *olivia* (Livental, 1938), and *Candona* (*Caspiolla*) *fastigata* (Freels, 1980) are commonly found in brackish (mainly oligo– to mesohaline) waters. Presumed freshwater dwellers that tolerate oligo−/mesohaline conditions are represented by: *Limnocythere* aff. *inopinata* (Baird, 1843), *Candona decimai* (Freels, 1980), *Candona* ex. gr. *neglecta* (Sars, 1887), *Cypris* cf. *pubera* (Müller, 1776), *Heterocypris salina* (Brady, 1868), and *Ilyocypris* spp. Typical freshwater ostracods are *Candona weltneri* (Hartwig, 1899) and *Prionocypris zenkeri* (Chyzer and Toth, 1858). The latter avoids limnic settings, and some occurrences of this taxon in the PLC and PLM sections may be the result of transportation by nearby rivers. Paleosalinity estimations are based on these autecological assumptions (for more details, see SI.1 for further information) (Fig. 16).

Paleobiogeographic considerations based on the current state of taxonomy (several taxa are left in open nomenclature) are problematic. However, *C. weltneri*, *C. pubera*, *H. salina* and *P. zenkeri*, which are widespread in the Holarctic today, have very early (possibly first) records in the Late Miocene of Anatolia (Freels, 1980; Meisch, 2000; Matzke-Karasz and Witt, 2005; Tunoğlu et al., 2012; Kayseri-Özer et al., 2017). *Candona neglecta*, also a present-day Holarctic taxon, was already common in Europe and the Anatolian peninsula during the Late Miocene and Pliocene (Meisch, 2000; Beker et al., 2008). *Candona decimai* occurs in Late Miocene-Pliocene times in northern Bulgaria, the Greek mainland and Aegean, as well as in Asia Minor (Matzke-Karasz and Witt, 2005). *C.* cf. *mehesi*, *C.* cf. *pontica*, and *C.* (*C.*) *fastigata* are possibly endemic in the Late Miocene–Pliocene basins of Anatolia but might be of

Table 2
Mineral composition and oxygen and carbon isotope values of various carbonate facies in the studied successions.

Facies association	Facies	Sample no	Mineralogy		Calcite		Dolomite	
			Carbonates	Siliciclastic components	$\delta^{18}O$ (‰ VPDB)	$\delta^{13}C$ (‰ VPDB)	$\delta^{18}O$ (‰ VPDB)	$\delta^{13}C$ (‰ VPDB)
Palustrine lake margin (PLM) (Gelinören section)	PLM2: Molluscan-ostracodal packstone-grainstone	GEK.1.1B	Cal	Clay>Mica>Q>Fel	−2,89	−5,31	-	-
		GEK.1.1A2			−4,15	−5,37	-	-
		GEK.1.1A1			−6,20	−7,20	−5,55	−6,44
		GEK.1.2B			−4,33	−4,49	-	-
		GEK.1.2A			−4,54	−4,61	-	-
	PLM3: Organic mudstone	GEK.2	Cal	Clay>Mica>Fel =Q	−5,44	−4,44	-	-
	PLM5: Laminated marlstone	GEK.3	Cal	Clay>Mica>Q>Fel	−2,37	−2,21	−2,66	−2,14
		GEK.4	Cal>Dol	Clay>Mica>Q>Fel	−1,34	−0,75	-	-
		GEK.5	Cal	Clay>Mica>Fel >Q	−2,14	−1,06	−1,62	−0,87
		GEK.6	Cal	Clay>Mica>Fel >Q	−2,53	−1,04	-	-
		GEK.7	Cal	Clay>Mica>Fel >Q	−3,73	−1,55	−2,55	−1,28
		GEK.8	Cal>Dol	Clay>Mica>Q>Fel	−1,45	−3,74	-	-
		GEK.9	Cal	Clay>Mica>Q>Fel	−2,33	−2,53	−2,02	−3,77
	PLM3: Organic mudstone	GEK.10	Cal	Clay>Mica>Fel =Q	−5,90	−8,45	-	-
	PLM1: Ostracodal−intraclastic packstone	GEK.11.2	Cal>Dol	Clay>Mica>Fel >Q	−1,30	−4,48	-	-
		GEK.11.1			−0,67	−4,97	−0,20	−3,00
	PLM3: Organic mudstone	GEK.12	Cal>Dol	Clay>Mica>Fel >Q	−1,18	−3,37	-	-
	PLM1: Ostracodal−intraclastic packstone	GEK.13.2	Cal>Dol	Clay>Mica>Q>Fel	−2,04	−5,05	-	-
		GEK.13.1			−1,77	−4,74	−3,20	−3,68
		GEK.14.2	Cal	Clay>Mica>Fel >Q	−3,78	−3,86	-	-
		GEK.14.1			−3,50	−4,05	−4,41	−3,68
Palustrine lake center (PLC) (Aşağıseyit−2 section)	PLC1: Peloidal-nodular-brecciated wackestone	AS.1.4	Dol>Cal	Clay>Mica>Q>Fel	3,68	−4,42	-	-
		AS.1.3			3,87	−4,48	3,92	−5,53
		AS.1.2			2,89	−4,29	-	-
		AS.1.1			2,66	−4,31	3,12	−5,71
	PLC3: Laminated marlstone	AS.1	Dol>Cal	Clay>Mica>Fel >Q	−0,81	−3,70	−1,35	−3,58
		AS.2	Cal>Dol	Clay>Mica>Fel >Q	−0,90	−2,08	-	-
		AS.3	Cal>Dol	Clay>Mica>Q>Fel	−2,03	−2,18	-	-
		AS.4	Dol	Clay>Mica>Q>Fel	−0,45	−5,31	−0,72	−5,07
		AS.4.1			1,90	−4,58	-	-
		AS.5.3	Cal>Dol	Clay>Mica>Q>Fel	−1,34	−2,63	0,52	−4,57
		AS.5.2			−1,40	−2,37	-	-
		AS.5.1			−0,32	−2,58	-	-
		AS.5	Cal>Dol	Clay>Mica>Fel >Q	−0,47	−3,84	−0,33	−3,84
		AS.6	Cal>Dol	Clay>Mica>Q>Fel	−1,85	−0,81	1,54	−4,59
		AS.6.1			2,53	−4,41	-	-
	PLC1: Peloidal-nodular-brecciated wackestone	AS.7.4	Dol	Clay>Mica>Q=Fel	2,99	−4,38	3,58	−5,21
		AS.7.3			3,15	−4,44	-	-
		AS.7.2			3,32	−4,37	1,38	−4,46
		AS.7.1			2,75	−4,29	-	-
	PLC3: Laminated marlstone	AS.8	Cal>Dol	Clay>Mica>Fel >Q	3,47	−4,08	2,01	−4,80
		AS.9	Cal>Dol	Clay>Mica>Fel >Q	2,01	−5,03	-	-
		AS.10	Cal>Dol	Clay>Mica>Q>Fel	−2,89	−5,31	-	-
Perennial shallow lake (PSL) (Aşağıseyit−1 section)	PSL4: Ostracodal− molluscan wackestone	GE.1.2	Dol>Cal	Clay>Mica>Fel>Q	1,57	−2,84	2,17	−2,85
		GE.1.1			1,63	−3,05	1,70	−2,87
	PSL3: Peloidal−brecciated−nodular wackestone	GE.2.2	Dol>Cal	Clay>Mica=Ara>Q>Fel	2,60	−4,24	-	-
		GE.2.1			2,38	−4,25	3,41	−1,08
	PSL6: Laminated marlstone	GE.3	Dol>Cal	Clay>Mica>Fel=Q	0,28	−4,60	2,48	−2,80
		GE.4	Dol>Cal	Clay>Mica>Ara>Fel>Q	0,90	−4,00	2,63	−2,03
	PSL1: Ostracodal packstone	GE.5.2	Cal>Dol	Clay>Mica=Ara>Fel>Q	3,40	−1,83	2,83	−2,81
		GE.5.1			3,71	−1,67		
	PSL6: Laminated marlstone	GE.6	Cal>Dol	Clay>Mica>Ara>Q>Fel	3,60	−3,19	-	-
	PSL2: Mudstone	GE.7.2	Dol	Clay>Mica>Q	4,08	−2,85	2,95	−3,08
		GE.7.1			3,92	−3,07	2,61	−3,09
	PSL6: Laminated marlstone	GE.8	Dol>Cal	Clay>Mica>Q>Fel	2,73	−3,00	3,33	−1,03
	PSL5: Organic mudstone	GE.9	Dol>Cal	Clay>Mica>Q>Fel	1,19	−3,44	3,64	−1,48
	PSL2: Mudstone	GE.10.2	Cal>Dol	Clay>Mica>Ara>Q=Fel	4,06	−2,74	2,19	−3,02
		GE.10.1			3,99	−2,65		
	PSL6: Laminated marlstone	GE.11	Dol>Cal	Clay>Mica>Fel >Q	3,32	−3,01	3,60	−2,45
		GE.12	Dol>Cal	Clay>Mica>Q>Fel	3,17	−3,11	-	-
		GE.13	Cal>Dol	Clay>Mica>Ara>Fel >Q	3,53	−2,95		
	PSL1: Ostracodal packstone	GE.14.2	Dol	Clay>Mica>Fel =Q	3,85	−2,82	-	-
		GE.14.1			4,02	−2,97	4,09	−1,55
	PSL6: Laminated marlstone	GE.15	Dol	Clay>Mica>Fel =Q	1,16	−3,90	3,16	−1,95
		GE.16			1,60	−3,95	2,60	−3,10

Paratethyan ancestry (e.g., Bassiouni, 1979; Dykan, 2016). *Tyrrhenocythere* and *Amnicythere* are supposed to be (Central) Paratethyan, of Middle and early Late Miocene origin, colonizing the Mediterranean and Ponto–Caspian region during the latest Miocene (e.g., Griffiths et al., 2002; Gliozzi et al., 2005; Pipík, 2007; Namiotko et al., 2012).

In summary, the Baklan ostracod fauna is composed of: i) widely distributed "freshwater" taxa (*C.* ex gr. *neglecta*, *C. weltneri*, *C.* cf. *pubera*, *H. salina*, *P. zenkeri*, *L.* aff. *inopinata*, *Ilyocypris* spp.), and ii) "brackish"

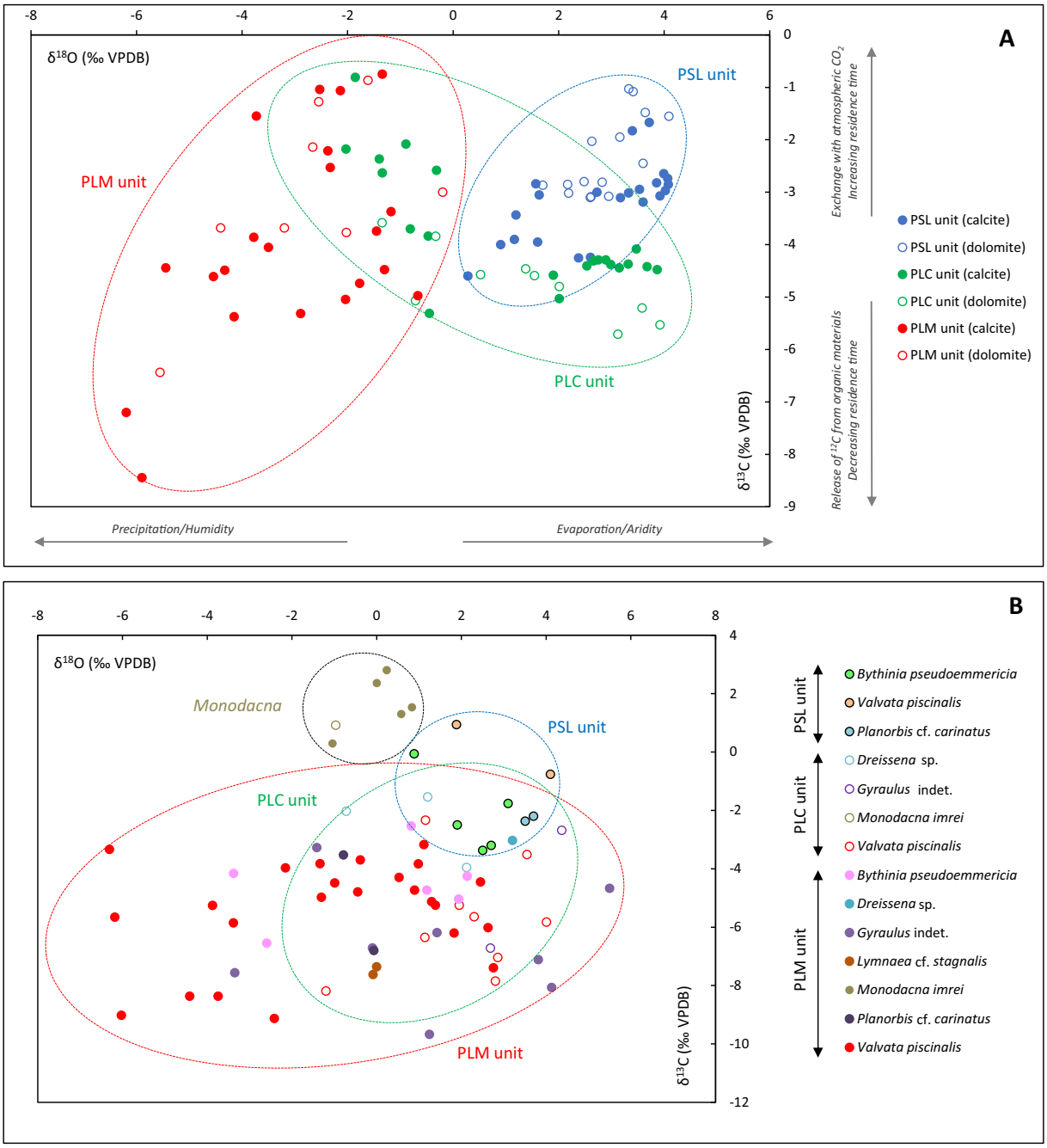

Fig. 15. (A) Scatter plot of stable oxygen and carbon isotope values in carbonate samples from the three facies associations of the studied succession, (B) Stable isotope values of selected species (data in Table 4). *Monodacna imrei* (inset, data in Fig. 13) has dissimilar $\delta^{13}C$ values.

water species with relationships to the Paratethyan realm (*C.* cf. *mehesi*, *C.* cf. *pontica*, *Tyrrhenocythere* sp., *Amnicythere* cf. *olivia*, *C. decimai*, *C.* (*C.*) *fastigata*). Freshwater taxa are dominated by modern Palearctic and Holartic forms, whereas brackish water taxa are dominated by fossil Palearctic with minor modern Palearctic forms (Table 4).

5.1.3. Molluscs

Three samples from the perennial shallow lake deposits (PSL association, Aşağıseyit-1 section, Fig. 4A), six samples from the palustrine lake center deposits (PLC association, Aşağıseyit-2 section, Fig. 4B), and eight samples from the palustrine lake margin deposits (PLM association, Gelinören section, Fig. 4C) were studied for their mollusc content and identified a total of 32 unique species [Figs. 10 and 13; Table 1 and 5; the opercula of the unidentified bithynid might belong to *Bithynia pseudemmericia* (Schütt, 1964)].

The mollusc fauna is dominated by *Valvata piscinalis* (Müller, 1774) in the Aşağıseyit-2 and Gelinören sections. Other common groups include planorbid and lymnaeid gastropods and dreissenid, sphaeriid, and cyrenid bivalves. The vast majority of species represents clear, slightly moving, vegetated freshwater. Two species [*Laevicaspia* ?*lincta* (Milaschewitsch, 1908) and *Monodacna imrei* (Wesselingh and Alçiçek, 2010)] are representatives of the so-called Pontocaspian fauna group that occupies coastal freshwater to lower mesohaline settings. *Bithynia pseudemmericia* and *Corbicula* species are generally considered to be intolerant to severe frost. Hence, the mollusc fauna from Baklan represents a Palearctic, shallow vegetated, slow-moving freshwater community with some freshwater to low mesohaline Pontocaspian elements in the Black Sea-Caspian Sea region.

Table 3
Oxygen and carbon isotope values of various mollusc species in the studied successions.

Facies assoc.	Sample no	Mollusc species	$\delta^{18}O$ (‰VPDB)	$\delta^{13}C$ (‰VPDB)	Sample no	Mollusc species	$\delta^{18}O$ (‰VPDB)	$\delta^{13}C$ (‰VPDB)
Palustrine lake	GEK1.1	*Bythinia pseudoemmericia*	1.18	−4.73	GEK2	*Valvata piscinalis*	−0.45	−4.79
margin	GEK1.1	*Bythinia pseudoemmericia*	0.81	−2.53	GEK2	*Valvata piscinalis*	0.53	−4.30
(PLM)	GEK1.2	*Bythinia pseudoemmericia*	1.93	−5.04	GEK4	*Monodacna imrei*	0.23	2.80
(Gelinören section)	GEK1.1	*Dreissena* sp.	3.20	−3.03	GEK4	*Monodacna imrei*	0.00	2.36
	GEK1.1	*Gyraulus* indet.	3.81	−7.11	GEK4	*Gyraulus* indet.	−1.41	−3.27
	GEK1.1	*Gyraulus* indet.	−0.10	−6.71	GEK4	*Valvata piscinalis*	−6.31	−3.33
	GEK1.1	*Gyraulus* indet.	5.49	−4.67	GEK4	*Valvata piscinalis*	−0.99	−4.49
	GEK1.1	*Gyraulus* indet.	1.24	−9.67	GEK4	*Valvata piscinalis*	2.45	−4.45
	GEK1.1	*Lymnaea* cf. *stagnalis*	0.00	−7.36	GEK4	*Valvata piscinalis*	1.38	−5.25
	GEK1.1	*Lymnaea* cf. *stagnalis*	−0.09	−7.62	GEK5	*Bythinia pseudoemmericia*	−2.59	−6.55
	GEK1.1	*Monodacna imrei*	−1.05	0.29	GEK5	*Bythinia pseudoemmericia*	2.14	−4.26
	GEK1.2	*Monodacna imrei*	0.58	1.30	GEK5	*Gyraulus* indet.	4.13	−8.07
	GEK1.2	*Monodacna imrei*	0.83	1.53	GEK5	*Gyraulus* indet.	−3.35	−7.56
	GEK1.1	*Planorbis* cf. *carinatus*	−0.07	−6.80	GEK5	*Valvata piscinalis*	1.11	−3.17
	GEK1.1	*Planorbis* cf. *carinatus*	−0.79	−3.53	GEK5	*Valvata piscinalis*	−3.88	−5.25
	GEK1.1	*Valvata piscinalis*	0.89	−4.73	GEK5	*Valvata piscinalis*	−6.18	−5.66
	GEK1.1	*Valvata piscinalis*	2.62	−6.02	GEK5	*Valvata piscinalis*	−4.41	−8.36
	GEK1.1	*Valvata piscinalis*	2.75	−7.39	GEK6	*Bythinia pseudoemmericia*	−3.38	−4.16
	GEK1.1	*Valvata piscinalis*	1.83	−6.20	GEK6	*Gyraulus* indet.	1.42	−6.18
	GEK1.1	*Valvata piscinalis*	0.98	−3.83	GEK6	*Valvata piscinalis*	−2.42	−9.13
	GEK1.2	*Valvata piscinalis*	−2.16	−3.97	GEK6	*Valvata piscinalis*	−3.75	−8.37
	GEK1.2	*Valvata piscinalis*	−1.31	−4.98	GEK6	*Valvata piscinalis*	1.30	−5.12
	GEK1.2	*Valvata piscinalis*	−1.34	−3.82	GEK6	*Valvata piscinalis*	−6.03	−9.02
	GEK1.2	*Valvata piscinalis*	−0.39	−3.69	GEK7	*Valvata piscinalis*	−3.39	−5.85
Palustrine lake	AS1	*Valvata piscinalis*	1.95	−5.25	AS2	*Valvata piscinalis*	1.14	−6.35
center	AS2	*Dreissena* sp.	−0.72	−2.03	AS2	*Valvata piscinalis*	3.55	−3.51
(PLC)	AS2	*Dreissena* sp.	1.20	−1.54	AS2	*Valvata piscinalis*	−1.20	−8.19
(Aşağıseyit−2 section)	AS2	*Dreissena* sp.	2.12	−3.95	AS6	*Valvata piscinalis*	2.30	−5.65
	AS2	*Gyraulus* indet.	2.68	−6.72	AS6	*Valvata piscinalis*	2.86	−7.03
	AS2	*Gyraulus* indet.	4.37	−2.68	AS6	*Valvata piscinalis*	1.15	−2.34
	AS2	*Monodacna imrei*	−0.97	0.92	AS6	*Valvata piscinalis*	2.80	−7.85
	AS2	*Valvata piscinalis*	4.00	−5.83				
Perennial shallow	GE4.1	*Bythinia pseudoemmericia*	0.88	−0.06	GE9	*Valvata piscinalis*	1.88	0.94
lake	GE4.1	*Bythinia pseudoemmericia*	3.10	−1.76	GE13	*Valvata piscinalis*	4.10	−0.76
(PSL)	GE4.1	*Bythinia pseudoemmericia*	2.50	−3.37	GE13	*Planorbis* cf. *carinatus*	3.50	−2.37
(Aşağıseyit−1 section)	GE9	*Bythinia pseudoemmericia*	2.70	−3.20	GE13	*Planorbis* cf. *carinatus*	3.70	−2.20
	GE9	*Bythinia pseudoemmericia*	1.90	−2.50				

The Baklan mollusc fauna contains many widespread Palearctic freshwater species, together with two Pontocaspian species (Table 4). The Pleistocene Pontocaspian species have been reported from other Anatolian lakes that may have served as refugia for these taxa (Büyükmeriç and Wesselingh, 2018). It is well possible that Anatolian lakes, such as Lake Baklan, also offered a refuge for Palearctic taxa during adverse time intervals in the Pleistocene. The identity of several taxa will require further, in-depth study that may deliver insights into more specific biogeographic affinities. We are uncertain as to the attribution of *Gyraulus* cf. *acronicus* (Férussac, 1807), as multiple resembling *Gyraulus* species are known from the region that we find difficult to differentiate. The exact identity of several other pulmonated species can only be established with more fully preserved specimens. The two *Corbicula* species resemble in outline modern *C. fluminalis* and *C. fluminea* (Müller, 1774), but the Baklan material contains coarse commarginal ribs near the umbo that are lacking in the modern species. Resolving such taxonomic matters is beyond the scope of this paper, but may provide additional insights into the evolution and biogeography of these faunas.

The age of the Baklan mollusc fauna has been revised here from Lower Pliocene to Lower-Upper Pleistocene. A direct comparison with Neogene faunas from nearby Denizli Basin is hampered by stratigraphic age differences and uncertainties in the latter basin. However, an Early Pleistocene fauna from lacustrine shore deposits in the vicinity of travertine terraces recently reported by Rausch et al. (2019) from the western Denizli Basin contains an unidentified *Monodacna* that may be conspecific with *Monodacna imrei* (Rausch et al., 2019). However, the remainder of the fauna is very different implying that both basins were separated at the time.

5.1.4. Fishes

Fish remains (Fig. 14) from the palustrine lake margin deposits (PLM, Gelinören section, Fig. 4C), predominantly teeth, as well as several vertebral centra and otoliths, were recovered from numerous sites. The most identifiable remains are pharyngeal teeth from cyprinoid fishes (this group is equivalent to the Cyprinidae of older literature, but is here regarded as a suborder following Tan and Armbruster, 2018). Assigning these teeth to a specific taxon is hampered by a lack of documentation of the diversity of morphologies exhibited in the pharyngeal teeth of many extant cyprinoids. Although the morphology of pharyngeal teeth is likely to be at least partly representative of phylogeny, there may also be a relationship with diet, and tooth form may vary with growth (Nakajima, 2018). Because of the possibility of convergent morphologies, and the lack of information on extant forms, the Baklan fossil teeth are not definitively assigned to species or genera, but instead referred to as morphotypes. One of the morphotypes is only identified as Teleostei because it is not comparable to any cyprinoid pharyngeal teeth figured in the literature or available in comparative collections. It is possible these belong instead to a non-cyprinoid fish.

Most of the identifiable fish material is assigned to the ostariophysan suborder Cyprinoidei. Cyprinoid fishes are restricted to fresh waters and are found throughout the Northern Hemisphere as well as having reached Africa by the Miocene (e.g., Stewart and Murray, 2017) (Table 4). A good diversity of cyprinoid species is present in Anatolia today.

The pharyngeal teeth from the Baklan Basin are most similar to those of *Leucisus, Capoeta, Scardinius* and *Phoxinus,* as well as possibly *Alburnus* and *Danio*. Of these genera, *Danio* is not currently found in Turkey (Çiçek et al., 2015), indicating this identification is less likely.

Table 4
Biogeographic zones of the dominant and minor species of the studied succession flora and fauna.

Fauna and flora (Facies associations)		Biogeographic zones	
		Dominant species	Minor species
Micromammals	Steppe and meadows	**Modern Palearctic:**	-
Palustrine lake margin (PLM)	(100%)	*Meriones* sp.	
		Modern Holarctic:	
		Microtus sp.	
Ostracods	Aquatic	**Modern Palearctic and Holarctic:**	**Modern Palearctic and Holarctic:**
Perennial shallow lake (PSL)	(freshwater)	*Candona* ex gr. *neglecta*	*Candona weltneri*
Palustrine lake center (PLC)	(72%)	*Heterocypris salina*	*Cypris* cf. *pubera*
Palustrine lake margin (PLM)		*Candona decimai*	
		Ilyocypris spp.	
		Prionocypris zenkeri	
		Limnocythere aff. *inopinata*	
	Aquatic	**Fossil Palearctic (endemic):**	**Modern Palearctic:**
	(brackish water)	*Cyprideis* cf. *pontica*	*Tyrrhenocythere* sp.
	(28%)	*Candona* (*Caspiolla*) *fastigata*	*Amnicythere* cf. *olivia*
		Cyprideis cf. *mehesi*	
Molluscs	Aquatic	**Modern Palearctic and Holarctic:**	**Modern Palearctic (endemic):**
Perennial shallow lake (PSL)	(freshwater)	*Bithynia pseudemmericia*	*Kirelia* cf. *carinata*
Palustrine lake center (PLC)	(95%)	*Bithynia* sp. (opercula)	**Modern Palearctic**
Palustrine lake margin (PLM)		*Valvata cristata*	*Segmentina* cf. *nitida*
		Valvata piscinalis	*Euglesa henslowana*
		Lymnaea cf. *stagnalis*	*Euglesa nitida*
		Radix sp.	*Euglesa ponderosa*
		Gyraulus cf. *acronicus*	*Euglesa subtruncata*
		Armiger crista	*Odhneripisidium moitessierianum*
		Corbicula aff. *fluminea*	*Odhneripisidium tenuilineatum*
		Corbicula aff. *fluminalis*	*Pisidium amnicum*
		Dreissena polymorpha s.l.	*Pisidium clessini*
			Pisidium s.l. sp.
			Planorbarius corneus
			Planorbis ?carinatus
			Sphaerium corneum s.l.
			Sphaerium rivicola
			Sphaerium sp.
			Stagnicola palustris
			Unionoidea sp. indet.
			?*Bythinella* sp.
	Aquatic (brackish water)	**Modern Palearctic (endemic, relict Neogene):**	**Modern Palearctic (endemic, relict Neogene):**
	(5%)	*Laevicaspia ?lincta*	*Theodoxus bukowskii*
		Monodacna imrei	
Characeae	Aquatic (100%)	**Modern Palearctic and Holarctic:**	*Chara* sp. 1, 2, 3
Palustrine lake center (PLC)	(freshwater and brackish)	*Chara* cf. *hispida*	
Palustrine lake margin (PLM)		*Chara* cf. *vulgaris*	
		Nitellopsis (*Tectochara*) *meriani*	
Fishes	Aquatic (100%)	**Modern Palearctic and Holarctic:**	-
Palustrine lake margin (PLM)	(freshwater)	Teleostei	
		Cyprinoidei	

Because the fish teeth recovered from the Baklan Basin cannot be precisely identified, they cannot be used for robust paleoecological or paleobiogeographic reconstructions. The most that can be said about the fish remains is that those identified as cyprinoids indicate a freshwater environment. The marginal lake environment of the Gelinören locality agrees with the habitat expected for these fish. One of the morphotypes of pharyngeal teeth (possibly corresponding to *Scardinius* or *Leuciscus*) is found in more localities than the other forms. This indicates that the fishes from which these teeth came might be more generalist than the other species, and able to inhabit a wider variety of habitats (see SI.2 for further information).

Most of the fish remains were found in marginal lake deposits, with a few remains coming from shallow lake and pond sediments. The lack of fish remains in the fluvial deposits is likely a result of their small size and relative fragility, as these water bodies should have been hospitable to the same fishes found in the lake deposits. Therefore, the lack of fish in some facies may be caused by preservational bias, not a true absence. On the other hand, fish are lacking or have a decreased diversity in the localities that are thought to have rising salinity based on the ostracods; in these cases, the absence of freshwater cyprinoids is likely a true absence caused by their intolerance to oligohaline waters.

5.1.5. Characeae

Of the investigated sections, nine samples yielded Characeae remains, three samples from the palustrine lake center (PLC, Aşağıseyit-2 section, Fig. 4B) and six samples from the palustrine lake margin (PLM, Gelinören section, Fig. 4C) were studied for their Characeae remains. Seven types could be distinguished, four of which were assigned to three species (Fig. 11). The Pliocene and Pleistocene Characeae gyrogonites and oospores extant species. *Chara* cf. *hispida* with 64% (Fig. 11a-b), *C.* cf. *vulgaris* with 13% (Fig. 11c), and *Nitellopsis* (*Tectochara*) *meriani* (Al. Braun ex Unger, 1852) with 19.5% (Fig. 11g) Only isolated and fragmented specimens of *Chara* sp. 1, *C.* sp. 2, and *C.* sp. 3 (Figs. 11d-f) were encountered. Extant members of the three identified species are found in freshwater but are tolerant of weakly brackish conditions with neutral to weakly alkaline pH (7–8.5) and grow in shallow, clear, slow-flowing, or standing waterbodies (see SI.3 for further information). The presence of weakly or not fully calcified oogonia of *Chara* cf. *hispida* is either a sign of immaturity, the ripening process was interrupted, or of greater water depth; in extant *Chara hispida*, oogonia only fully mature to gyrogonites in shallow waters (Soulié-Märsche and García, 2015). All taxa are dominated by modern Palearctic and Holarctic forms (Table 4).

Table 5
Mollusc data from the studied sections (GE samples from Aşağıseyit-1 section; AS samples from Aşağıseyit-2 section; GEK samples from Gelinören section).

Taxon	Authorship	GEK1.1	GEK1.2	GEK2	GEK3	GEK4	GEK5	GEK6	GEK7	GEK13	AS1	AS2	AS5	AS6	AS8	AS9	GE4.1	GE9	GE13	#spec.
Theodoxus bukowskii	(Oppenheim, 1919)	0	0	0	0	0	1	0	0	0	0	0	0	0	0	0	0	0	0	1
Kirelia carinata	Radoman, 1973	0	0	0	0	1	0	1	0	0	0	0	0	0	0	0	0	0	0	2
Laevicaspia ?lincta	(Milaschewitsch, 1908)	1	16	14	3	37	13	2	0	0	4	31	0	0	0	0	0	0	0	121
?Bythinella sp.		0	0	0	0	0	5	0	0	0	0	0	0	0	0	0	0	0	0	5
Bithynia pseudemmericia	Schütt, 1964	1	9	4	0	10	65	32	0	0	3	3	0	0	0	0	0	10	0	137
Bithynia sp. (opercula)		0	12	0	0	0	5	9	0	0	0	4	0	0	0	1	0	0	0	31
Valvata cristata	Müller, 1774	3	11	2	5	10	21	21	2	0	4	1	0	0	0	0	11	15	19	125
Valvata piscinalis	(Müller, 1774)	27	95	52	22	152	750	295	14	0	33	320	0	83	1	0	0	0	0	1844
Lymnaea cf. *stagnalis*	(Linnaeus, 1758)	1	0	0	0	3	9	4	0	0	0	6	0	0	0	0	0	0	0	23
Stagnicola palustris	(Müller, 1774)	0	1	0	0	0	4	6	0	0	0	0	0	0	0	0	0	0	0	11
Radix sp.		0	3	2	0	1	1	0	0	0	0	19	0	1	0	0	0	0	0	27
Planorbarius corneus	(Linnaeus, 1758)	0	0	0	0	1	1	1	0	0	5	2	0	0	0	0	0	10	16	36
Planorbis ?carinatus	(Müller, 1774)	0	0	0	1	4	8	2	0	0	0	0	0	0	0	1	10	5	13	44
Gyraulus cf. *acronicus*	(Férussac, 1807)	8	22	11	4	51	54	21	2	0	2	56	2	0	0	0	15	25	32	305
Armiger crista	(Linnaeus, 1758)	2	11	0	0	5	0	0	0	0	1	8	0	1	0	0	0	0	0	28
Segmentina aff. *nitida*	(Müller, 1774)	0	0	0	0	0	0	0	0	0	0	0	0	1	0	0	0	0	0	1
Monodacna imrei	Wesselingh and Alçiçek, 2010	2	2	2	0	5	0	0	0	0	0	14	0	0	0	0	0	0	0	25
Corbicula aff. *fluminalis*	(Müller, 1774)	2	0	4	5	7	0	0	0	0	0	0	0	0	0	0	0	0	0	18
Corbicula aff. *fluminea*	(Müller, 1774)	1	0	5	4	18	29	5	0	0	0	1	0	0	0	0	0	0	0	63
Sphaerium rivicola	(Lamarck, 1818)	0	0	0	0	0	2	0	0	0	0	0	0	0	0	0	0	0	0	2
Sphaerium corneum s.l.	(Linnaeus, 1758)	0	0	0	0	0	3	3	0	0	0	0	0	0	0	0	0	0	0	6
Sphaerium sp.		0	0	0	0	0	1	0	0	0	0	0	0	0	0	0	0	0	0	1
Pisidium amnicum	(Müller, 1774)	0	0	0	0	0	4	0	0	0	0	1	0	0	0	0	0	0	0	5
Pisidium clessini	Neumayr and Paul, 1875	0	0	0	0	0	0	0	0	15	0	1	0	0	0	0	0	0	0	16
Pisidium s.l. sp.		0	0	0	0	0	0	1	0	0	0	0	2	0	0	1	0	0	0	4
Euglesa nitida	(Jenyns, 1832)	0	0	0	0	2	4	1	0	0	1	0	0	0	0	0	0	0	0	8
Euglesa subtruncata	(Malm, 1855)	2	0	0	0	1	4	0	0	0	0	1	0	1	0	0	0	0	0	9
Euglesa henslowana	(Sheppard, 1825)	0	0	0	0	0	3	0	0	0	0	0	1	0	0	0	0	0	0	4
Euglesa ponderosa	(Stelfox, 1918)	0	0	0	0	1	0	0	0	0	0	0	0	0	0	0	0	0	0	1
Odhneripisidium tenuilineatum	(Stelfox, 1918)	0	0	1	0	0	1	0	0	0	0	1	0	0	0	0	0	0	0	3
Odhneripisidium moitessierianum	(Paladilhe, 1866)	0	0	0	0	1	0	0	0	0	0	0	0	0	0	0	0	0	0	1
Unionoidea sp. indet.		0	0	0	0	0	1	0	0	0	0	0	4	1	0	0	0	0	0	6
Dreissena polymorpha s.l.	(Pallas, 1771)	0	2	1	1	0	8	0	0	0	0	27	0	0	0	0	0	0	0	39
		50	184	98	45	310	997	404	18	15	53	496	9	88	1	3	36	65	80	2952

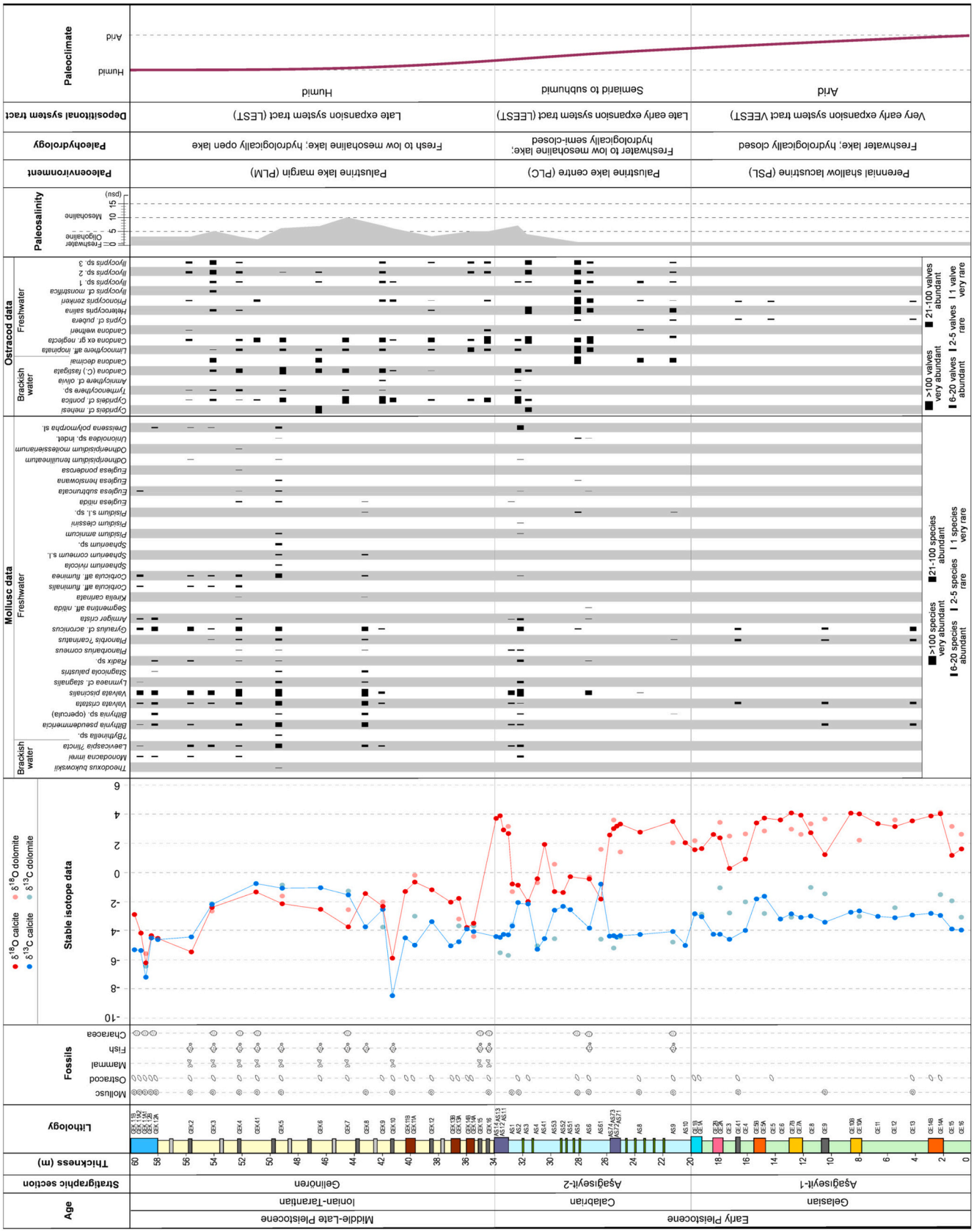

Fig. 16. A summary of the Early-Late Pleistocene depositional history of the Baklan Basin, including sedimentological, paleontological and geochemical data and their paleoenvironmental interpretation.

5.2. Depositional model and facies stacking pattern: paleohydrological and paleoclimatic implications

The approximately 60 m thick, the Lower-Upper Pleistocene succession of the Baklan Basin consists of an overall carbonate-dominated sequence predominantly composed of Palearctic freshwater fauna with a contribution of brackish water (oligohaline to low mesohaline) Pontocaspian fauna (Fig. 16; Table 4). Sedimentological and paleontological data indicate that the Lower-Upper Pleistocene lacustrine-palustrine system in the Baklan Basin developed in a low-gradient 'ramp'-type margins environment as described by Platt and Wright (1991). Well-documented modern and fossil examples of the low-gradient 'ramp'-type margins environment have been reported in various sequences all over the world, including the Late Pliocene sequences of the Çal Basin (southwestern Turkey; Alçiçek and Alçiçek, 2014), the Cretaceous-Tertiary sequences in southern France (Freytet and Plaziat, 1982), the Middle Miocene sequences of the Ebro Basin, Spain (Vázquez-Urbez et al., 2013; the Miocene-Pliocene sequences of the Calama Basin, Chile (de Wet et al., 2015), the Late Eocene sequences of Hampshire Basin, England (Armenteros et al., 1997), the Miocene sequences of the Teruel Basin, Spain (Alonso-Zarza and Calvo, 2000), and the Eocene-Oligocene sequences of the Alès–Saint-Chaptes–Issirac basins in southeastern France (Lettéron et al., 2017, 2018, 2022).

Such lakes occur favorably in low-relief topography, as exemplified in the Lower-Upper Pleistocene Baklan paleolake, which developed during periods of the decreased subsidence rates coupled with a carbonate source area. The lake sedimentation has been controlled by a combination of tectonic, climate, and source rock factors. The formation of shallow lacustrine-palustrine carbonates depends on the relationship between the subsidence rate and sediment+water supply in depositional basins (Alonso-Zarza, 2003). The progressive reduction of tectonic activity along basin margins or topographic changes resulting from basin infilling can lead to low-relief areas that eventually receive carbonate sediments from carbonate source areas (Platt and Wright, 1991; Alonso-Zarza and Wright, 2010). The vertical and lateral relationships and paleoenvironmental interpretations of the facies and facies associations, faunal and floral assemblages, diagenetic features, and stable isotope compositions of the studied successions allow the reconstruction of the lake evolution in response to tectonic and climatic factors, corresponding to three depositional intervals of the Lower-Upper Pleistocene Baklan paleolake system (Figs. 16 and 17). These depositional intervals correspond to different stages of the lake expansion system tract, according to the classification of Li et al. (2019).

5.2.1. Interval I: Early Pleistocene (Gelasian) lake

The first interval is marked by the deposition of perennial shallow lake deposits (PSL facies association, Aşağıseyit-1 section, Fig. 4A) in the lower part of the Early Expansion System Tract (VEEST), representing the very early stage of the lake transgression in the Baklan Basin (Fig. 17A). The PSL deposits are particularly well developed in the basin`s northern part (Fig. 2).

The remarkable lateral continuity of the PSL deposits (Fig. 5A) suggests low-gradient "ramp" type margins where deposition frequently occurred in semiarid or arid climatic conditions (Platt and Wright, 1991). The predominance of mudstone to wackestone textures supports that the deposition of PSL1 to PSL4 carbonates took place under low-energy conditions (Alonso-Zarza et al., 2011). Early diagenetic modifications of the PSL3 carbonates, leading to brecciation, nodularization, and planar and circumgranular desiccation cracking (Fig. 5B-5C and 5E-5F) occurred under evaporative conditions when the lake gradually lowered and the carbonates became exposed in the marginal zones (Freytet and Plaziat, 1982; Alonso-Zarza, 2003). The formation of the PSL carbonates reflects calcium- and magnesium-rich, alkaline waters. Calcium and magnesium ions would have been supplied from upland drainage of carbonate bedrock. These aerobic lake conditions are suggested by diverse biotal assemblage (ostracods; (Fig. 7 (9–10) and (17–20) and molluscs (Table 1).

The PSL carbonates and molluscs exhibit a relatively narrow range of positive $\delta^{18}O$ values (Table 2 and 3; Fig. 15A-15B), suggesting evaporative enrichment of ^{18}O in the lake water (Leng and Marshall, 2004). Lake water became enriched in ^{18}O through evaporation, indicating arid climate conditions. Similar conditions have also been documented in the neighboring Çameli Basin (Fig. 1B, van den Hoek Ostende et al., 2015; Jiménez-Moreno et al., 2015), Acıgöl Basin (Fig. 1B, Demory et al., 2020; Andrieu-Ponel et al., 2021), and Karacasu Basin (Fig. 1B, Alçiçek and Jiménez-Moreno, 2013). The freshwater ostracod and mollusc taxa and positive $\delta^{18}O$ values indicate that the deposition of PSL occurred in freshwater, shallow water settings. The mean $\delta^{18}O$ values of the calcite (+0.28 to +4.08‰, mean = +2.76‰) and dolomite (+1.70 to +4.09‰, mean = +2.89‰) (Fig. 15A; Table 2) are quite similar and indicate that calcite and dolomite precipitated in similar conditions. Positive, good $\delta^{18}O/\delta^{13}C$ correlations (r-values of +0.67 for calcite and +0.71 for dolomite) in the PLC unit indicate a hydrologically closed lake. Such lakes are sensitive to changes in precipitation/evaporation ratios (P/E) and evolve under low P/E ratios (Talbot, 1990; Lamb et al., 2002). Such a covariant trend is indicative of periods with negative precipitation/evaporation balance (enrichment in $^{13}C_{DIC}$ and $^{18}O_{water}$). In this stage, lake level was controlled by negative precipitation/evaporation balance (P < E) and active subsidence due to a normal fault located on the basin's northern margin (Fig. 2). The PLC succession is interpreted as an underfilled lake, characterized by the rates of accommodation exceeding the rates of sediment+water supply (Figs. 16 and 17A; Bohacs et al., 2000). The PSL deposits include limited ostracod and mollusc faunas compared to the PLC and PLM deposits due to the fact that hydrologically closed lakes are isolated and stressful environments.

5.2.2. Interval II: Early Pleistocene (Calabrian) lake

During this second interval, the palustrine lake centre deposits (PLC facies association, Aşağıseyit-2 section, Fig. 4B) formed in the upper part of the Early Expansion System Tract (LEEST), indicating continued lake expansion (Fig. 17B). The PLC deposits conformably overlie the PSL deposits (Fig. 5A) and pass upward into the palustrine lake margin facies association (PLM). These deposits are particularly well exposed in the northern part of the basin (Fig. 2).

The progressive reduction of tectonic activity along basin margins or topographic changes resulting from basin infilling caused low-relief areas, leading to the widespread deposition of carbonate deposits (PLC facies association) in a palustrine lake-dominated setting. The pedogenic features of the peloidal-nodular-brecciated wackestone (facies PLC1) and marlstone (facies PLC3) (brecciation, planar and circumgranular cracks, and root traces) indicate the low-gradient 'ramp' type margins-low energy (Platt and Wright, 1991) dominated by micritic carbonates (facies PLC1). These features formed under evaporative conditions (semiarid climate) when the lake level gradually decreased and carbonate sediments were exposed (Alonso-Zarza et al., 2011).

The PLC deposits and molluscs show a relatively narrow range of $\delta^{18}O$ values and slightly lower $\delta^{18}O$ values than those of the PSL deposits (Table 2 and 3; Fig. 15A-15B), indicating evaporative enrichment of ^{18}O in lake water and semiarid-subhumid conditions. The mean $\delta^{18}O$ values of the calcite (−2.03 to +3.87‰, mean = +1.22‰) and dolomite (−1.35 to +3.92‰, mean = +1.37‰) (Fig. 15A; Table 2) are very similar and reflect that calcite and dolomite occurred in similar conditions. The PLC lake reflects a hydrologically semi-closed lake, confirmed by a good $\delta^{18}O/\delta^{13}C$ correlation (r-values of −0.74 for calcite and −0.79 for dolomite). These conditions indicate that precipitation and evaporation are in balance (P = E) and that there are low rates of tectonic subsidence due to a normal fault located on the basin's northern margin (Fig. 2). The negative covariance indicates concomitant enrichment in ^{18}O and ^{12}C, reflecting a decrease in freshwater input, and evaporative effects generate an enrichment of ^{18}O and organic productivity that can lead to ^{12}C enrichment (Li and Ku, 1997).

The abundant supply of dissolved calcium and magnesium in the

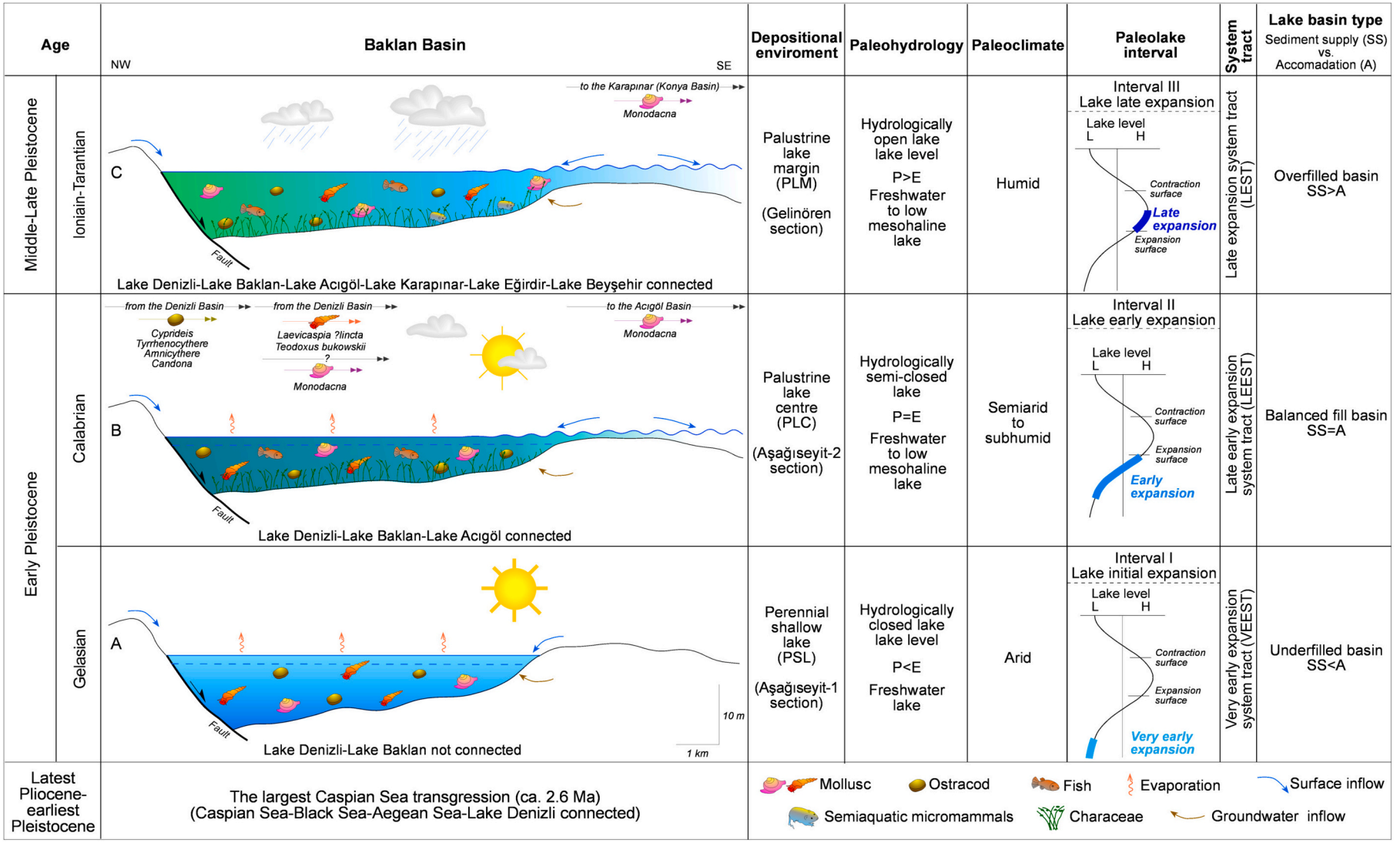

Fig. 17. The evolution of the Baklan paleolake in response to climatic and tectonic factors during the Early-Late Pleistocene.

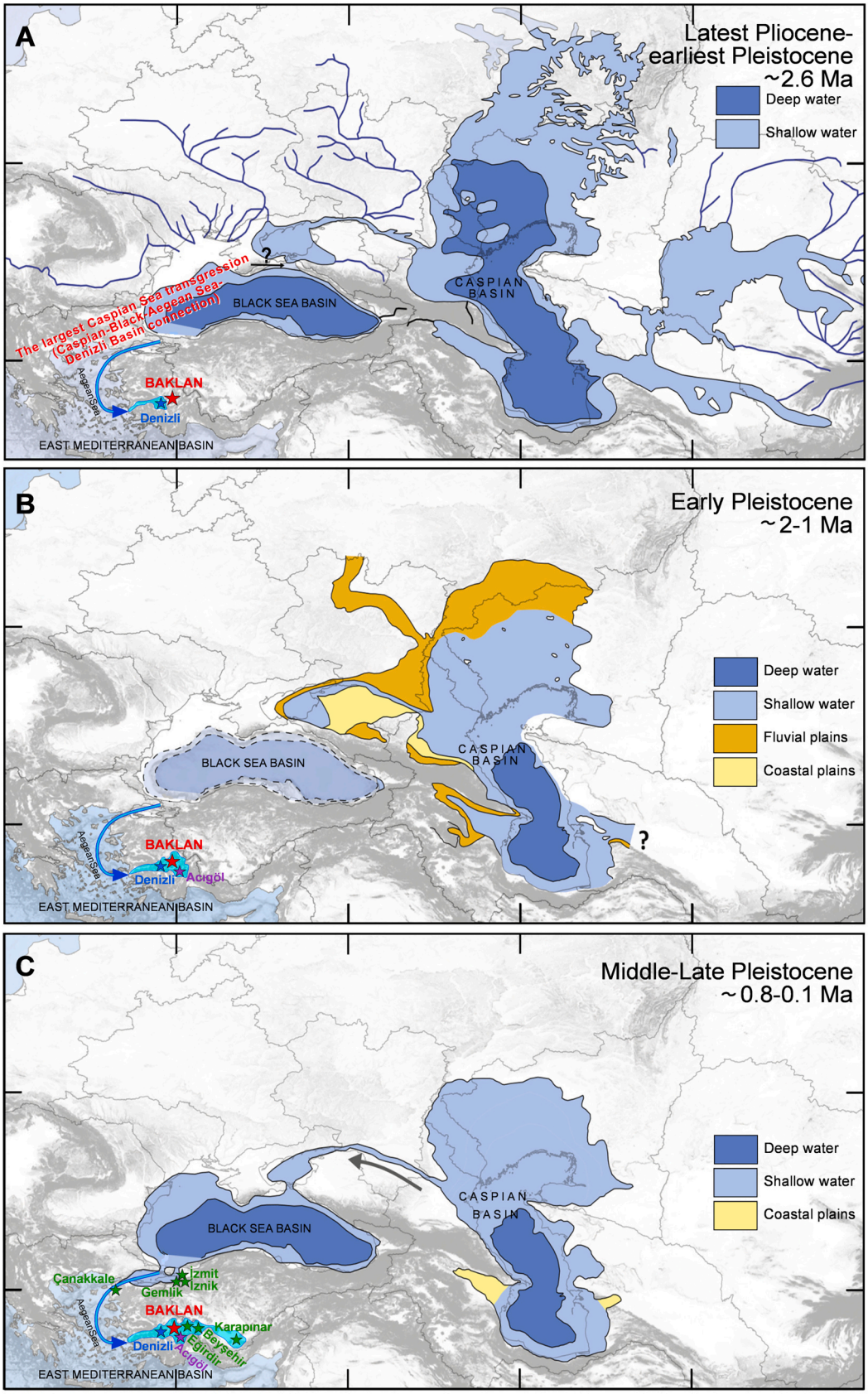

Fig. 18. Paleogeographic maps showing the extension of the largest Caspian transgression during the latest Pliocene-Pleistocene in the Pontocaspian region and southwestern Anatolia: (A) Latest Pliocene-earliest Pleistocene (~2.6 Ma), (B) Early Pleistocene (~2–1 Ma), (C) Middle-Late Pleistocene (~0.8–0.1 Ma). Arrows indicate the water flow direction in the gateway regions. Modified from Krijgsman et al. (2019).

influx waters, originating from the Mesozoic carbonates in the source area, led to the predominance of dolomitic limestones and dolostones under low evaporative conditions. This is confirmed by the decreasing upward trend in $\delta^{18}O$ values of the PLC carbonates, which indicates a transition from an arid to a semiarid-subhumid climate (Figs. 16 and 17A-17B). Similar climatic conditions have also been reported in the neighboring Çal Basin (Alçiçek et al., 2012). The vertical distribution of mollusc and ostracod fauna in the PLC deposits also supports this trend. The freshwater to oligohaline water-tolerant ostracod taxa [Fig. 7 (1–4), (13–16), (29–32) and Fig. 9 (1-4) (9–12), (17-40)] and mollusc taxa [Fig. 10 (a, c, j, l-n)] of the PLC association (Table 1) indicate a freshwater to slightly brackish water (oligohaline-low mesohaline) lake setting. Ostracod associations in samples AS.9–AS.5 from the Aşağıseyit-2 section point to freshwater setting (Fig. 16). Up–section (sample AS.3), the occurrence of *Cyprideis* suggests an increase in salinity towards oligohaline waters. In sample AS.2, *Cyprideis* cf. *pontica* becomes the dominant taxon, accompanied by the brackish water species *Tyrrhenocythere* sp., *A.* cf. *olivia*, and *C.* (*C.*) *fastigata*. This may indicate low mesohaline conditions were reached in this sample.

The PLC succession represents a balanced-fill lake (Fig. 17) proposed by Bohacs et al. (2000). Such lake basins occur when the rates of sediment+water supply and potential accommodation are roughly in balance over the time span of sequence development. In these conditions, water inflows are occasionally insufficient to periodically fill accommodation space, but they are not always in equilibrium with outflows, resulting in common climatically-driven lake level fluctuations, as seen in the PLC lake. Since the hydrologically open lakes host relatively diverse and abundant fauna, the PLC deposits are rich in ostracod and mollusc faunas compared to the PSL deposits.

In the second interval, the PLC lake level was predominantly controlled by the balance between precipitation and evaporation (P = E). The lake level may have also been governed by neighboring lakes, such as Denizli and Acıgöl. The connections between the Baklan and Denizli basins were established due to the presence of Pontocaspian mollusc species (*Theodoxus bukowski* and *Laevicaspia* ?*lincta*) and ostracod genera (*Cyprideis*, *Tyrrhenocythere* sp., *Amnicythere*, and *Candona*) in both the PLC deposits of the Baklan Basin and lacustrine deposits of the Denizli Basin located in the west of the Baklan Basin (Figs. 1B and 2). This indicates that these brackish water mollusc and ostracod species may have entered from the Denizli Basin to the Baklan Basin (Fig. 17B). During this time, a connection was also established between the Baklan and Acıgöl basins due to the presence of *Monodacna* in the Acıgöl Basin (F.P. Wesselingh, pers. obs.) (Fig. 17B). An increase in precipitation and a decrease in subsidence caused the relative rise of the lake level compared to the first lake interval, resulting in the establishment of a connection between Lake Baklan, Lake Denizli and Lake Acıgöl. Many studies reported that western and central Anatolian lakes united to constitute a single mega-lake (known as the Pisidic Lake) during the Pliocene and Pleistocene (Spratt and Forbes, 1847; Becker-Platen, 1970; Bering, 1971; Luttig and Steffens, 1976).

5.2.3. Interval III: Middle-Late Pleistocene (Ionian-Tarantian) lake

In the third interval, the palustrine lake center deposits (PLC) passed upwards into the palustrine lake margin (PLM) deposits of the upper part of the studied succession (Gelinören section, Fig. 4C). The overlying progradational wedge of PLM deposits developed during the Late Expansion System Tract (LEST) associated with humid conditions (Fig. 17C), as supported by negative $\delta^{18}O$ values throughout the section (Fig. 16).

The predominance of packstone to grainstone textures of the facies PLM1 and facies PLM2 indicates that the deposition of PLM deposits occurred in a low-energy, low-gradient 'ramp' type margin environment (Platt and Wright, 1991; Alonso-Zarza et al., 2011). Pedogenic features (i.e., brecciation, nodularization, cracking, and coated grains) suggest that littoral lake areas were subaerially exposed due to seasonal fluctuations (Freytet and Plaziat, 1982; Alonso-Zarza, 2003). Fossiliferous marlstone–siltstone–sandstone–mudstone alternations formed in this palustrine setting (Fig. 17). The PLM carbonates and molluscs exhibit negative $\delta^{18}O$ and $\delta^{13}C$ values (Table 2 and 3; Fig. 15A-15B). The low $\delta^{18}O$ values in this unit suggest that isotopically light, ^{18}O-depleted meteoric water entered into the area (Leng and Marshall, 2004). The negative $\delta^{13}C$ values indicate that the isotopically light CO_2 entered the system through biological processes related to pond vegetation or decay of organic matter (Talbot and Kelts, 1990; Leng and Marshall, 2004). The mean $\delta^{18}O$ values of the calcite (−6.20 to −0.67‰, mean = −3.03‰) and dolomite (−5.55 to −0.20‰, mean = −2.78‰) (Fig. 15A; Table 2) are quite similar and imply that calcite and dolomite precipitated in similar conditions. The PLM carbonates and mollusc fauna do not exhibit a clear trend (correlation r-values +0.52 for calcite and +0.62 of dolomite; Fig. 15A-15B), indicating a hydrologically open lake with a positive precipitation/evaporation balance (P > E ratios), leading to a depletion in $^{13}C_{DIC}$ and $^{18}O_{water}$ (Talbot, 1990; Lamb et al., 2002). This lake was predominantly diluted by meteoric water input with low $\delta^{18}O$ and $\delta^{13}C$ values. This is supported by intolerant to elevated salinities to most mollusc species, such as the sphaeriid clams and planorbid gastropods. However, *Monodacna imrei* stands out with strongly elevated $\delta^{13}C$ values than those other species (Fig. 15B). Strongly elevated $\delta^{13}C$ values point to prolonged water residence times (Vonhof et al., 1998), and the specific isotope signature may suggest that *Monodacna* did not live exactly coeval with, but instead within adjacent biotopes of the other species.

The PLM succession is interpreted as an overfilled lake (Figs. 16 and 17), as suggested by Bohacs et al. (2000). This lake-basin type occurs when the rate of sediment+water supply exceeds potential accommodation. These conditions usually take place when P/E ratio is relatively high or rates of tectonic subsidence are relatively low (Bohacs et al., 2000). The resulting lake hydrology is predominantly open, as in the PLM deposits, indicating that the lake level was controlled by a positive precipitation/evaporation balance (P > E) (Fig. 17C). It is thought that the connections between Baklan, Denizli and Acıgöl basins continued due to the presence of Pontocaspian mollusc species and ostracod species. A strong increase in precipitation promoted the establishment of connections with further southwestern Anatolian lakes (Eğirdir and Beyşehir lakes, Wilke et al., 2007; Glöer and Girod, 2013) and central Anatolian lakes (Lake Karapınar, Konya Basin; Büyükmeriç and Wesselingh, 2018). These interbasinal connections may have formed during the outflow periods. In particular, the presence of bivalve genus *Monodacna* in the PLM deposits may have entered Lake Karapınar during the outflow periods in the Late Pleistocene.

The upward decreasing trend in $\delta^{18}O$ values of this succession (Fig. 16) reflects humid conditions throughout the section, supported by mollusc and ostracod distributions. The freshwater to low mesohaline ostracod taxa (Fig. 7 (5–8), (11−12), (21-28), (33–36) and Fig. 9 (5–8), (13–16)) and mollusc taxa (Fig. 10 (b, d-i, k, o-p) and Fig. 13 (a-r)) (Table 1) in this section indicate freshwater to low mesohaline lake conditions. In the Gelinören section, the ostracod fauna (samples GEK.15, GEK.14, and GEK.12) is formed by *Cyprideis* cf. *pontica*, *L.* aff. *inopinata*, *C.* ex gr. *neglecta* and *Ilyocypris* spp., indicating shallow, oligohaline waters (Fig. 16). Above (GEK.10–GEK.7) the abundance of *C.* cf. *pontica* and *C.* (*C.*) *fastigata* successively increases and rare brackish water taxa (*Tyrrhenocythere* sp. and *A.* cf. *olivia*) appear. The faunal change points to a gradual rise in salinity, which peaks in sample GEK.7 with supposedly low mesohaline conditions. Afterwards (samples GEK.6–GEK.2), salinity drops back to oligohaline waters.

5.3. Regional significance of the Baklan Basin

The Pontocaspian region comprises a series of basins (Fig. 18; including the Black Sea, Azov Sea, and Caspian Sea basins) that represent remnants of the Eastern Paratethys, with their own specific biota and paleogeographic evolution (e.g., Rögl, 1999; Yanina, 2014; Krijgsman et al., 2019). During the Eocene-Oligocene transition, a southern

Mediterranean Sea was formed at the western end of the Tethys, while an intercontinental Paratethys Sea emerged to the north of the Alpine tectonic belt (Rögl, 1999). At this time, several continental microplates, such as the Aegean–Anatolian region, developed in this area. The Aegean-Western Anatolian region separated the Mediterranean and the Eastern Paratethys at that time. The Aegean-Anatolian microplate represents a semi-continuous crossroads between Europe, Africa, and Asia, facilitating continental faunal migration (Rögl, 1999). This region also hosted aquatic corridors with the Mediterranean and Paratethys during episodic connections (Neubauer et al., 2015; Krijgsman et al., 2019).

In the Pontocaspian region, significant regional paleoenvironmental and paleobiogeographic developments occurred during the Pleistocene (e.g., Yanina, 2014; Krijgsman et al., 2019). Since the onset of the Northern Hemisphere Glaciation about 2.6 million years ago, the global climate has been dominated by glacial–interglacial variations (e.g., Lisiecki and Raymo, 2007). During the Pleistocene, several significant transgressive–regressive cycles resulted in recurrent connections between the Black Sea and Caspian basins, accompanied by dramatic changes in lake size, salinity, and biotic assemblages (Neubauer et al., 2015).

During the latest Pliocene-earliest Pleistocene (around 2.6 million years ago), the largest Caspian transgression occurred, with shores extending well into the middle Volga and southern Urals to the north, as well as the Azov Sea in the west and the Aral Sea in the east (Krijgsman et al., 2019; Fig. 18A). This transgression led to the establishment of connectivity between the Caspian Sea, Black Sea, and Aegean Sea, enabling various fauna such as fishes, molluscs, and ostracods to migrate from the Caspian Sea to the Black Sea and eventually to the Aegean Sea. The biota of the Pontocaspian region comprises a high diversity of taxa that have evolved in the brackish habitats of the Caspian Sea-Black Sea-Aral Sea region and surrounding rivers over the past few million years.

The Caspian Sea Basin has been a series of lakes with varying levels of salinity, ranging from anomalohaline to freshwater since the Late Miocene (late Messinian; Popov et al., 2006). This extended period allowed for the development of a diverse and highly endemic Pontocaspian biota, especially since the Early Pleistocene (Neubauer et al., 2018). Fossil evidence indicates a close relationship between the northern Aegean and the Eastern Paratethys from the Tortonian onwards (Popov and Nevesskaya, 2000). Wide-ranging Pontocaspian species (fishes, molluscs, crustaceans, dinoflagellates, and diatoms) are found in the northern Black Sea, the Caspian Sea, and the former Lake Aral, and have evolved to adapt to the unusual salinity regimes in these lakes and seas in the past two million years (Nevesskaya et al., 2005). The Pontocaspian biota's development mostly occurred around the Caspian Sea, Black Sea, and Marmara Sea basins (e.g., Nevesskaja et al., 2001; İslamoğlu, 2009; Yanina, 2014), but satellite areas such as the Balkans and Anatolia may have played a role in their evolution as well. Some fossil and modern Pontocaspian genera are found in the western and central Anatolian lake systems (Wesselingh et al., 2008; Wesselingh and Alçiçek, 2010; Alçiçek et al., 2015; Büyükmeriç and Wesselingh, 2018) and northeastern Marmara Sea Basin (İslamoğlu, 2009; Büyükmeriç et al., 2016; Taviani et al., 2014).

During the Late Pliocene-Pleistocene, the Aegean-Anatolian region experienced regional extension, leading to the formation of a complex basin configuration. During this period, southwestern Anatolia was located between the Eastern Paratethys in the north and the Mediterranean basins in the south (Fig. 18A-18C). This region is a hotspot for continental aquatic biodiversity, featuring Graeco-Anatolian and Pontocaspian faunal elements (Wesselingh et al., 2008; Wilke et al., 2010; Büyükmeriç and Wesselingh, 2018; Rausch et al., 2019, 2020). In southwestern Anatolian region, the Denizli Basin contains the Pliocene-Pleistocene successions, which hosted endemic Pontocaspian faunas (Nebert, 1958; Taner, 1974a, 1974b, 1975; Alçiçek et al., 2015; Rausch et al., 2019, 2020; Lazarev, 2020a, 2020b). Meanwhile, the Baklan Basin includes the Lower-Upper Pleistocene succession comprising similar endemic Pontocaspian ostracod and mollusc faunas. This suggests that the largest Caspian transgression extended to the Denizli Basin (Fig. 17A and 18A) during the latest Pliocene-earliest Pleistocene transgression (ca. 2.6 Ma) and then arrived in the Baklan Basin (lake interval II; Fig. 17B and 18B) during the Early-Late Pleistocene. This means that there was interbasinal connectivity between the Denizli and Baklan basins in southwestern Anatolia during the Early-Middle Pleistocene (Fig. 17B). The Pontocaspian mollusc species (*Theodoxus bukowski* and *Laevicaspia ?lincta*) and ostracod species (*Cyprideis*, *Tyrrhenocythere*, *Amnicythere*, *Candona*) initially entered to the Denizli Basin during the latest Pliocene-earliest Pleistocene transgression (Gelasian) (ca. 2.6 Ma) (Fig. 17A; Alçiçek et al., 2015; Rausch et al., 2019, 2020) and subsequently migrated to the Baklan Basin during the Early Pleistocene (Calabrian; ca. 1.8 Ma) (Fig. 17B). During the Calabrian, there was also interbasinal connectivity between the Baklan and Acıgöl basins because of the presence of *Monodacna* species in both basins (Fig. 17B and 18B). At this time, *Monodacna* species may have migrated from the Baklan Basin to the Acıgöl Basin (Fig. 17B). Meanwhile, the absence of *Monodacna* in the Denizli Basin suggests that the *Monodacna* species of the Baklan Basin may have arrived through another gateway.

The Middle-Late Pleistocene (Ionian-Tarantian) conditions (lake interval III) show similarities to the Calabrian conditions (lake interval II) due to the presence of Pontocaspian brackish water ostracod and mollusc species in the PLM deposits (Table 4) of the Baklan Basin (Fig. 17C). During this time, interbasinal connectivity was established between the Baklan, Denizli, Acıgöl, Eğirdir, and Beyşehir lake basins in southwestern Anatolia and the Konya Basin (Lake Karapınar; Büyükmeriç and Wesselingh, 2018) in central Anatolia (Fig. 18C). The Upper Pleistocene Pontocaspian brackish water fauna has been also recorded in Lake İznik (İslamoğlu, 2009), Lake İzmit (Büyükmeriç et al., 2016) and Lake Gemlik (Taviani et al., 2014) in the eastern Marmara Sea Basin (Fig. 18C), indicating marine connections between the Mediterranean and Black Sea basins during the Late Pleistocene (130–71 ka). These findings suggest a closer biogeographic relationship with contemporaneous Black Sea faunas than with Mediterranean faunas (Büyükmeriç et al., 2016). In the western of Marmara Sea Basin, the presence of Middle-Upper Pleistocene fauna from the Çanakkale-Dardanelles region (Fig. 18C), which includes both Pontocaspian and Mediterranean faunas, indicates the significant role of gateway tectonics in the connectivity history between the Black Sea and Mediterranean region (Büyükmeriç et al., 2018; Alçiçek et al., 2023). The fossil and modern freshwater and brackish water faunas are well known from other western and central Anatolian basins, most of which are dominated by freshwater taxa. These include the Çameli Basin (Alçiçek et al., 2017), the Burdur-Salda Basin, (H. Alçiçek, pers. obs.), the Burdur Basin (Yıldırım, 1999; Kebabçı and Yıldırım, 2010); the Beyşehir-Eğirdir Basin (Wilke et al., 2007; Glöer and Girod, 2013), and the Konya Basin (Karabıyıkoğlu et al., 1999).

Consequently, the presence of Pontocaspian fauna in the Baklan Basin and other Anatolian lake basins, such as Denizli and Karapınar, can be explained by the establishment of interbasinal connectivity between the Paratethys via the Aegean region to the lake basins during highstands. This allowed faunal migration via possible intra-west Anatolian gateways. The Aegean migration corridor enabled Pontocaspian faunas, such as molluscs and ostracods, to colonize the Baklan Basin and the adjacent Denizli Basin (Wesselingh et al., 2008; Alçiçek et al., 2015; Rausch et al., 2019, 2020; Lazarev, 2020a, 2020b). This indicates that the region was once a connected paleobay of the Paratethys, and the influence of the Paratethys extended further south than previously believed (Freels, 1980; Wesselingh et al., 2008; Wesselingh and Alçiçek, 2010; Rausch et al., 2019, 2020). Further studies in southwestern Anatolia will enhance our understanding of the southern boundary of the Paratethys, the location of the gateways, and when the region served as a refugium for the Pontocaspian fauna.

6. Conclusions

The stratigraphic, sedimentological, and paleontological analyses, and stable isotopic data from the Lower-Upper Pleistocene sedimentary record in the northern sector of the Baklan Basin have enabled the investigation of the paleoenvironmental, paleoclimatic, paleoecological, and paleobiogeographical evolution of its Quaternary fill stage.

The studied successions serve as an excellent example of lacustrine and palustrine deposition in a laterally extensive, low-gradient, shallow lake system in the semi-isolated Pontocaspian freshwater to slightly brackish water (oligohaline-low mesohaline) long-lived lake.

Three major types of depositional environments have been identified: freshwater perennial shallow lake (PSL deposits), and freshwater to low mesohaline palustrine carbonate lake center (PLC deposits) and palustrine lake margin (PLM deposits) depositional environments. These environments correspond to the different intervals of the lake expansion cycle: (i) During the lake interval I, the perennial shallow lake environment represents the very early stage of Early Expansion System Tract (VEEST), indicating a stage of the very early lake transgression in arid conditions in the basin; (ii) During the lake interval II, the palustrine carbonate lake center environment corresponds to the late stage of the Early Expansion System Tract (LEEST), suggesting a stage of the late early lake transgression in semiarid to subhumid climates; and (iii) During the lake interval III, the palustrine lake margin environment reflects the Late Expansion System Tract (LEST) under humid conditions.

During the Early-Late Pleistocene, the Baklan Basin hosted a wide variety of landscape mosaics represented by the Palearctic taxa, dominanted by an open-steppe ecosystem. The study area and surroundings still hosts a rich and varied biota with cosmopolitan, regional, and local endemic Pontocaspian taxa. The mammal fauna of the PLM deposits still inhabits the area today. The ostracod and mollusc faunas of the PSL, PLC, and PLM deposits are predominantly composed of modern Palearctic-Holarctic species with minor fossil (endemic) species. The fish fauna of the PLM deposits is most similar to modern Palearctic forms. This study shows that Lake Baklan represents a refuge for Palearctic taxa during adverse time intervals during the Early-Late Pleistocene, as well as in other Anatolian lakes (e.g., Denizli, Karapınar).

This study demonstrates that lacustrine-palustrine deposits in intermontane basins serve as excellent records of paleohydrology and paleoclimate. Therefore, detailed stratigraphic, sedimentological, and geochemical analyses are important to interpreting drainage patterns, lake hydrology, and depositional evolution in response to tectonism and climate. These results highlight the importance of considering allocyclic factors when interpreting other lake systems, as well as inferring the causes of the occurrence and evolution of open- and closed-lake basins. As a result, this study shows the combined influence of tectonics, climate changes, and the largest major Caspian Sea transgression on the evolution of the final fill stage of the Baklan Basin.

Declaration of Competing Interest

The authors declare that they have no known competing financial interests or personal relationships that could have appeared to influence the work reported in this paper.

Data availability

The data that has been used is confidential. All data are available in the publication and the supplementary material.

Acknowledgments

This study was supported by the Scientific and Technological Research Council of Turkey (TÜBİTAK research grants ÇAYDAG 105Y280). H. Alçiçek, A. Tesakov and M.C. Alçiçek received Martin, Temminck and Synthesys fellowships to visit Naturalis for comparative studies. M.C. Alçiçek is indebted to the Outstanding Young Scientis Award by Turkish Academy of Sciences (TUBA-GEBIP). The authors would like to express their gratitude to the editor Lucia Angiolini, the reviewer François Fournier, and an anonymous reviewer for their helpful comments and suggestions.

Appendix A. Supplementary data

Supplementary data to this article can be found online at https://doi.org/10.1016/j.palaeo.2023.111649.

References

Alçiçek, H., Alçiçek, M.C., 2014. Palustrine carbonates and pedogenic calcretes in the Çal Basin of SW Anatolia: Implication on the Plio-Pleistocene regional climatic pattern in the Eastern Mediterranean. Catena 112, 48–55.

Alçiçek, H., Jiménez-Moreno, G., 2013. Late Miocene to Pliocene fluvio-lacustrine system in Karacasu Basin (SW Anatolia, Turkey): depositional, palaeogeographic and palaeoclimatic implications. Sediment. Geol. 291, 62–83.

Alçiçek, M.C., Mayda, S., 2012. Faunal and palaeoenvironmental changes in the Çal Basin, SW Anatolia: Implications for regional stratigraphic correlation of late Cenozoic basins. Comptes Rendus Geosci. 344, 89–98.

Alçiçek, M.C., Mayda, S., Ten Veen, J.H., Boulton, S.J., Alçiçek, H., Tesakov, A., Saraç, G., Hakyemez, Y., Göktaş, F., Murray, A., Wesselingh, F.P., Jimenez-Moreno, G., Büyükmeriç, Y., Bouchal, J.M., Demirel, F.A., Kaya, T.T., Halaçlar, K., Bilgin, M., van den Hoek Ostende, L.W., 2019. Reconciling the stratigraphy and sedimentation history of the Lycian orogen-top basins, SW Anatolia. Palaeobiodiversity and Palaeoenvironments 99, 551–570.

Alçiçek, M.C., Ten Veen, J.H., 2008. The late Early Miocene Acipayam piggy-back basin: refining the last stages of Lycian nappe emplacement in SW Turkey. Sediment. Geol. 208, 101–113.

Alçiçek, H., Varol, B., Özkul, M., 2007. Sedimentary facies, depositional environments and palaeogeographic evolution of the Neogene Denizli Basin of SW Anatolia, Turkey. Sediment. Geol. 202, 596–637.

Alçiçek, M.C., Brogi, A., Capezzuoli, E., Liotta, D., Meccheri, M., 2013. Superimposed basin formation during Neogene–Quaternary extension in SW-Anatolia (Turkey): insights from the kinematics of the Dinar fault zone. Tectonophysics 608, 713–727.

Alçiçek, H., Wesselingh, F., Alçiçek, M.C., 2015. Paleoenvironmental evolution of the late Pliocene-early Pleistocene fluvio-deltaic sequence of the Denizli Basin (SW Turkey). Palaeogeogr. Palaeoclimatol. Palaeoecol. 437, 98–116.

Alçiçek, H., Wesselingh, F.P., Alçiçek, M.C., Jimenez-Moréno, G., Feijen, F.J., van den Hoek Ostende, L.W., Mayda, S., Tesakov, A., 2017. A multiproxy study of the early Pleistocene palaeoenvironmental and palaeoclimatic conditions of an anastomosed fluvial sequence from the Çameli Basin (SW Anatolia, Turkey). Palaeogeogr. Palaeoclimatol. Palaeoecol. 467, 232–252.

Alçiçek, H., Büyükmeriç, Y., Krijgsman, W., Shen, C.-C., Yu, T.-L., Alçiçek, M.C., Wesselingh, F.P., 2023. A new Middle-Late Pleistocene succession from the southern Dardanelles (Turkey) sheds lights on the Mediterranean-Black Sea gateway evolution. XXI. In: INQUA Congress, Roma, Italy.

Alonso-Zarza, A.M., 2003. Palaeoenvironmental significance of palustrine carbonates and calcretes in the geological record. Earth Sci. Rev. 60, 261–298.

Alonso-Zarza, A.M., Calvo, J.P., 2000. Palustrine sedimentation in an episodically subsiding basin: the Miocene of the northern Teruel Graben (Spain). Palaeogeogr. Palaeoclimatol. Palaeoecol. 160, 1–21.

Alonso-Zarza, A.M., Wright, V.P., 2010. Palustrine Carbonates. In: Alonso-Zarza, A.M., Tanner, L.H. (Eds.), Carbonates in Continental Settings: Processes, Facies, and Application, Developments in Sedimentology. Elsevier, Amsterdam (The Netherlands), pp. 103–131.

Alonso-Zarza, A.M., Genise, J.F., Verde, M., 2011. Sedimentology, diagenesis and ichnology of cretaceous and Palaeogene calcretes and palustrine carbonates from Uruguay. Sediment. Geol. 236, 45–61.

Anadón, P., Orti, F., Rosell, L., 2000. Neogene lacustrine systems of the southern Teruel Graben (Spain). In: Gierlowski-Kordesch, E.H., Kelts, K.R. (Eds.), Lake Basins Through Space and Time, 46. AAPG Stud. Geol, Tulsa, pp. 497–504.

Andrieu-Ponel, V., Rochette, P., Demory, F., Alçiçek, H., Boulbes, N., Bourlès, D., Helvacı, C., Lebatard, A.E., Mayda, S., Michaud, H., Moigne, A.M., Nomade, S., Perrin, M., Ponel, P., Rambeau, C., Vialet, A., Gambin, B., Alçiçek, M.C., 2021. Continuous presence of proto-cereals in Anatolia since 2.3 Ma, and their possible co-evolution with large herbivores and hominins. Sci. Rep. 11, 8914.

Armenteros, I., Daley, B., García, E., 1997. Lacustrine and palustrine facies in the Bembridge Limestone (late Eocene, Hamshire Basin) of Isle of Wight, southern England. Palaeogeogr. Palaeoclimatol. Palaeoecol. 128, 111–132.

Badertscher, S., Fleitmann, D., Cheng, H., Edwards, R.L., Göktürk, O.M., Zumbühl, A., Leuenberger, M., Tüysüz, O., 2011. Pleistocene water intrusions from the Mediterranean and Caspian seas into the Black Sea. Nat. Geosci. 4, 236–239.

Baird, W., 1843. The Natural history of the British Entomostraca. Ann. Mag. Nat. Hist. 68, 81–95.

Bassiouni, M.A.A., 1979. Brackische und marine Ostracoden (Cytherideinae, Hemicytherinae, Trachyleberidinae) aus dem Oligozän und Neogen der Türkei. Geol. Jahrbuch B 31, 3–195.

Becker-Platen, J.D., 1970. Lithostratigraphische Unterschungen im Kanozoikum Südwest Anatoliens (Türkei)- Kanozoikum und Braunkohlen der Turkei. Beiheftezum Geol. Jahrbuch 97. Hannover, 244 p.
Beker, K., Tunoğlu, C., Ertekin, K., 2008. Pliocene–Lower Pleistocene Ostracoda Fauna from İnsuyu Limestone (Karapınar–Konya/Central Turkey) and its paleoenvironmental implications. Geol. Bull. Turkey 51 (1), 1–31.
Bering, D., 1971. The development of the Neogene and Quaternary intramontane basins within the Pisidic lake district in S.Anatolia. Newsl. Stratigr. 1, 27–32.
Bernoulli, D., Graciansky, P.C., Monod, O., 1974. The extension of the Lycian nappes (SW Turkey) into the southwestern Aegean islands. Eclogae Geol. Helv. 67, 39–90.
Bohacs, K.M., Carroll, A.R., Neal, J.E., Mankiewwicz, P.Z., 2000. Lake-basin type, source potential, and hydrocarbon character: An integrated sequence-stratigraphic-geochemical framework. In: Gierlowski-Kordesch, E.H., Kerry, K.R. (Eds.), Lake Basins through Space and Time, Am. Assoc. Petrol. Geol. Stud. Geol., vol. 46, pp. 3–33.
Bozkurt, E., 2003. Origin of NE-trending basins in western Turkey. Geodin. Acta 16, 61–81.
Brady, G., 1868. A monograph of the recent British Ostracoda. Trans. Linnean Soc. Lond. 26, 353–495.
Büyükmeriç, Y., Wesselingh, F., 2018. New cockles (Bivalvia: Cardiidae: Lymnocardiinae) from late Pleistocene Lake Karapınar (Turkey): Discovery of a Pontocaspian refuge? Quat. Int. 465, 37–45.
Büyükmeriç, Y., Wesselingh, F.P., Alçiçek, M.C., 2016. Middle–late Pleistocene marine molluscs from Izmit Bay area (eastern Marmara Sea, Turkey) and the nature of Marmara – Black Sea corridors. Quat. Int. 401, 153–161.
Büyükmeriç, Y., Alçiçek, H., Alçiçek, M.C., 2018. Çanakkale Boğazı Güney Kıyılarındaki orta-geç Pleyistosen Yaşlı Birimlerin Mollusk Faunasına Dayalı Stratigrafisi, Paleoekolojisi ve Paleobiyocoğrafyası. Tübitak Proj. 116Y541, 80 p.
Chyzer, C., Toth, A., 1858. *Cypris zenkeri* n. sp. In: Chyzer, C., Ueber die Crustaceen-Fauna Ungarns. Verhandlungen des zoologisch-botanischen Vereins in Wien 8, 514–515.
Çiçek, E., Birecikligil, S.S., Fricke, R., 2015. Freshwater fishes of Turkey: a revised and updated annotated checklist. Biharean Biol. 9, 141–157.
Collins, A.S., Robertson, A.H.F., 1998. Processes of late cretaceous to late Miocene episodic thrust–sheet translations in the Lycian Taurides, SW Turkey. J. Geol. Soc. Lond. 155, 759–772.
Demory, F., Rambeau, C., Lebatard, A-E., Perrin, M., Blawal, S., Andrieu-Ponel, V., Alçiçek, H., Boulbes, N., Bourlès, D., Helvaci, C., Petschick, R., Mayda, S., Moigne, A-M., Nomade, S., Ponel, P., Rochette, P., Vialet, A., Alçiçek, M.C., 2020. Chronostratigraphy, depositional patterns and climatic imprints in Lake Acigöl (SW Anatolia) during the Quaternary. Quat. Geochronol. 56, 101038.
Dunham, R.J., 1962. Classification of carbonate rocks according to depositional texture. In: Ham, W.E. (Ed.), Classification of Carbonate Rocks. American Association of Petroleum Geologists, Tulsa, pp. 108–121. AAPG Memoir 1.
Dykan, N.I., 2016. The species of *Cyprideis pontica* Krstić, 1968 (Ostracoda, Crustacea) – the indicator of the boundary of the Pliocene and Quaternary sediments (the NW Black Sea). Geol. Miner. Resour. World Ocean 2016 (1), 19–32.
Férussac, J.B.L., 1807. Essai d'une méthode conchyliologique appliquée aux mollusques fluviatiles et terrestres d'après la considération de l'animal et de son test, par M. Daudebard de Férussac. Nouvelle édition augmentée d'une synonymie des espèces les plus remarquables, d'une table de concordance systématique de celles qui ont été décrites par Géoffroy, Poiret et Draparnaud, avec Müller et Linné, et terminée par un catalogue d'espèces observées en divers lieux de la France, par J. Daudebard fils pp. j-xvj [= 1–16], 1–142. Paris.
Freels, D., 1980. Limnische Ostrakoden aus Jungtertiär und Quartär der Türkei. Geol. Jahrbuch B 39, 3–169.
Freytet, P., Plaziat, J.C., 1982. Continental carbonate sedimentation and pedogenesis-Late Cretaceous and Early Tertiary of Southern France. Contrib. Sedimentol. 12, 213 pp.
Geraards, D., 2017. Late Miocene large mammals from Mahmutgazi, Denizli province, Western Turkey. Neues Jahrbuch Geol. Paläontol. Abhandlungen 284 (3), 241–245.
Gittenberger, E., Janssen, A.W., Kuijper, W.J., Kuijper, J.G.J., Meijer, T., van der Velde, G., De Vries, J.N., 1998. De Nederlandse zoetwatermollusken. Recente en fossiele weekdieren uit zoet en brak water. Nederlandse Fauna, 2. Nationaal Natuurhistorisch Museum Naturalis, KNNV Uitgeverij & EIS-Nederland, Leiden.
Gliozzi, E., Rodriguez-Lazaro, J., Nachite, D., Martin-Rubio, M., Bekkali, R., 2005. An overview of Neogene brackish leptocytherids from Italy and Spain: Biochronological and palaeogeographical implications. Palaeogeogr. Palaeoclimatol. Palaeoecol. 225, 283–301.
Glöer, P., 2002. Die Tierwelt Deutschlands, 73. Teil: Süßwassergastropoden Nord- Und Mitteleuropas. Bestimmungsschlüssel, Lebensweise, Verbreitung. Conchbooks, Hackenheim, p. 327.
Glöer, P., Girod, A., 2013. New Pleistocene *Valvata* species from Lake Beyşehir and two new *Gyraulus* species from Lake Eğirdir (Mollusca: Gastropoda: Valvatidae, Planorbidae) in Turkey. Folia Malacol. 21/1, 25–31.
Gogaladze, A., Son, M.O., Lattuada, M., Anistratenko, V.V., Syomin, V.L., Pavel, A.B., Popa, O.P., Popa, L.O., ter Poorten, J.-J., Biesmeijer, J.C., Raes, N., Wilke, T., Sands, A.F., Trichkova, T., Hubenov, Z.K., Vinarski, M.V., Anistratenko, O.Y., Alexenko, T.L., Wesselingh, F.P., 2021. Decline of unique Pontocaspian biodiversity in the Black Sea Basin: a review. Ecol. Evol. 11, 12923–12947.
Göktaş, F., Çakmakoğlu, A., Tarı, E., Sütçü, Y.F., Sarıkaya, H., 1989. Çivril-Çardak arasındaki bölgenin jeolojisi: Maden Tetkik ve Arama Genel Müdürlüğü, Report no: 8701. Ankara (unpublished).
Griffiths, S.J., Griffiths, H.I., Altinsaçli, S., Tzedakis, P.C., 2002. Interpreting the *Tyrrhenocythere* (Ostracoda) signal from Palaeolake Kopais, Central Greece. Boreas 31, 250–259.
Gündoğdu, M.N., 1982. Neojen yaşlı Bigadiç Sedimanter Baseninin Jeolojik, Mineralojik Ve Jeokimyasal Incelenmesi (Geological, Mineralogical and Geochemical Investigation of the Bigadiç Neogene Volcano-Sedimentary Basin). Ph.D. Dissertation,. Hacettepe University, Ankara, 386 pp.
Hartwig, W., 1899. *Candona euplectella* (Robertson 1880) bildet eine selbständige Gattung. Zool. Anz. 22, 309–311.
İslamoğlu, Y., 2009. Middle Pleistocene bivalves of the İznik lake basin (Eastern Marmara, NW Turkey) and a new paleobiogeographical approach. Int. J. Earth Sci. (Geol. Rundsch.) 98, 1981–1990.
Jenyns, L., 1832. A monograph on the British species of *Cyclas* and *Pisidium*. Transactions of the Cambridge Philosophical Society 4, 289–312.
Jiménez-Moreno, G., Alçiçek, H., Alçiçek, M.C., van den Hoek Ostende, L.W., Wesselingh, F.P., 2015. Vegetation and climatic cycles during the late Pliocene and early Pleistocene in SW Anatolia, Turkey. Quat. Res. 84, 448–456.
Karabıyıkoğlu, M., Kuzucuoğlu, C., Fontugne, M., Kaiser, B., Mouralis, D., 1999. Facies and depositional sequences of the late Pleistocene Göçü shoreline system, Konya Basin, Central Anatolia: Implications for reconstructing lake-level changes. Quat. Sci. Rev. 18, 593–609.
Kaymakçı, N., Langereis, C., Özkaptan, M., Özacar, A.A., Gülyüz, E., Uzel, B., Sözbilir, H., Koç, A., 2018. Paleomagnetic evidences for upper plate response to a STEP fault, SW Anatolia. Earth and Planetary Science Letters 498, 101–115.
Kayseri-Özer, M.S., Karadenizli, L., Akgün, F., Oyal, N., Saraç, G., Şen, Ş., Tunoğlu, C., Tuncer, A., 2017. Palaeoclimatic and palaeoenvironmental interpretations of the Late Oligocene, Late Miocene–Early Pliocene in the Çankırı–Çorum Basin. Palaeogeogr. Palaeoclimatol. Palaeoecol. 467, 16–36.
Kebabçı, Ü., Yıldırım, M.Z., 2010. Freshwater snails fauna of lakes region (Göller Bölgesi), Turkey. Oltenia 26, 75–83.
Konak, N., 2002. Geological map of Turkey in 1/500.000 scale: İzmir sheet. Publ. Miner. Res. Explor. Direct. Ankara, Turkey.
Konak, N., Şenel, M., 2002. Geological map of Turkey in 1/500.000 scale. Publ. Miner. Res. Explor. Direct. Ankara, Turkey.
Konak, N., Akdeniz, N., Çakir, M.H., 1986. Çal-Çivril-Karahallı dolayının jeolojisi [Geology of Çal-Çivril-Karahallı regions]. Mineral Research and Exploration Institute of Turkey (MTA), unpublished report No: 8945, Ankara, 122 pp. (in Turkish).
Krijgsman, W., Tesakov, A., Yanina, T., Lazarev, S., Danukalova, G., Van Baak, G.C.G., Agustí, J., Alçiçek, M.C., Aliyeva, E., Bista, D., Bruch, A., Büyükmeriç, Y., Bukhsianidze, M., Flecker, R., Frolov, P., Hoyle, T.M., Jorissen, E.L., Kirscher, U., Koriche, S.A., Oms, O., Rausch, L., Singarayer, J., Stoica, M., Van de Velde, S.V., Titov, V.V., Wesselingh, F.P., 2019. Quaternary time scales for the Pontocaspian domain: Interbasinal connectivity and faunal evolution. Earth Sci. Rev. 188, 1–40.
Kuss, S.E., Storch, G., 1978. Eine Säugetierfauna (Mammalia: Artiodactyla, Rodentia) des älteren Pleistozäns von der Insel Kalymnos (Dodekanés, Griechenland). Neues Jahrbuch für Geologie und Paläontologie. Monatshefte 4, 206–227.
Lamarck, J.B., 1818. Histoire naturelle des animaux sans vertebres, 5. Bailliere, Paris, p. 612.
Lamb, A.L., Leng, M.J., Lamb, H.F., Telford, R.J., Mohammed, M.U., 2002. Climatic and non-climatic effects on the $\delta^{18}O$ and $\delta^{13}C$ compositions of Lake Awassa, Ethiopia, during the last 6.5 ka. Quat. Sci. Rev. 21, 2199–2211.
Lazarev, S., 2020a. Constraining Biogeographic Evolution at Interbasinal Crossroads: Age and Environmental Evolution of the Late Neogene Denizli Basin Succession (Turkey). PhD Thesis,. Utrect University, pp. 85–115.
Lazarev, S., 2020b. Depositional Architecture and Drivers of Sublacustrine Channel-Fans in the Extensional Denizli Basin (Early Zanclean, SW Anatolia). PhD Thesis,. Utrect University, pp. 117–142.
Leng, M.J., Marshall, J.D., 2004. Palaeoclimate interpretation of stable isotope data from lake sediments. Quat. Sci. Rev. 23, 811–831.
Lettéron, A., Fournier, F., Hamon, Y., Villier, L., Margerel, J.-P., Bouche, A., Feist, M., Joseph, P., 2017. Multi-proxy paleoenvironmental reconstruction of saline lake carbonates: Paleoclimatic and paleogeographic implications (Priabonian-Rupelian, Issirac Basin, SE France). Sediment. Geol. 358, 97–120.
Lettéron, A., Hamon, Y., Fournier, F., Séranne, M., Pellenard, P., Joseph, P., 2018. Reconstruction of a saline, lacustrine carbonate system (Priabonian, St-Chaptes Basin, SE France): depositional models, paleogeographic and paleoclimatic implications. Sediment. Geol. 367, 20–47.
Lettéron, A., Hamoun, Y., Fournier, F., Demory, F., Séranne, M., Joseph, P., 2022. Stratigraphic architecture of a saline lake system: from lake depocenter (Alès Basin) to margins (Saint-Chaptes and Issirac basins), Eocene-Oligocene transition, south-East France. Sedimentology 69, 651–695.
Li, H.C., Ku, T.L., 1997. $\delta^{13}C$–$\delta^{18}O$ covariance as a paleohydrological indicator for closed–basin lakes. Palaeogeogr. Palaeoclimatol. Palaeoecol. 133, 69–80.
Li, Z., Yang, W., Wang, Y., Zhang, L., Luo, H., Liu, S., Zhang, L., Luo, X., 2019. Anatomy of a lacustrine stratigraphic sequence within the fourth member of the Eocene Shahejie Formation along the steep margin of the Dongying depression, eastern China. AAPG Bulletin 103, 469–504.
Linnaeus, C., 1758. Systema naturae per regna tria naturae, secundum classes, ordines, genera, species, cum characteribus, differentiis, synonymis, locis. Tomus I. Editio decima, reformata. Laurentius Salvius, Holmiae. iv + 824.
Lisiecki, L.E., Raymo, M.E., 2007. Plio-Pleistocene climate evolution: trends and transitions in glacial cycle dynamics. Quat. Sci. Rev. 26, 56–69.
Livental, V.E., 1938. Deposits and microfauna of the Baku area. Azerbaijan Sci. Res. Inst. Petrol. Trans. 1, 46–67 (In Russian).
Luttig, G., Steffens, D., 1976. Explanatory Notes for the Paleogeographic Atlas of Turkey from Oligocene to Pleistocene, 64pp. Bundesanstalt für Geowissenschaften und Rohstoffe, Hannover.
Malm, A.W., 1855. Om Svenska landt- och söttvattens mollusker, med särskilt afseende på de arter och former, som förkomma i grannskapet af Christianstad (C) och

Götheborg (G). Götheborgs Kongliga Vetenskaps och Vitterhets Samhälles Handlingar (Ny. Tidsföljd) 3, 73–152.
Matzke-Karasz, R., Witt, W., 2005. Ostracods of the Paratethyan Neogene Kilic and Yalakdere Formations near Yalova (Izmit Province, Turkey). Zitteliana A45, 115–133.
Meisch, C., 2000. Freshwater Ostracoda of Western and Central Europe. In: Schwoerbel, J., Zwick, P. (Eds.), Süßwasserfauna von Mitteleuropa, 8(3). Spektrum Akademischer Verlag, Heidelberg/Berlin, pp. 1–522.
Milaschewitsch, K.O., 1908. Molluscs collected during the excursion of S.a. Zernov on the torpedo-boat no. 264 on the Danube River from June 28 to July 3, 1907.
Müller, O.F., 1774. Vermivm terrestriumet fluviatilium, seu animalium infusoriorum, helminthicorum, ettestaceorum, nonmarinorum, succincta historia. Testacea 2, 214. Havniaeet Lipsiae.
Müller, O.F., 1776. Zoologiae Danicae Prodromus, Seu Animalium Daniae et Norvegiae Indigenarum: Characteres, Nomina, et Synonyma Imprimis Popularium. Typis Hallagerii, Havni, Copenhagen, 282 pp.
Nakajima, T., 2018. Comparative Studies on the Pharyngeal Teeth of Cyprinids. Tokai University Press, Kanagawa, Japan, 166 pp.
Namiotko, T., Danielopol, D.L., Belmecheri, S., Gross, M., Grafenstein Von, U., 2012. On the Leptocytheridae Ostracods of the Long–Lived Lake Ohrid: a Reappraisal of their Taxonomic Assignment and Biogeographic Origin. Int. Rev. Hydrobiol. 97 (4), 356–374.
Nebert, K., 1958. Denizli Pliyosen teressübatı ve bunların Batı Anadolu tatlı su Neojen stratigrafisi için ehemmiyeti. Bull. Mineral Res. Expl. Direct. Turkey (MTA) 51, 7–20.
Neumayr, M., Paul, C.M., 1875. Die Congerien- und Paludienschichten Slavoniens und deren Faunen. Abhandlungen der k. k. Geologischen Reichsanstalt 7 (3), 1–106.
Nemec, W., Alçiçek, M.C., Özaksoy, V., 2018. Sedimentation in a foreland basin within synorogenic orocline: Palaeogene of the Isparta Bend, Taurides, SW Turkey. Basin Res. 30, 650–670.
Neubauer, T.A., Harzhauser, M., Kroh, A., Georgopoulou, E., Mandic, O., 2015. A gastropod-based biogeographic scheme for the European Neogene freshwater systems. Earth Sci. Rev. 143, 98–116.
Neubauer, T.A., van de Velde, S., Yanina, T., Wesselingh, F.P., 2018. A late Pleistocene gastropod fauna from the northern Caspian Sea with implications for Pontocaspian gastropod taxonomy. Zookeys 770, 43–103.
Nevesskaja, L.A., Paramonova, N.P., Popov, S.V., 2001. History of the Lymnocardiinae (Bivalvia, Cardiidae). Paleontol. J. 35, 147–217.
Nevesskaya, L.A., Goncharova, I.A., Iljiana, L.B., 2005. Types of Neogene Marine and Non-marine basins exemplified by the Eastern Paratethys. Paleontol. J. 39, 227–235.
Nissen, E., Cambaz, M.D., Gaudreau, E., Howell, A., Karasözen, E., Savidge, E., 2022. Areappraisal of active tectonics along the Fethiye-Burdur trend southwestern Turkey. Geophysical Journal International 230, 1031–1051.
Oppenheim, P., 1919. Das Neogen in Kleinasien. Zeitschrift der Deutschen Geologischen Gesellschaft 70, 1–210.
Özgül, N., Arpat, E., 1973. Structural units of the Taurus orogenic belt and their continuation in neighbouring regions; selection of papers on the Eastern Mediterranean region, the 23rd congress of CIESM in Athens. Bull. Geol. Soc. Greece 10 (1), 155–164.
Paladilhe, A., 1866. Nouvelles miscellanées malacologiques. II. Espèces inédites, nouvelles ou peu connues du départment de l'Herault - Suite. Revue et Magasin de Zoologie pure et 18 (appliquée (2)), 168–171.
Pallas, P.S., 1771. Reise durch verschiedene Provinzen des Russischen Reichs. Erster Theil. Kaiserliche Academie der Wissenschaften, Saint Petersburg, p. 504.
Pickford, M., 2016. *Hippopotamodon erymanthius* (Suidae, Mammalia) from Mahmutgazi, Denizli–Çal Basin, Turkey. Fossil Imprint 72, 183–201.
Pipík, R., 2007. Phylogeny, palaeoecology, and invasion of non–marine waters by the late Miocene hemicytherid ostracod *Tyrrhenocythere* from Lake Pannon. Acta Palaeontol. Pol. 52 (2), 351–368.
Platt, N.H., Wright, V.P., 1991. Lacustrine carbonates: Facies models, facies distributions and hydrocarbon aspects. In: Anadón, A., Cabrera, L., Kelts, K. (Eds.), Lacustrine Facies Analysis, Int. Assoc. Sedimentol. Spec. Publ., vol. 13, pp. 57–74.
Popov, S.V., Nevesskaya, L.A., 2000. Late Miocene Brackish-Water Mollusks and the history of the Aegean Basin. Stratigr. Geol. Correl. 8, 195–205.
Popov, S.V., Shcherba, I.G., Ilyina, L.B., Nevesskaya, L.A., Paramonova, N.P., Khondkarian, S.O., Magyar, I., 2006. Late Miocene to Pliocene palaeogeography of the Paratethys and its relation to the Mediterranean. Palaeogeogr. Palaeoclimatol. Palaeoecol. 238, 91–106.
Radoman, P., 1973. New Classification of Fresh and Brackish Water Prosobranchia from the Balkans and Asia Minor. Posebna Izdanja, Prirodnjacki Muzej u Beogradu 32, 13–30.
Rausch, L., Alçiçek, H., Vialet, A., Boulbes, N., Mayda, S., Titov, V.V., Stoica, M., Charbonnier, S., Abels, H.A., Tesakov, A.S., Moigne, A.-M., Andrieu-Ponel, V., Franceschi, D.D., Neubauer, T.A., Wesselingh, F.P., Alçiçek, M.C., 2019. An integrated reconstruction of the early Pleistocene palaeoenvironment of *Homo erectus* in the Denizli Basin (SW Turkey). Geobios 57, 77–95.
Rausch, L., Stoica, M., Lazarev, S., 2020. A late Miocene-early Pliocene Paratethyan type ostracod fauna from the Denizli Basin (SW Anatolia) and its palaeogeographic implications. Acta Palaeontol. Roman. 16, 3–56.
Rögl, F., 1999. Mediterranean and Paratethys. Facts and hypotheses of an Oligocene to Miocene Paleogeography (short overview). Geol. Carpathica 50, 339–349.
Rutte, E., Becker-Platen, J.D., 1980. Cypriniden–Schlundzähne (Pisces) aus dem Känozoikum der Türkei. Newsl. Stratigr. 8, 191–222.
Sars, G.O., 1887. Nye Bidrag til Kundskaben om Middelhavets In-vertebratfauna 4: Ostracoda Mediterranea (Sydeuropaeiske Ostracoder). Arch. Math. Nat. 12, 173–324 (In Norwegian).
Schütt, H., 1964. Die Molluskenfauna eines reliktären Quellsees der südlichen Türkei. Arch. Molluskenkunde 93 (5/6), 173–180.
Şenel, M., 1997. Geological Maps of Turkey in 1:100 000 Scale: Denizli K9 Sheet, Mineral Research and Exploration Directorate of Turkey (MTA). Ankara, Turkey, 17 p.
Şenel, M., 2002. Geological Map of Turkey in 1/500.000 Scale: Konya sheet. Publication of Mineral Research and Exploration Directorate of Turkey (MTA). Ankara, Turkey.
Sheppard, R., 1825. Descriptions of seven new British land and fresh-water shells, with observations upon many other species, including a list of such as have been found in the County of Suffolk. The Transactions of the Linnean Society of London 14 (1), 148–170.
Sickenberg, O., Tobien, H., 1971. New Neogene and lower Quaternary vertebrate faunas in Turkey. Newsl. Stratigr. 1, 51–61.
Soulié-Märsche, I., García, A., 2015. Gyrogonites and oospores, complementary viewpoints to improve the study of the charophytes (Charales). Aquat. Bot. 120, 7–17.
Sözbilir, H., 1997. Stratigraphy and Sedimentology of the Tertiary Sequences in the Northeastern Denizli Province (Southwest Turkey). PhD Thesis. Dokuz Eylül University, İzmir-Turkey, 195 p.
Spratt, T.A.B., Forbes, E., 1847. Travels in Lycia, Milyas and the Cibyrates, 244pp. VanVoorst, London.
Stelfox, A.W., 1918. The *Pisidium* fauna of the Grand Junction Canal in Herts. and Bucks. Journal of Conchology 15 (10), 289–304.
Stewart, K.M., Murray, A.M., 2017. Biogeographical implications of fossil fishes from the Awash River, Ethiopia. J. Vertebr. Paleontol. 37 (1), 1269115.
Storch, G., 1988. Eine jungpleistozäne/altholozäne Nager–Abfolge von Antalya, SW–Anatolien (Mammalia, Rodentia). Zeitschrift Säugetierkunde 53, 76–82.
Sun, S., 1990. Denizli-Uşak Arasının Jeolojisi ve Linyit Olanakları. Mineral Res. Expl. Direct. Turkey (MTA), Scientific Report No: 9985. Ankara, Turkey (in Turkish, unpublished).
Swart, P.K., Burns, S.J., Leder, J.J., 1991. Fractionation of stable isotopes of O and C in CO_2 during the reaction of calcite with phosphoric acid as a function of temperature and technique. Chem. Geol. (Isot. Geosci. Sect.) 86, 89–96.
Talbot, M.R., 1990. A review of the palaeohydrological interpretation of carbon and oxygen isotopic ratios in primary lacustrine carbonates. Chem. Geol. 80, 261–279.
Talbot, M.R., Kelts, K., 1990. Paleolimnological signatures from carbon and oxygen isotopic ratios in organic carbon rich lacustrine sediments. In: Katz, B.J. (Ed.), Lacustrine Basin Exploration – Case Studies and Modern Analogs, AAPG Memoir, vol. 50, pp. 99–112.
Tan, M., Armbruster, J.W., 2018. Phylogenetic classification of extant genera of fishes of the order Cypriniformes (Teleostei: Ostariophysi). Zootaxa 4476, 6–39.
Taner, G., 1974a. Denizli bölgesi Neojen'inin paleontolojik ve stratigrafik etüdü. Bull. Mineral Res. Expl. Direct. Turkey (MTA) 82, 89–126.
Taner, G., 1974b. Denizli bölgesi Neojen'inin paleontolojik ve stratigrafik etüdü. Bull. Mineral Res. Expl. Direct. Turkey (MTA) 83, 145–177.
Taner, G., 1975. Denizli bölgesi Neojen'inin paleontolojik ve stratigrafik etüdü. Bull. Mineral Res. Expl. Direct. Turkey (MTA) 85, 45–66.
Taviani, M., Angeletti, L., Çağatay, M.N., Gasperini, L., Polonia, A., Wesselingh, F.P., 2014. Sedimentary and faunal signatures of the post-glacial marine drowning of the Pontocaspian Gemlik "lake" (Sea of Marmara). Quat. Int. 345, 11–17.
Temel, A., Gündoğdu, M.N., 1996. Zeolite occurrences and erionite-mesothelioma relationship in Cappadocia region, Central Anatolia, Turkey. Mineral. Deposita 31, 539–547.
Ten Veen, J.H., Boulton, S.J., Alçiçek, M.C., 2009. From palaeotectonics to neotectonics in the Neotethys realm: the importance of kinematic decoupling and inherited structural grain in SW Anatolia (Turkey). Tectonophysics 473, 261–281.
Tunoğlu, C., Besbelli, B., Ertekin, I.K., 2012. Ostracoda (Crustacea) association and a new species (*Dolerocypris anatolia* nov. sp.) from the Pliocene–Pleistocene Afşin–Elbistan (Kahraman Maraş) Coal Basin of Turkey. Geol. Carpath. 63 (2), 165–174.
Turan, N., 2002. Geological map of Turkey in 1/500.000 scale: Ankara sheet. Publ. Miner. Res. Explor. Direct. Ankara, Turkey..
Unger, F., 1852. Iconographia plantarum fossilium. In: Denkschriften Akademie der Wissenschaften, Mathematisch-Naturwissenchaftliche Klasse, Wien, 4, pp. 73–118.
van den Hoek Ostende, L.W., Diepeveen, F., Tesakov., A.S., Saraç, G., Mayhew, D., Alçiçek, M.C., 2015. On the brink: micromammals from the latest Villanyian from Bıçakçı (Anatolia). Geol. J. 50, 30–245.
Vázquez-Urbez, M., Arenas, C., Pardo, G., Pérez-Rivares, J., 2013. The effect of drainage reorganization and climate on the sedimentologic evolution of intermontane lake systems: the final fill stage of the Tertiary Ebro Basin (Spain). J. Sediment. Res. 83, 562–590.
van de Velde, S., Jorissen, E.L., Neubauer, T.A., Radan, S., Pavel, A.B., Stoica, M., Van Baak, C.G.C., Martínez Gándara, A., Popa, L., de Stigter, H., Abels, H.A., Krijgsman, W., Wesselingh, F.P., 2019. A conservation palaeobiological approach to assess faunal response of threatened biota under natural and anthropogenic environmental change. Biogeosciences 16, 2423–2442.
Vonhof, H.B., Wesselingh, F.P., Ganssen, G.M., 1998. Reconstruction of the Miocene western Amazonian aquatic system using molluscan isotopic signatures. Palaeogeogr. Palaeoclimatol. Palaeoecol. 141, 85–93.
Welter-Schultes, F.W., 2012. European Non-marine Molluscs, a Guide for Species Identification. Planet Poster Editions, Göttingen, 674 pp.
Wesselingh, F.P., Alçiçek, H., 2010. A new cardiid bivalve from the Pliocene Baklan Basin (Turkey) and the origin of modern Pontocaspian taxa. Paleontology 53, 711–719.
Wesselingh, F.P., Alçiçek, H., Magyar, I., 2008. A late Miocene Paratethyan type mollusc fauna from the Denizli Basin (southwestern Anatolia, Turkey) and its regional palaeobiogeographic implications. Geobios 41, 861–879.

Wesselingh, F.P., Neubauer, T.A., Anistratenko, V.V., Vinarski, M.V., Yanina, T., Ter Poorten, J.J., Kijashko, P., Albrecht, C., Anistratenko, O.Y., D'Hont, A., Frolov, P., Gándara, A.M., Gittenberger, A., Gogaladze, A., Karpinsky, M., Lattuada, M., Popa, L., Sands, A.F., de Velde, S.V., Vandendorpe, J., Wilke, T., 2019. Mollusc species from the Pontocaspian region - an expert opinion list. Zookeys 827, 31–124.

de Wet, C.B., Godfrey, L., de Wet, A.P., 2015. Sedimentology and stable isotopes from a lacustrine-to-palustrine limestone deposited in an arid setting, climatic and tectonic factors: Miocene-Pliocene Opache Formation, Atacama Desert, Chile. Palaeogeogr. Palaeoclimatol. Palaeoecol. 426, 46–67.

Wilke, T., Albrecht, C., Anistratenko, V.V., Şahin, S.K., Yıldırım, M.Z., 2007. Testing biogeographical hypotheses in space and time: faunal relationships of the putative ancient Lake Eğirdir in Asia Minor. J. Biogeogr. 34, 1807–1821.

Wilke, T., Schultheiß, R., Albrecht, C., Bornmann, N., Trajanovski, S., Kevrekidis, T., 2010. Native *Dreissena* freshwater mussels in the Balkans: in and out of ancient lakes. Biogeosciences 7, 3051–3065.

Yanina, T.A., 2014. The Ponto-Caspian region: environmental consequences of climate change during the late Pleistocene. Quat. Int. 345, 88–99.

Yıldırım, M.Z., 1999. Living and fossil molluscs of the Burdur Lake Basin. Club Conchylia Inform. 31 (1/2), 27–35.